In vitro analysis of polymeric microspheres containing human vocal fold fibroblasts for vocal fold lamina propria regeneration

Submitted by

Alicia Reyes Valenzuela

Department of Biological and Biomedical Engineering

McGill University- Montreal

A thesis submitted to McGill University in partial fulfillment of the requirements for the degree of Master of Engineering

To my family

To my parents, Felipe Reyes, and Nay Valenzuela, to my brother Felipe R.V, and to my sister Beatriz R.V

Thank for your support and your unconditional love

Words cannot express how grateful I am to you all

Table of contents

Abstract

Voice disorders can be defined as the absence of normal voice production which interferes with speech communication. These disorders have a functional impact with economic repercussions. It is estimated that these problems cost in the United States a total of $2.5 billion annually. Voice problems can affect 3 to 9% of the general population at any given point in life. The most common disorders occur in the vocal fold Lamina Propria (VF-LP), specifically in the superficial layer. Material injection is the most frequently used strategy to regenerate the injured VF-LP. But recent work has shown that commonly used materials may be rapidly cleared by the mononuclear phagocyte system (MPS) after injection, hampering their regeneration function. It has been previously demonstrated that microspheres (Ms) with a diameter of 500 µm are able to reduce the immune response. Thus, Ms can remain in the body for a longer time period. In addition, Ms are considered ideal substrates for cell delivery due to their optimal diffusion properties. The aim of the present study was to evaluate the feasibility of using Ms containing human vocal fold fibroblasts to induce VF-LP regeneration. This evaluation was done through the fabrication and *in vitro* characterization of Ms.

Electrospraying was used to fabricate alginate Ms. Taking advantage of the electronegative surface of alginate, layer-by-layer (LBL) assembly of polyelectrolytes was used to fabricate different Ms configurations, including Alginate-Poly-L-Lysine-Alginate (APA) and Alginate-Chitosan (Al-Cs). Homogeneous size distribution, and a spherical morphology with a diameter of 552.74±7.72 µm were obtained. The optimal load cell concentration, $4x10^5$ cells/ml, of the Ms was determined based on the morphology and integrity of the Ms using optical microscope. In the case of Al Ms and Al-Cs Ms, excessive cell concentration caused many Ms to be deformed. Conversely, APA Ms were less prone to deformation upon high cell concentration. In all cases, the Ms swelled and ruptured when $10x10^5$ cells/ml were loaded into the Ms. The results indicate that cells were

randomly distributed within the Ms. The cells added pressure on the edges of the Ms causing their rupture. The mechanical stability at 37°C was determined. Alginate-Ms and Al-Cs Ms were stable. Only 7% and 6% of the Ms, respectively, were found to be broken after 10 days of testing. In contrast 28% of APA Ms broke on day 10. Osmotic pressure test showed that Al Ms were the toughest. The stiffness of the materials was evaluated using a torsional rheometer and an atomic force microscope (AFM). The Young's modulus of pure alginate hydrogel crosslinked with $CaCl_2$ was 3 kPa. The modification with an additional layer of PLL and additional diluted alginate decreased the stiffness to 1.92 kPa. The addition of one Cs layer increased the local stiffness to 12.23 kPa. The results indicate that all hydrogels stiffness was matched with native tissue. Swelling properties were evaluated by measuring the diameter changes of the Ms when stored in PBS. In the present study, alginate, APA, and Al-Cs Ms had swelling percentages of 33.67%, 2.32%, and 52.76%, respectively. The thickness of the Cs and PLL membrane was characterized using genipin as a fluorogenic marker, and confocal laser scanning microscopy. It was found that the PLL membrane was thicker, 21.55±1.88 µm, and more uniform than that of Cs membrane, 10.625 ± 0.88 µm. In terms of cytotoxicity, none of the three configurations of Ms compromised the viability of fibroblasts. All of them indicated proliferation of the cells after 24h and 48h of incubation. Alginate and Al-Cs Ms doubled the initial cell concentration, while APA Ms increased the initial cell population by up to 72%.

Overall, the best balance of desirable properties was obtained for the alginate Ms, which also were the easiest group to fabricate. These results thus represent a first step in Ms design and fabrication to promote the regeneration of the VF. As such, alginate Ms were found to be a stable and functional cell delivery tool. Although Ms are extensively used for other organs, this is the first time that they are used and characterized with the purpose to induce the regeneration of the VF-LP, to the author's knowledge.

Résumé

Les troubles de la voix résultent en une altération de production vocale ce qui interfère avec la communication parlée. Ces troubles ont un impact fonctionnel mais aussi des répercutions économiques. Aux États-Unis, le coût annuel total de ces troubles est estimé à 2,5 milliards de dollars, incluant les interventions médicales, l'absentéisme et la perte de productivité. Les problèmes de voix touchent de 3 à 9% de la population générale à un stade ou à un autre de la vie. Le trouble le plus fréquent survient dans la couche superficielle de la lamina propria des cordes vocales. L'injection de substances telles que le gras ou un hydrogel est la stratégie la plus communément utilisée pour permettre la régénération de cette zone. Cependant, de travaux récents ont montré. Qu'après injection, ces matériaux peuvent être rapidement éliminés par le système phagocytaire mononucléaire, stoppant leur fonction régénérative. Il a notamment déjà été montré que l'encapsulation dans des microsphères d'un diamètre de 500 µm supprimer la réponse immunitaire. Ces microsphères ont une longue durée de vie. De plus, leurs favorise la diffusion excellente des cellules. Le but de la présente étude est d'évaluer l'efficacité des microsphères contenant des fibroblastes de cordes vocales pour induire la régénération de la lamina propria des cordes vocales humaines. La fabrication et la caractérisation *in vitro* de microsphères est l'objet premier de cette recherche.

L'électrodéposition a été utilisé afin de fabriquer des microsphères en alginate. Exploitant la surface électronégative de l'alginate, la technique d'assemblage de poly-électrolytes couche par couche a permis d'obtenir différentes conformations, incluant de l'alginate-poly-L-lysine-alginate (APA) et alginate-chitosane (Al-Cs). Des microsphères réparties de manière homogènes, ayant une forme sphérique ainsi qu'un diamètre de 552.74 ±7.72 µm ont été obtenues. Une distribution de taille homogène est nécessaire pour obtenir un taux de transport uniforme ainsi que la période de

dégradation voulue, et des particules de consistance stable. La concentration optimale de cellules insérées dans les microsphères a été estimée en utilisant un microscope. Pour les microsphères d'alginate et Al-Cs, une grande concentration cellulaire cause un grand nombre de malformation. Au contraire, les microsphères APA ont moins tendance à se déformer lorsqu'elles sont chargées avec une grande concentration de cellules. Dans tous les cas, les microsphères remplies de $10x10^5$ cellules se gonflent et se déchirent. Les résultats indiquent une répartition aléatoire des cellules dans les microsphères. Les cellules exercent une pression sur les a bords des microsphères provoquant leur rupture. Leurs propriétés mécaniques ont été mesurées, entre autres: 1) la stabilité mécanique à 37°C et 2) la pression osmotique. La rigidité des matériaux a été évaluée à l'aide d'un rhéomètre à torsion et d'un microscope à force atomique. Les tests de stabilité mécanique et de pression osmotique ont montré que la microsphère d'alginate est la plus stable et est la moins fragile après implantation. La microsphère APA est moins stable dans le temps que les autres types de microsphères. Le module d'Young de l'hydrogel d'alginate pur réticulé avec $CaCl_2$ est de 3 kPa. La modification avec une couche supplémentaire de PLL et d'alginate dilué a diminué la rigidité jusqu'à 1,92 kPa. La couche supplémentaire de chitosane a augmenté la rigidité locale jusqu'à 12,23 kPa. Les résultats indiquent que tous les hydrogels conviennent à la régénération de la lamina propria des cordes vocales.

Les propriétés de gonflement ont été évaluées en mesurant les changements de diamètre des microsphères lorsque celles-ci sont stockés dans du PBS. Les microsphères d'alginate, APA et Al-Cs ont respectivement un pourcentage de gonflement de 33,67%, 2,32% et 52,76%. L'épaisseur de la membrane de chitosane et PLL a été caractérisée en utilisant la génipine comme marqueur fluorogène et un microscope confocal à balayage laser. La membrane PLL est plus épaisse et plus uniforme que la membrane de chitosane. En termes de cytotoxicité, nulle des trois configurations

de microsphères n'ont compromis la viabilité des fibroblastes. Toutes ont induit la prolifération des cellules après 24 h et 48 h d'incubation.

Dans l'ensemble, les propriétés des microsphères d'alginate semblent des plus propices, c’est aussi le type de microsphère le plus facile à fabriquer. Les microsphères d'alginates semblent être un outil stable et fonctionnel de transport de cellules. Même si les microsphères sont souvent utilisées, leur emploi pour induire la régénération de la lamina propria des cordes vocales est originale à cette étude.

Acknowledgments

I wish to express my most sincere gratitude to my supervisor, Professor Luc Mongeau, for his guidance, constant support, his encouragement, motivation, and trust to develop innovative ideas. I appreciate all the tools, that Professor Mongeau provided me to learn new techniques, and to increase my skills to succeed in my master, and in my scientific career, including special training courses, workshops, and conferences. I also thank Professor Mongeau for helping me to improve the quality of my writing.

I am especially in debt with my co-supervisor Professor Satya Prakash. I am grateful for his collaboration, discussions, and feedback on my research. I express my gratitude to him for giving me access to his biomedical and cell therapy research laboratory, and his facilities, without which my work would be extremely difficult if not impossible. I thank him for his patient and guidance that helped me to reach my research objectives.

I express my deepest gratitude to my colleagues, Hongmei Chen, and Umar Iqbal for their orientation, and discussion related to the fabrication of Ms. Their expertise and ideas were extremely appreciated. Special thanks to my colleague, Nikita Lomis for her training and orientation related to the proliferation assays.

I extend my sincere thanks to my laboratory colleague Guangyu Bao who freely gave his time to perform the indentation assays on the atomic force microscopy and torsional rheometer. His contributions are deeply appreciated. Similarly, I thank my laboratory colleagues Rayane Ait Oubahou and Marion Lacroix for translating my abstract to French. In addition, I thank all my laboratory colleagues and laboratory manager Huijie Wang. They all provided a cooperative and enthusiastic research environment which makes me be extremely grateful. Thank you all for your advice, helpfulness, and emotional support through all this work.

The National Institute of Health is acknowledged for providing funding for this experimental research work through grant DC-005788 (Mongeau, PI).

Some special words of gratitude go to my dear friend Rolando Rojas, who has been a major source of caring, support, and encouragement during my studies. I thank him for being always for me and for being available to help me even at the distance. Words can't describe how grateful I am to have you in my life.

I would also like to acknowledge my friend Ali Mehdi. I thank him for being part of my journey and adventures at McGill. I am gratefully indebted to his emotional support, and his valuable comments in this thesis. Thank you for making this experience more enriching.

My special gratitude to my family, my parents Felipe Reyes and Nay Valenzuela, for their love, care, encouragement, for their constant support during my studies, and for all the sacrifices they have done for me. I also thank my brother Felipe R.V, and my sister Beatriz R.V for their love, encouragement, and friendship. I dedicate this thesis to my family, without whom this work would not have been possible.

Contributions of authors

This thesis has been entirely written by the candidate, in collaboration with her supervisor, Dr. Luc Mongeau, and co-supervisor, Dr. Satya Prakash. The résumé was translated by my dear friends and colleagues Marion Lacroix and Rayane Ait Oubahou. The data was collected and analyzed by the candidate. The stiffness of hydrogels using the AFM and torsional rheometer was done with the help of my colleague Guangyu Bao, who performed the experiments. The lymph nodes of fresh dead mice were isolated for my colleague Qiman Gao.

List of tables

List of figures

Nomenclature

Symbols

abs_b	absorbance of the media without cells
abs_c	absorbance of the media with cells in control conditions
abs_s	absorbance of the sample
D_0	initial diameter of microspheres
D	final diameter of microspheres
G´(ω)	storage modulus
G´´(ω)	loss modulus
nc	number of cells
t	time
τ	mechanical response of viscoelastic material
γ	sinusoidal stress
Y_0	stress amplitude
ω	the oscillation frequency

Abbreviations

Al	alginate
Al-Cs	alginate-chitosan
AFM	atomic force microscopy
APA	alginate-poly-l-lysine-alginate
bFGF	basic fibroblast growth factor
Cs	chitosan

CLSM	confocal laser scanning microscopy
DLP	deep lamina propria
DMEM	dulbecco's modified eagle medium
DMSO	dimethyl sulfoxide
DNC	distance between the nozzle and collector
ECM	extracellular matrix
ELISA	enzyme-linked immunosorbent assay
FAK	focal adhesion kinase
FBS	fetal bovine serum
GAGs	glycosaminoglycans
HA	hyaluronic acid
HAS	hyaluronic acid synthase
HEPES	4-(2-hydroxyethyl)-1-piperazineethanesulfonic acid
HGF	including Hepatocyte Growth Factor
hVFF	human vocal fold fibroblasts
IL-β1	interleukin 1 Beta
IL-4	interleukin 4
ILP	intermediate lamina propria
LP	lamina propria
LPS	liposaccharides
MOPS	3-N-morpholino propanesulfonic acid
MPs	metalloproteinases
MPS	mononuclear phagocyte system
Ms	Microspheres
MTT	3-(4,5-Dimethylthiazol-2-Yl)-2,5-Diphenyltetrazolium Bromide
NaOH	sodium hydroxide
PBS	phosphate buffered saline
PLL	poly-l-lysine

PS	physiological saline
RPMI-1640	Roswell Park Memorial Institute medium
SID	syringe internal diameter
SLP	superficial lamina propria
TA	thyroarytenoid muscle
TIMPs	tissue inhibitors metalloproteinases
VF	vocal folds
VF-LP	vocal fold lamina propria

CHAPTER 1

Introduction

1.1 Motivation

Voice disorders can be defined as the absence of normal voice production, which interferes with speech communication [1]. A total of 29% of the adult population has experienced a voice disorder at least once over its lifespan. These disorders have a functional impact with economic repercussions. It is estimated that these problems cost in the United Sates a total of $2.5 billion annually [2], including medical interventions, absenteeism and lost productivity [1]. Although most voice disorders are short-term, others display chronic conditions (3-9%), which are linked to gender and profession [1, 3]. For instance, women have a higher prevalence of voice disorders than men. It is hypothesized that the laryngeal anatomy differences between both genders make women more vulnerable [1]. Teachers, singers, and salespersons are prone to develop voice disorders [3].

Voice problems are often caused by damage to the VFs. Previous studies have reported that the vibrational amplitude and vibrational frequency of the VF cause repeated VF impact or collision over the time. Excessive vibration dosage may contribute to VF injury [1].

The vocal folds include a functional mucosa, which has the ability of vibrate at frequencies up to 3 kHz [4]. The vocal folds are located on opposite sides of the larynx, laterally. They are separated by the glottis, which is the orifice created by the gap between the VFs during vibrations. Fig. 1.1 A) shows the anatomy of the human larynx including the VFs. Phonation is produced when the air is expelled by the lungs through the airway, driving the oscillation of the VF [5]. Fig. 1. B) and C) show one cycle of oscillation [6].

The ability of the VF to oscillate is supported by its histological characteristics, including a well-defined layered structure, which is shown in Fig. 1.2. The VF layers include the epithelium, the lamina propria, and the thyroarytenoid muscle (TA). The epithelium protects the VFs from contaminants in the external environment. It provides protection, structure, and stability to the VF. The Lamina Propria (LP) is divided into three layers referred to as the superficial, intermediate and deep layers. The Superficial Lamina Propria (SLP) is a pliable and amorphous structure, which allows the mucosa to vibrate, and therefore to sustain phonation. The Intermediate Lamina Propria (ILP) is formed by elastin fibers, while the Deep Lamina Propria (DLP) is composed mostly of collagen fibers. Both the ILP and the DLP form the ligament, which limits the movement of the VF and allows the vibration of the SLP. The TA is the contractile muscle that provides support to the VF. It is the stiffest and least pliable of all the structures [4].

Most voice disorders, short-lived and chronic, affect the Lamina Propria (LP), specifically the SLP. Scarring is a state in which the mucosa of the VF becomes stiff. During phonation, the vibration of the VF is compromised causing asymmetric amplitude, voice changes, and even aphonic conditions [4]. This state is characterized by disorganized collagen deposition, which forms thick bundles and alters the biological properties of the VF-LP [4, 7]. Some of the biological changes include a decrease in elastic fibers and hyaluronic acid (HA) [4]. Scarring currently does not have any effective treatment [4].

Biomaterials injections are commonly used to restore the functionality of the vocal fold lamina propria (VF-LP). Ideally, these biomaterials attract an influx of cells and growth factors to eventually form new permanent tissues. None of the materials used so far have been very successful in cell recruitment [4]. One reason is that the bulky size of the scaffolds induces their faster

degradation [8]. The drawbacks and limitations of the scaffolds is discussed in more detail in section 2.4.1.

Few studies have used cell therapy to target the regeneration of the VF-LP. The implanted cells proliferate, migrate and produce several ECM proteins and growth factors which have the potential to regenerate the tissue [8, 9]. But the cells are foreign bodies, and they are frequently destroyed by the host immune response before they achieve any regeneration [9].

Microspheres (i.e. artificial cells) are structures which protect the cells from the host immunological response. Therefore, they improve the cell retention at the site of the injury, increasing the regeneration efficiency. These structures have been used in regenerative medicine targeting organs like liver, heart, knee, and eyes [9-13]. The principles and properties of Ms (i.e. artificial cells) is discussed in more detail in the section 1.4. The motivation of this study was to apply the principles of artificial cells to induce the regeneration of the VF-LP through the fabrication of Ms made of selected materials. This approach therefore combines injectable biomaterials (Ms) and cell therapy.

1. 2 Literature review and background

1.2.1 Scar formation in wound healing and in response to biomaterials

Diverse growth factors, cytokines, biologically active proteins, and peptides modulate cell functions to induce wound healing [14]. The immediate response of the body after injury includes clot formation and the invasion of inflammatory cells into the wound area. This process sterilizes the injury site, removing damaged cells. The inflammatory and anti-inflammatory responses can help or inhibit the regeneration process. The effect of these cells on the process depends on the wound microenvironment [15, 17]. The control of the microenvironment can redirect healing

strategies to achieve effective and efficient regeneration, as for example in other species such as the salamander [14]. The microenvironment regulates cell survival, growth function, differentiation, and cellular interactions with ECM [14].

Biomaterials, host and donor cells, and the local matrix are key parameters for tissue regeneration [15, 16]. The 2nd phase of the healing process is characterized by the migration and the proliferation of fibroblasts and other cells to produce new extracellular matrix structural components such as collagen and fibronectin [15, 16]. At the same time, cells grow and cover the injury site. Wound contraction, which is a part of the 2nd phase, helps to decrease the wound area [16]. The proliferative phase is also regulated by the metalloproteinases (MPs) and the tissue inhibitors metalloproteinases (TIMPs). These factors determine the rate of the creation, maintenance, and degradation of the extracellular matrix components (ECM). The 3rd and final stage of the regenerative process is the maturation and remodeling phase, when collagen is realigned along tension lines and unnecessary cells are removed by apoptosis signals [16]. However, the wound healing cascade previously described can induce scar formation, in particular for large tissue defects. Fig. 1.3 shows the immediate response of the body after injury in ideal conditions to achieve tissue regeneration (Fig. 1.3 c). The response of the body in aberrant conditions is illustrated in Fig. 1.3 d). In this case excessive recruitment of inflammatory cells impairs tissue remodelling, causing scar formation [17]. Other parameters promoting scar formation include an increment in tissue tension and fibrous deposition. To avoid increased tension, the biomaterials should not be stiffer than the native tissue. The cells can sense the stiffness of the environment and produce factors which signal scar formation [16]. Some of these factors are the Focal Adhesion Kinase (FAK), the P13K growth factor and excess of Calcium [18].

When scaffolds are implanted, the immune cells join native cells to lead the generation of a fibrous capsule around the biomaterial. The process starts with Chemokines and Cytokines. Both lead to neutrophils recruitment, followed by macrophages and monocytes which degrade and digest the material. This process competes with the scaffold designed to regenerate the tissue. Several studies have shown that the addition of cells to the biomaterials enhances tissue regeneration and decreases scar formation, since the cells start the regeneration process after they are implanted while keeping their growth factors upregulated [15, 16]. The regeneration time is also related to scar formation. It is believed that reducing the time over which new tissue is regenerated prevents scar formation [9]. A combination of cells and biomaterials promises to be more efficient. In the case of VF-LP, the duration of remodeling process is not clear. Most authors consider that is between 1 to 3 months [19] while scar formation is expected to appear over a period of 2 to 8 weeks [7,20]. Therefore, it is important to develop a system that can restore the VF-LP over a relatively short time.

1.2.2 Cellular and glycoproteins components of the vocal fold lamina propria

The Superficial Lamina Propria (SLP) is the site of most VF problems, such as scarring and atrophy [4]. Therefore, it is the preferred most study site for targeting wound healing [4]. The properties of the SLP are regulated by interstitial proteins, including proteoglycans and glycosaminoglycans (GAGs). One of the most important GAGs is hyaluronic acid (HA), which determinates the viscoelasticity of the SLP. Other important GAGs are fibronectin, decorin, fibromodulin, and biglycan. However, their functions have not completely been elucidated [4].

The fibroblasts within the LP produce the Extra Cellular Matrix proteins (ECM). Two types of fibroblasts may be found in the LP. Fibroblast cells are in the SLP. Fibroblasts in the macula flava are also called VF stellate cells. The macula flava is located at the anterior and posterior ends of the ILP. Fibroblasts in the SLP are sparse, with low protein production because of the absence

of intracellular organelles such as Golgi apparatus and endoplasmic reticulum. Conversely, vocal fold stellate cells are abundant in the macula flava and are associated with high production of ECM proteins. Few studies have been used this kind of cells [4].

1.2.3 Stiffness of the vocal folds

In the voice production, the VF experience complex mechanical deformation and stresses related to tensile, contractile, aerodynamic, impact and shear forces. When the glottis closes, the shear stress associated with impact between folds are in the range between of 0.1-5 kPa [6].

The vocal cord structure, Fig. 1.1, its biomechanical, and its geometry characteristics play an active role in the voice production. For instance, the stiffness of the VF determinates the speed of surface waves propagating over the surface of the SLP [21].

The VF regulate the airflow during breathing and protects the airway from external particles. The VF oscillate at high frequency with a small amplitude during phonation [21]. The voice pitch depends on many factors, including the amplitude of VF vibrations, the traveling wave speed and the elastic modulus of the tissue [21].

Several techniques have been used to determinate the stiffness (Young's modulus) and elastic properties of the human VFs. However, the results vary according to the instrumentation, protocols and the conditions of the VF. The indentation test is a well know and accurate methodology. This technique was used with spherical probe in conjunction with atomic force microscopy (AFM) due to its sensitivity in load and displacement. The reported values of Young's modulus of human tissues were in the range between 5.3 kPa and 13.1 kPa for in situ measurements. Values in the range between 3.9 kPa-5.7 kPa were reported for in vitro measurements [21]. Traction

testing has also been used, reporting values between 60-145 kPa for the cover of the tissue, and 20-40 kPa for the body tissue [21].

These values provide estimates of the mechanical properties of the healthy VFs. Given the relationship between biomaterials and scar formation (section 1.2.1) the stiffness of Ms used in the present study should fall within these ranges. It also contributes to efficient tissue regeneration, without compromising neither its rheological characteristics nor its produced pitch [4].

1.3 Regeneration strategies for the vocal fold

1.3. 1 Scaffolding

Scaffold materials have been used to target the VF regeneration [4, 7, 9, 19, 20]. Scaffolds need to be biocompatible and biodegradable. One important requirement is to recruit an influx of cells and growth factors from the surrounding tissues, as illustrated in Fig. 1.4. The fast degradation of the material can hamper its ability to regenerate tissue as described in the section 1.2.1. Mechanical stiffness should be tuned to match the viscoelastic properties of the tissues. The material should be injectable with a needle and withstand the mechanical stress caused by phonation. In other words, the material needs to be strong enough to support mechanical fatigue, but it should not be too stiff, which promote scarring [4, 7, 19, 20, 22-34].

The scaffold degradation is sped up by the host immune response, mechanical fatigue, and enzymatic reactions. All these factors impede the regeneration process [4, 22].

A variety of scaffold materials have been used for VF regeneration, including gelatine, hyaluronic acid, collagen, Cs, and composites which combine varied materials. Until now, no material has been found optimal or efficient [4]. Some materials promote cell migration, and proliferation but their enzymatic degradation is too fast, starting a few minutes after implantation.

A minimum residence time is needed to achieve a significant regeneration [24-31]. Other materials, as gelatin and collagen, are strong enough to support collision but their viscoelastic properties compromise the tissue, causing scarring problems [4, 22-32]. *Bioscaffolds* are derived from decellularized ECM from animals, including bovine and porcine [4, 30, 32]. These materials are promising for their regenerative properties, but they can have problems related to the biocompatibility of the xenografts and reproducibility. Some characteristics of these materials, such as their vibratory response have not yet been studied [4, 30, 32].

1.3. 2 Cell therapy

Cell therapy is considered one of the most effective strategies for tissue regeneration [9, 33-36]. Previous studies have shown that implanted cells do proliferate, migrate, and produce the ECM proteins needed for remodeling [4, 23, 28, 29, 32]. Stem cells have often been used for VF cell therapy, as they can differentiate in multiple cell types and proliferate at higher rates. Mesenchymal stem cells (MSC) and adipose stem cells (ASC) produce growth factors (GF) associated with VF remodeling, including Hepatocyte GF (HGF), and feature high levels of hyaluronic acid synthase (HAS), all desirable attributes [23, 28, 29, 32]. But MSC or ASC therapy alone may negatively alter the viscoelastic properties of the host tissue [4]. Alternately, hVFF can be used. They also produce HGF, which stimulate anti-fibrotic activity and the production of hyaluronic acid (HA), while reducing the production of collagen. They also produce basic Fibroblast GF (bFGF), which induces cell proliferation and migration, and HA. Several animal studies have shown improvements of the VF after the injection of hVFF [23, 28, 29, 32]. In some cases, the VFs remain damaged after treatment [4]. Overall, cell therapy has so far yielded better results than scaffold-based treatments [4]. The main challenge of cell therapy is the immunological rejection of the host to donor cells. The CDT-8 and CDT-4 cells recognize the

donor cells as foreign bodies, and they kill them directly or by producing strong local inflammation [16].

1.3.3 Growth factors therapy

Another interesting strategy to regenerate the host VFs is through the injection of growth factors, specifically, bFGF and HGF. Both growth factors, as it was stated above, have regenerative effects. Usually, one type of growth factor is injected into the solution. There is insufficient information to elucidate which growth factor is the best to target VF regeneration. Although growth factors can help to tissue regeneration, periodic re-injection is often needed to improve the damaged tissue [4]. Another alternative to the re-injection can be the use of drug delivery systems as Ms (i.e. artificial cells) which promise to deliver the growth factors in a controllable way, preventing burst release and therefore scar formation [9].

1.4 Microspheres for regenerative medicine

The idea of Ms emerged in 1964 when Thomas Chang encapsulated erythrocytes in isotonic solution of hemolysate containing 10% of hemoglobin. This solution was added dropwise to the crosslinker solution containing diacid, sebacoyl chloride, and silicon liquid [9, 37]. This principle was based on the cell structure, in which the membrane is permeable to certain substances, as oxygen and carbon dioxide, but impermeable to other molecules. At the same time, this structure decreases the immunological reactions in the body [37]. This application started the concept of Ms (i.e artificial cells) which some years later was defined by Thomas Chang, as follows: *"Artificial cell is not a specific physical entity. It is an idea involving the preparation of artificial structures of cellular dimensions for possible replacement or supplement of deficient cell functions"* [37].

Since then several materials have been used for the fabrication of Ms, including biological materials such as proteins and polysaccharides, and synthetic polymers which vary according to

the application [37]. The content of artificial cells is also variable and has evolved over the time. It includes enzymes, microorganisms, pharmaceutical agents, several types of cells including stem cells, genetically engineered cells, and ordinary cells such as fibroblasts, hepatocytes, islets, and others [9]. Alginate is a frequently used material as the main component of the capsules for cell therapy [9]. Multiple studies done by Thomas Chang point out the universal characteristics of artificial cells in the field of regenerative medicine [9]. It is expected that Ms protects the cells from destruction and from severe immunological responses [34]. A greater cell retention is expected when cells are injected inside Ms than when cells are injected into single aggregations without any protection. The efficiency of treatment of cell therapy using Ms is expected to be better than another methodology [9, 12, 33]. This fact has been proved in different applications including the treatment of myocardial infarction [12]. Microspheres should be permeable to nutrients to keep the cells alive and function properly. They should be permeable to the specific growth factors that are fabricated by cells to regenerate the tissue. The typical structure of Ms for regenerative medicine is illustrated in Fig. 1.5.

A spherical shape is preferred to ensure good mechanical properties, including stability at 37°C. The membrane of the Ms is flexible to allow deformation within narrow spaces. It can recover its original spherical shape after passage through a constriction, which is the reason why artificial cells are good structures for injection [33]. Additionally, Ms can support shear stress and collision. The membrane tension has been reported to be 2520 ±20 dynes/cm independently of their diameter [33].

Other studies have found that tuning the geometry and volume distribution of the biomaterials can decrease or increase the immune body reactions, as well as their biocompatibility and functionality. For instance, when scaffolds of 4 mm of diameter were injected subcutaneously in non-human

primates for either 14- and 28-days retrieval time points, the scaffolds were embedded in host tissues and fibrosis. Conversely, when Ms with diameters among 0.5-1.5 mm were injected and retrieved at the same time points, they were devoid of cellular overgrowth and fibrosis [8].

1.5 Rationale

Effective Lamina Propria regeneration using scaffolds requires the recruitment of cells and growth factors from the surrounding native tissue after 5-15 days of being implanted [4] Generally, the mononuclear phagocyte system (MPS) clears the scaffolds after injection rapidly, hampering the regeneration function of scaffolds [8, 38] The MPS response can be modulated with the biomaterial size and surface properties [8, 38]. It has been previously demonstrated that Ms with standard dimeter, around 500 µm to 1 mm, reduce MPS and other foreign body responses. Consequently, the Ms can be in the body for longer time than scaffolds without being covered by fibrosis or cellular overgrowth [8].

In comparison with scaffolds, Ms are better biomaterials for cell delivery, since using the bulky size of scaffolds hampers the successful incorporation of cells because their diffusion properties are compromised. Therefore, the cells are more prone to die for lack of oxygen and other nutrients [8, 39]. The main challenge of scaffolds is to sustain vascularization. Conversely, the morphology of Ms is associated with better diffusion properties which allow the supply of oxygen and nutrients to the encapsulated cells in a more efficient way than in scaffolds [7-38].

As it was mentioned in section 1.4, the membrane of the Ms is flexible to allow deformation in narrow spaces, and after passing through the narrow space, it can recover its original spherical shape [9, 14, 37], that is the reason why artificial cells are good structures to be injectable. At the

same time, the Ms can support shear stress and collision, which are required properties for the VF regeneration [4, 37].

Microspheres are being used as a treatment for organ failures, degenerative, chronic diseases as diabetes, injuries, and to induce liver, heart, bone, cartilage and spinal cord regeneration. However, the emphasis of these studies is based on the cell line, and not on the mechanical properties of the Ms [9, 10, 40-42]. In the present study a proper characterization of the Ms was done to determine their feasibility as optimal substrates for the regeneration of VF-LP. In addition, to the best of our knowledge, this is the first time that Ms acting as cell carriers are studied for the regeneration of the VF-LP.

1.6 Hypothesis

Microspheres loaded with human vocal fold fibroblasts (hVFF) may be a feasible method to promote the permanent regeneration of the Superficial Lamina Propria. It may restore the tissue faster and more efficiently than traditional strategies as scaffolding and cell therapy alone. Consequently, it can be possible to avoid biomaterials re-injection, reducing the cost of the treatment.

1.7. Objective

The objective of this project is to asses the potential of the Ms based on natural polymers containing hVFF to regenerate and restore the vocal fold superficial lamina propria (VF-SLP) and their functionality in scarring conditions. Fig. 1.6 illustrates the desirable behavior of the Ms.

To achieve the main objective, three different configurations of Ms were fabricated including alginate (Al), Alginate-Poly-L-Lysine (APA) and Alginate-chitosan (Al-Cs) using electrospraying and Layer-by-Layer. The aim of the present study was to characterize the Ms and

considering their biocompatibility, physiological degradation, and mechanical properties to determine the type of microsphere which is more adequate to use for VF-LP regeneration.

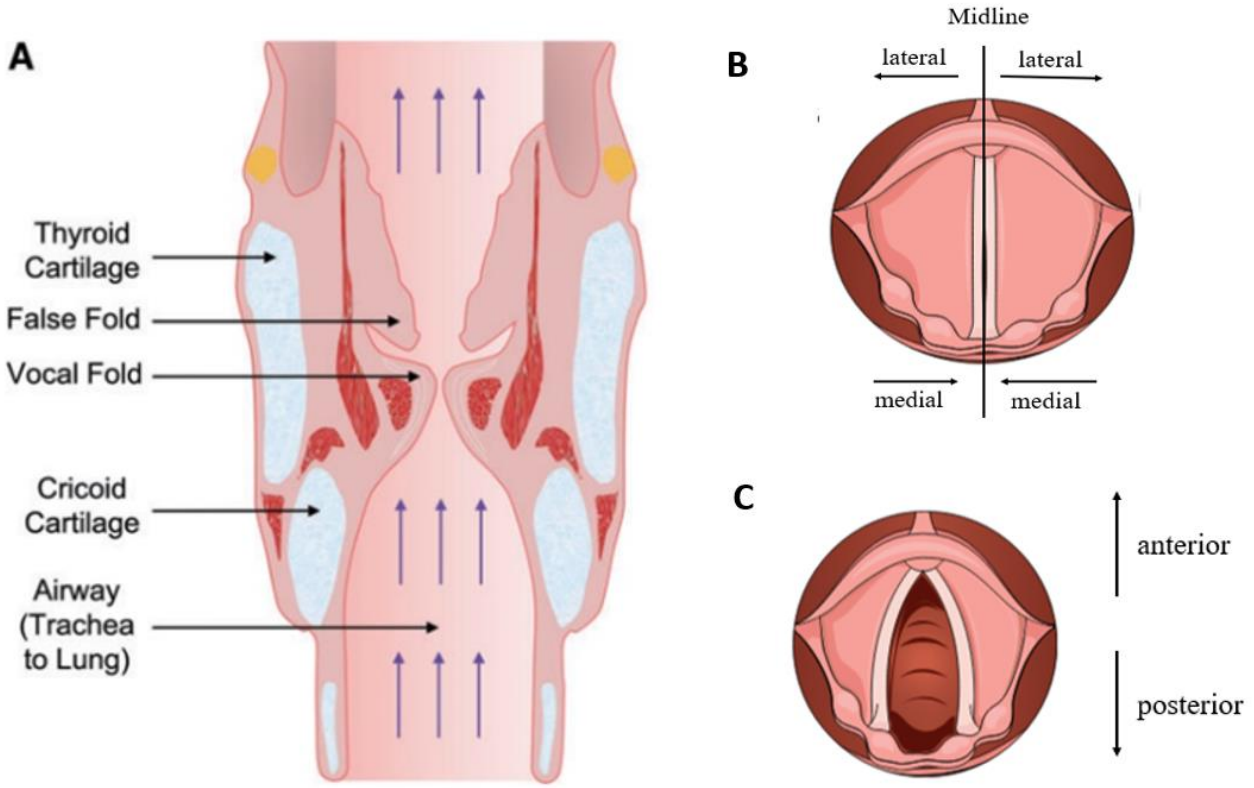

Fig. 1.1 Anatomy of the Larynx. A) The vocal folds are on opposite sides of the larynx. The structures are separated by the glottis. Phonation is produced by flow in by the lungs, and the flow-induce oscillations of the VF. B) and C) Closing and opening of the glottis during phonation. Image modified from [6].

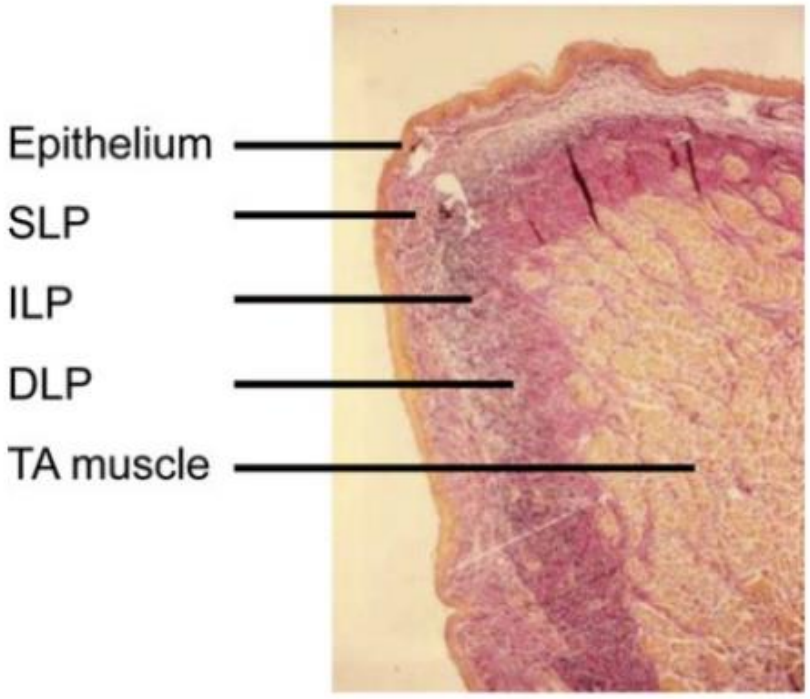

Fig. 1.2 Layered structure of the VF. Three layers form the VF: The epithelium, lamina propria, and thyroarytenoide muscle. The lamina propria is divided in three layers: superficial, intermediate and deep layer. Image reproduced with Springer permission of [4].

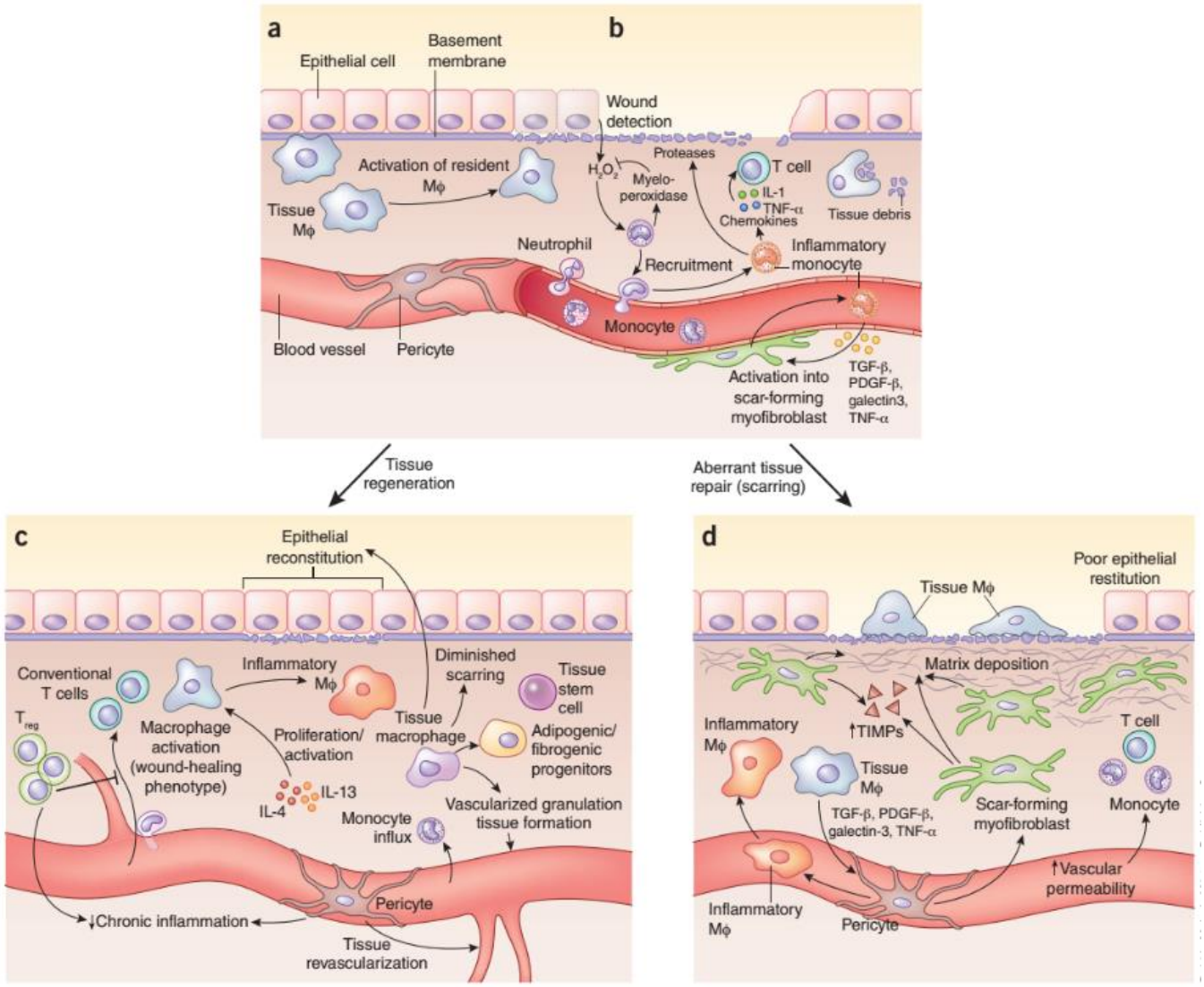

Fig. 1. 3 General models of wound healing and scar formation. a) Healthy tissue microenvironment. Intact basement membrane. b) Damaged tissue and rupture of the basement membrane. The influx of neutrophils and monocytes. c) Wound healing microenvironment. The basement membrane is restored efficiently by the balance of inflammatory cells regulated by T_{reg}, epithelial proliferation and macrophages with wound-healing phenotype. d) Aberrant microenvironment promotes scar formation because of the continuous activation of inflammatory cells impaired with epithelial proliferation. Image reproduced with the permission of Springer Nature from [17].

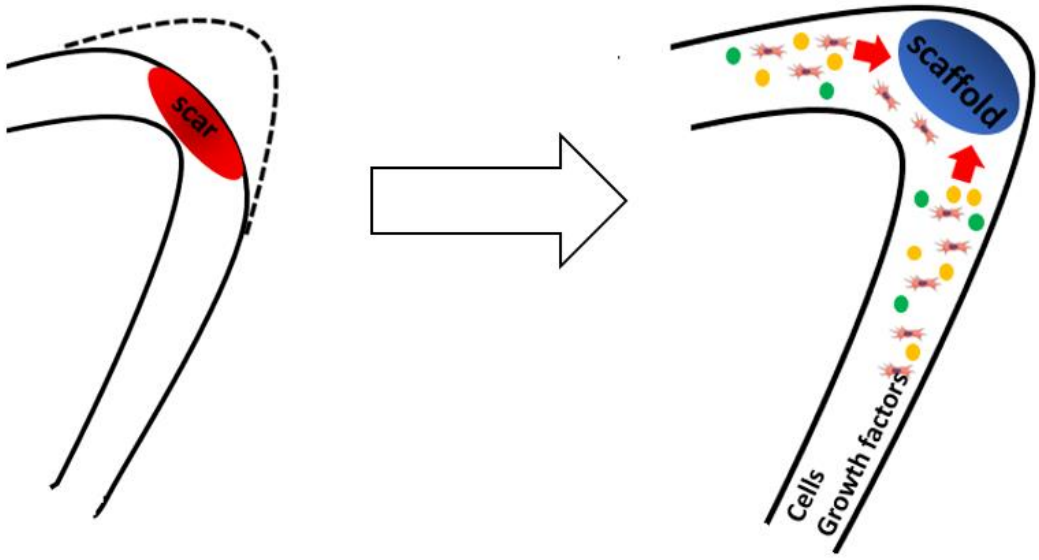

Fig. 1.4 Scaffold concept. The scaffold should attract cells and growth factors of surrounding tissues to form a new and healthy tissue. Image modified from [4].

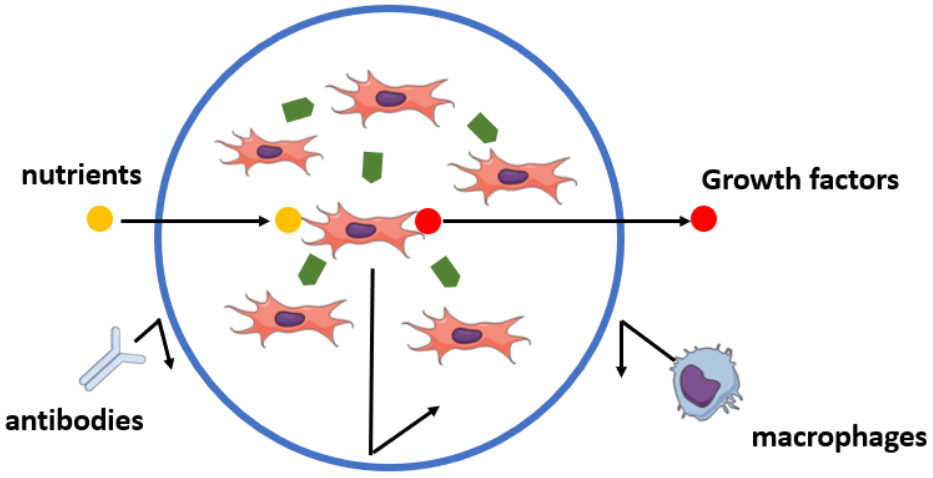

Fig. 1.5 Microspheres representation. Viable and metabolic active cells inside of the microsphere. The structure protects cells from being destroyed or degraded from immunological reactions, while it is permeable to growth factors to regenerate the tissue. Image modified from [9].

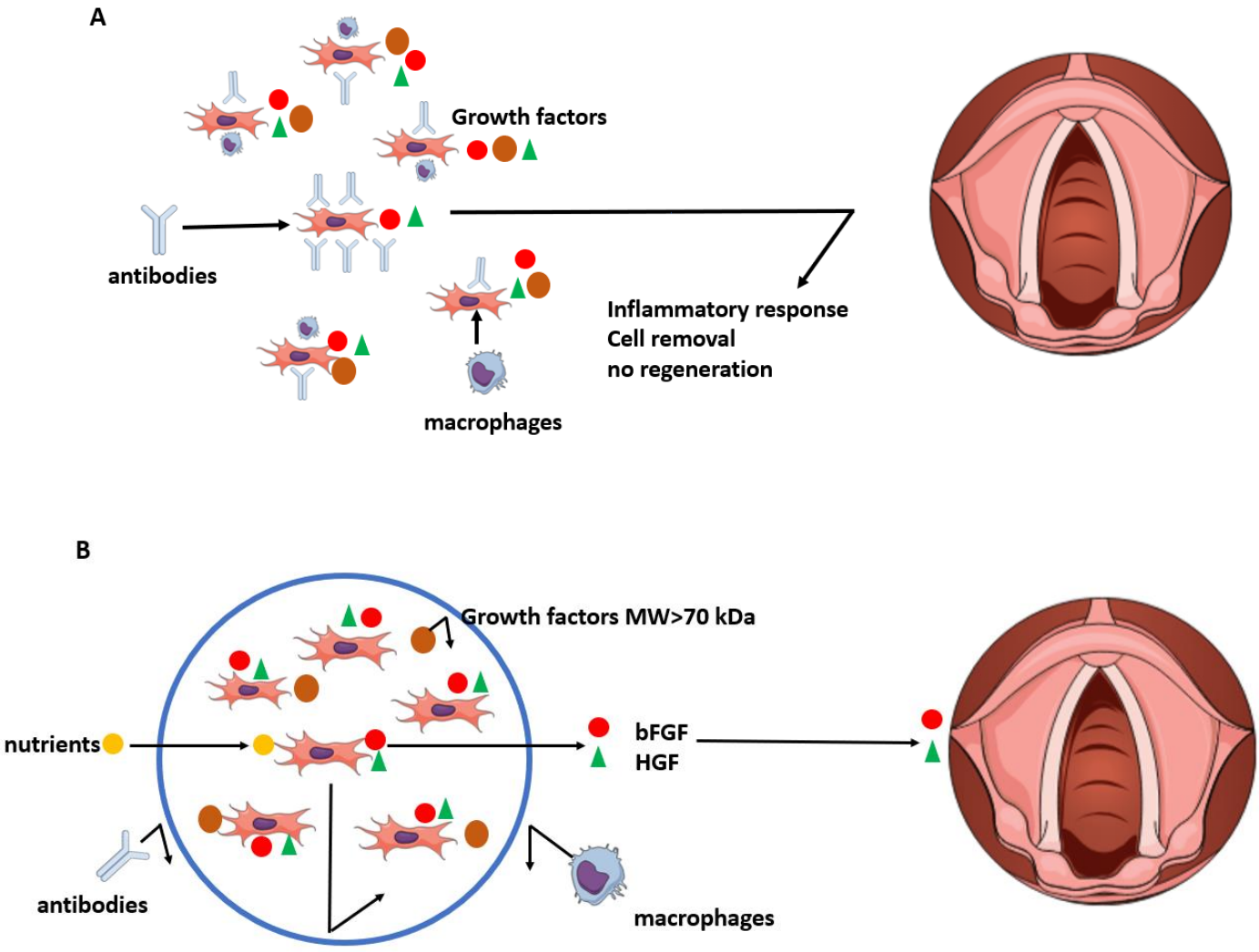

Fig.1.6. Schematic representation of the regenerative system. A) Free cells (hVFF) injection. The immunological response and macrophages remove the cells before the regeneration. B) Ms containing cells (hVFF) The system protects the fibroblasts from the immune system, while they produce basic fibroblast growth factor (bFGF) and hepatocyte growth factor (HGF) which can go outside of the system to regenerate the superficial lamina propria.

CHAPTER 2

Microspheres design

2.1 Design objectives

To regenerate and restore effectively the VF-LP, the Ms should have good mechanical strength to resist stress caused by phonation [4, 6]. The degradation rate of the Ms should be at least two weeks in the VF-LP before scar is formed [7, 20]. They should be permeable to therapeutic subcellular products such as the bFGF and HGF, with a molecular weight of 18 kDa and 34 kDa respectively. These growth factors are produced by the VFF and they target the regeneration of the tissue [43]. The release of the growth factors should be controlled to avoid scarring problems [16]. It has been reported that Ms with smaller pore sizes are less permeable, resulting in higher encapsulation efficiency and slower release rates than Ms with large pore sizes [44]. Moreover, the Ms should provide a temporary microenvironment to support the viability of the VFF [9]. The stiffness of the Ms should match the native VF-LP. Previously reported with values between 3.9 kPa and 13.1 kPa [21].

2.2 Injectable biomaterials for cell encapsulation

2.2.1 Alginate

Alginate is a natural and hydrophilic polysaccharide, one of the most abundant in nature. It is derived from brown seaweed [45, 46, 51]. Alginate is the most used material for cell encapsulation due to its biocompatibility, biodegradability, and non-antigenicity [45, 46]. Biomaterials made primarily of Al have a longer circulation time in the host, due to the hydrophilic properties and electronegative surface of the Al [48]. It is speculated that these properties delay the macrophage

response [47]. Alginate is classified as a mucoadhesive polymer, which can create hydrogen bonds with mucin-type glycoproteins.

Alginate's chemical structure, illustrated in Fig 2.1, is characterized by two different blocks: (1-4)-linked β-D-mannuronic acid (M) and α-L-guluronic acid(G). The polymer is composed of segments of mannuronic acid, followed by segments of guluronic acid, and alternating mannuronic and guluronic acid segments [38]. The amount and distribution of each monomer depend on the age of the seaweed from which the Al is isolated. Alginate with higher guluronic acid is stronger and more ductile than with mannuronic acid, but it has a higher porosity [49, 50]. Alginate with higher mannuronic acid content decreases the number of reactive positions available for hydrolysis. Therefore, the material is less prone to degradation and to variations in molecular structure changes [51].

Alginate can form three-dimensional gel structures by ionic crosslinking with divalent cations. The process is called EGG box, since the cations penetrate the guluronic acid segment resembling "eggs" in a box [45, 50]. As illustrated in Fig. 2.2. Usually, Al is crosslinked by Ca^{2+}, but it has affinity also for strontium Sr^{2+} and barium Ba^{2+} [10, 45, 52].

The resulting Al structures (hydrogels or Ms) resemble the basic ECM, including the high-water content needed for the cell physiological processes as the transport of oxygen, nutrients, waste, and soluble factors [53]. In addition, their mechanical properties are similar to the ones of soft tissues in the body as cartilage, fibroblasts, ganglion, peripheral nerve, smooth and striated muscle [45, 54, 55].

2.2.2 Alginate modifications

Alginate beads can provide protection to the allogeneic cells against the immune response [9, 45]. Alginate Ms have some drawbacks. For instance, Al Ms have poor cell adhesion, and high

porosity, which may lead to the burst release of growth factors and other cellular products, or immune response when xenografts are used as cell sources [45, 56-58]. The mechanical strength of Al beads is not well understood. It has been reported that as optimal and weak [45].

The properties of the Al Ms can be modified using cationic polyelectrolytes and proteoglycans to interact with the electronegative surface of Al [45, 51]. The Al Ms are usually coated with polycations that act like a semipermeable membrane allowing the diffusion of subcellular products, oxygen, nutrients and cellular waste, improving their immune protection, mechanical properties, and the diffusion rate of therapeutic agents [9, 45]. Fig. 2.3 A illustrates the potential problems that Al beads can cause in the regeneration of VF-LP. Fig 2.3 B illustrates the selective and semipermeable membrane which interacts with the electronegative surface of the Al.

2.2.3 Poly-L-Lysine

Poly-L-Lysine (PLL) is one of the most frequently used polycations to interact with the Al [9, 45]. The PLL binding is influenced by the ratio of the mannuronic and guluronic content of the Al. It was shown that PLL has more affinity for mannuronic acid blocks [57].

Poly-L-Lysine has been used to reinforce the outer shell of Al Ms, and to control their permeability [9, 45, 57, 59]. For instance, a PLL membrane with 0.05% concentration allows the influx and outlet of molecules up to a molecular weight between 60, 000 and 70, 000 Da, excluding in this way molecules as Focal Adhesion Kinase (FAK), collagen and P13k, which can hamper the regeneration process [4, 9, 60]. Conversely, small molecules, including elastin, hydroxyproline and oxygen can cross the membrane [9].

Microparticles of PLL with Al were successfully used to improve the strength and resistance in acidic environments such as the intestine [57]. Nevertheless, PLL triggers a strong immunological reaction when implanted in the organism. The PLL induces the production of interleukin 1 (IL-1)

by the macrophages [50]. It has poor biocompatibility and poor strength [45, 50]. To improve the biocompatibility of PLL, an external and diluted layer of Al is frequently used, resulting in APA microcapsules [9, 45]. The use of PLL and Al can decrease the deformation capacity of Al beads [61]. Alternative polycations can be used to coat the Al spheres, including Cs [45, 57, 62, 63].

2.2.4 Chitosan

Chitosan is naturally derived from chitin. It is a semi-crystalline polysaccharide composed of (1, 4)-2-acetamido-2-deoxy-b-D-glucan (N-acetyl D-glucosamine) and (1, 4)-2-amino-2-deoxyb-D-glucan (D-glucosamine) units. Fig. 2.4 shows its chemical structure. The number of amino groups is related to their viscoelastic properties, and it is given by their deacetylation degree [64].

The amino groups of Cs can be positively charged in acidic conditions (pH<6) [57, 64]. The positive charge of the Cs is responsible for its analgesic effect. Chitosan is also considered antibacterial [64], and an accelerator of wound healing. It was shown that Cs stimulates the production of the transforming growth factor beta 1 (TGF-*B*1) and the platelet-derived growth factor (PDGF) by the macrophages, leading to the acceleration of ECM production [65].

Chitosan has been reported to be biocompatible and biodegradable. It does not trigger a strong immune response. The degradation rate of Cs is stable in physiological conditions. It has been reported that only 10% of the material is lost after 4 weeks [22].

Chitosan has been used to coat Al Ms for protein and enzyme delivery. It was found that greater protein concentrations can be loaded into these structures that in Al beads. Al-Cs spheres have been found to protect the enzymes in gastrointestinal conditions [58, 63]. The Cs membrane modifies the release properties of Al beads. For instance, for bacteria delivery, the addition of this membrane resulted in ordered release [56].

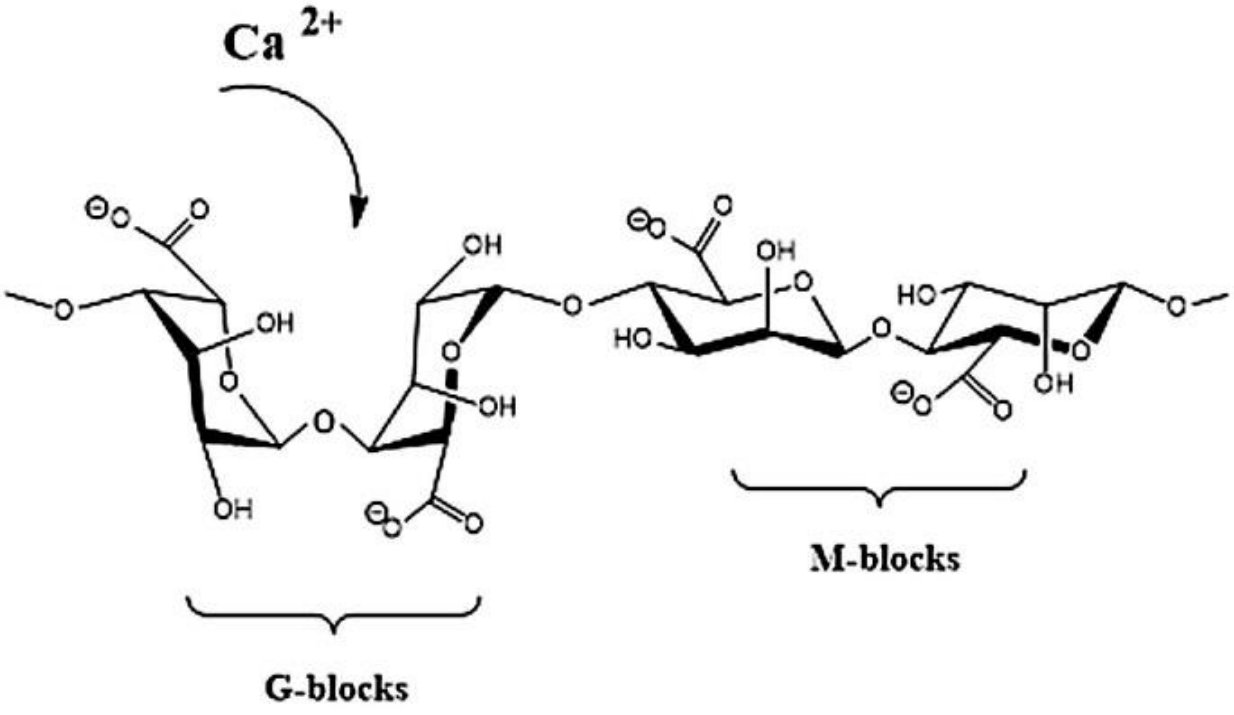

Fig. 2.1 Chemical composition of Al. Al is composed of two blocks (1,4)-linked β-D-mannuronic acid (M) and its C5-epimer α-L-guluronate (G). Image reproduced with the permission of Elsevier from [118].

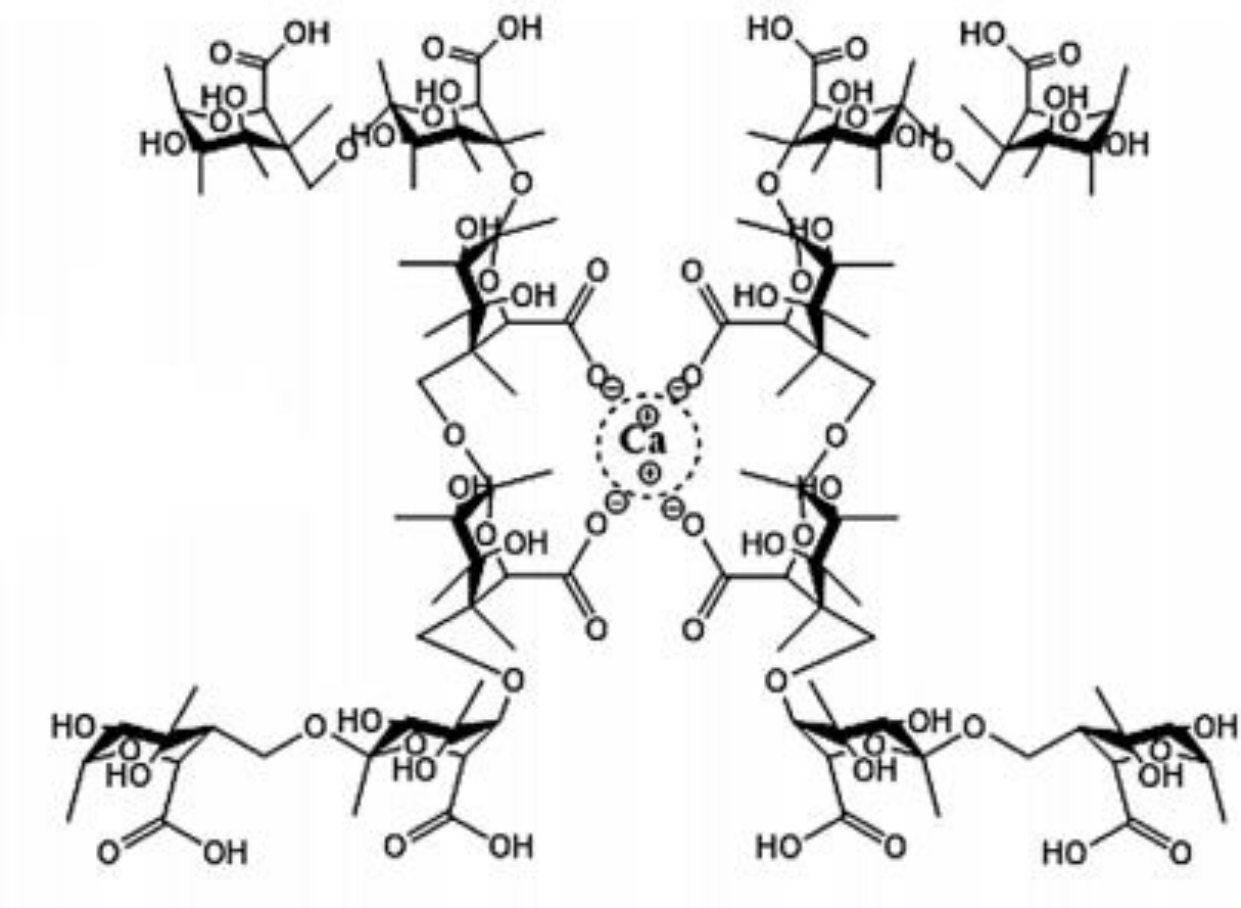

Fig. 2.2 Egg box model. The divalent cations as Ca^{2+} penetrate the guluronic acid segment of the alginate. Image reproduced with the permission of Elsevier from [118].

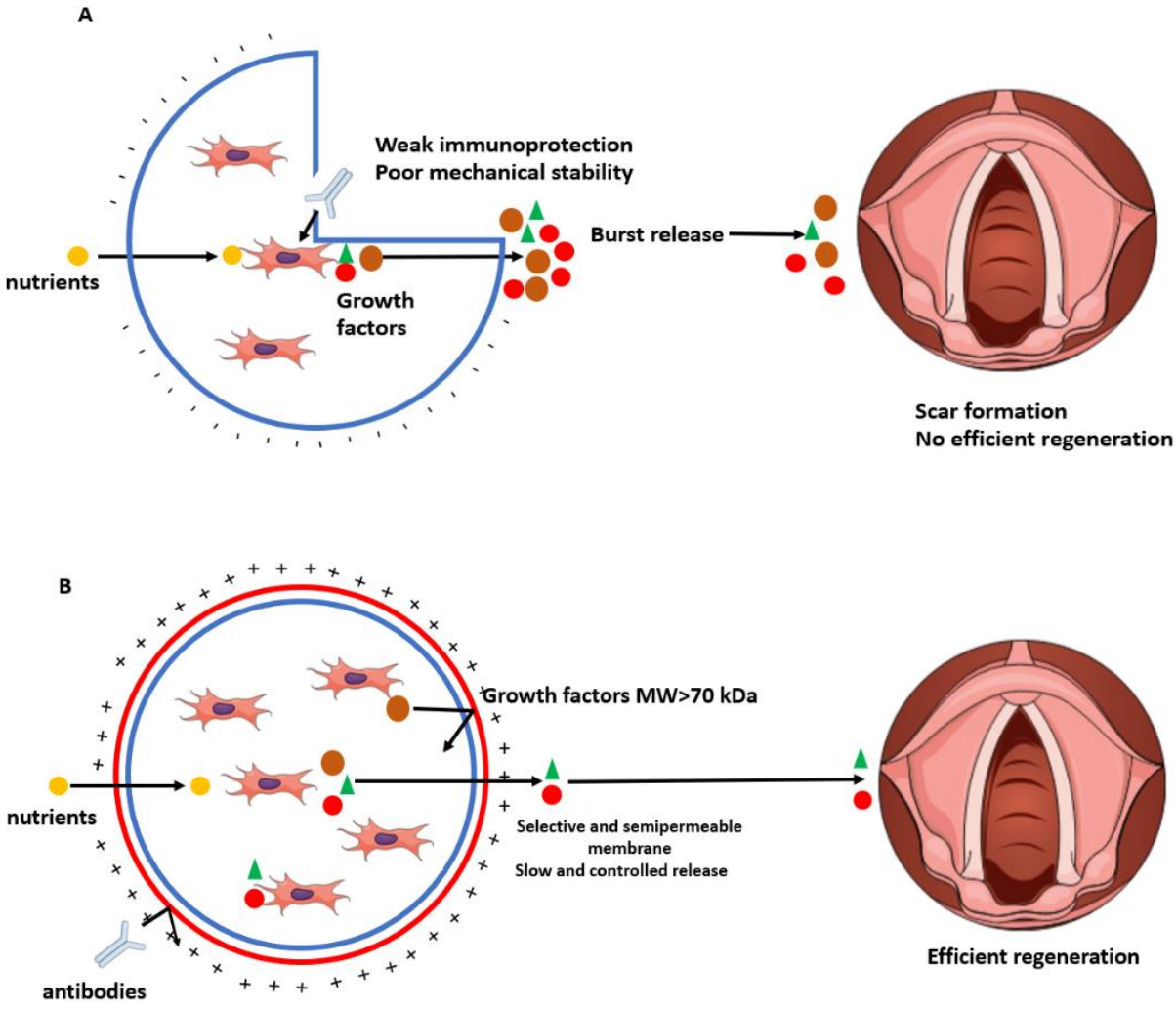

Fig. 2.3 Microspheres for vocal fold regeneration. A) Potential problems of Al Ms. The Al beads can lead to burst release of therapeutic factors and ultimately scar formation. B) The semipermeable membrane is formed by the interaction of polycations with the electronegative surface of the Al. The membrane can improve the mechanical stability, release properties, and immune protection of the beads. Image designed with information [9, 45,51].

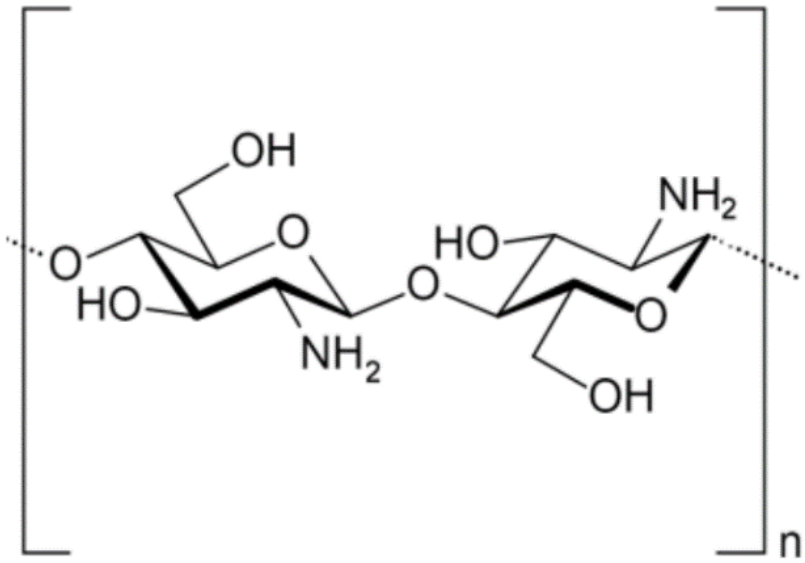

Fig. 2.4 Chitosan chemical composition. The chitosan is characterized by amino groups. Image reproduced from [119]. Open access, permission is not required.

CHAPTER 3

Experimental methods

3.1 Fabrication

3.1.1 Introduction

Different microsphere fabrication processes are used depending on the characteristics of the Ms [44, 52, 66]. Their size, distribution, and morphology [52]. In emulsion, the cells and polymers are dissolved in an aqueous solution, and subsequently dispersed in a non-aqueous medium such as oil. The solution is exposed to chemical crosslinking, and finally Ms are centrifuged and washed [67]. The viability and metabolic activity of the cells may be compromised by toxic organic solvents and acidic pH during the process [68]. The nature of the surfactants used in the emulsion, Ms with a heterogeneous size distribution, hampering clinical translation [52, 69]. A homogeneous size distribution is needed in order to obtain uniform release properties as well as known and well-tuned degradation properties, and strong particles [70].

Electrospraying is one-step-technique which allows Ms formation and cell immobilization under safe and mild conditions without compromising cell viability. The encapsulation process using electrospraying is fast thereby avoiding the need to manipulate cells over a long time period [45, 51]. Electrospraying yields a uniform size distribution and prevents agglomeration [71]. An electric field is applied creating an electrostatic force that deforms the interface of the liquid drop [52, 72, 74]. This Coulomb force competes with the cohesive intrinsic force of the droplet. When the Coulomb force is stronger than the cohesive force, the droplet breaks into microscopic droplets because of the surface tension generated in the droplet [52]. This process is illustrated in Fig. 3.1. Fig. 3.1 a) shows the liquid rinsing in the nozzle, the formation, and the elongation of the droplet. Fig. 3.1 b) illustrates the Taylor cone in which the charged Ms break up into a cone and smaller droplets are ejected in response to the surface tension [52, 75].

Several parameters are involved in the process of electrospraying, including voltage, distance to the collector, nozzle diameter, flow rate, and polymer concentration. These parameters influence microsphere size, morphology, loading capacities, viscosity, and conductivity [52].

The polymer concentration and molecular weight affect the viscosity and surface tension of the solution. The viscosity, strength, and flexibility of the polymer increases when the molecular weight increases [76]. In contrast, the polymer solubility decreases when the molecular weight increases [77]. The jet can be destabilized for low polymer concentration. The size of the particles can be controlled by changing the concentration of the polymer [71]. The voltage controls the strength of the electrical field between the nozzle and the collector. Frequently, high voltages (kV) are needed to form the microdroplets. The electrical force determines the initial shape of the solution in the nozzle, described previously. The cone jet needs to be formed in order to produce stable Ms [78].

Fig. 3.2 summarizes the effects of polymer concentration, voltage, and flow rate on the size of the Ms. The size of the particle can be modulated varying the polymer solution flow rate. The flow rate determines the amount of polymer available at the nozzle during electrospraying. There is a specific value of flow rate for each selected voltage for which Taylor Cone is stable. An unstable jet is formed when the flow rate is disproportionate to the given voltage causing irregular mass transfer at the nozzle end, or when the voltage is too high. In consequence, the polymer is discharged before sufficient charge is accumulated in the droplet [79]. In general, high flow rates generate large Ms in which the volatilization of the solvent is incomplete [80].

The distance between the nozzle and collector influences the electrostatic field strength, particle size, and morphology, due to the evaporation rate of the solvent. When the distance is not sufficiently large, the solvent does not have time to evaporate and solidify to form particles before reaching the collector. Consequently, the Ms are large and unstable [78].

3.1.2 Methods

Sodium Al (MW 216.121 g/mol. 61% mannuronic acid, 39% guluronic acid. low viscosity), MOPS (MW 209.3 g/mol. buffering range: pH 6.5-7.9), and HEPES (MW 238.30g/mol. Titration rate 99.5% with NaOH) D-(-)-Fructose (MW 180.16 g/mol) were purchased from Sigma-Aldrich (Ontario, Canada). $CaCl_2$ (MW 147.02 g/mol) was purchased from ACP Chemicals (Montreal, Canada). NaOH (MW 40 g/mol), and the pH Benchtop meter were purchased from Fisher Scientific (USA). Syringes with internal diameter of 19.13 mm and 26.7 mm were purchased from Cole-Parmer (Canada). The magnetic stirrer was purchased form Ika Werke basic. The encapsulator IER-20, and nozzles of 300 µm of diameter were purchased from Inotech. Corp. A Pyrex dish of 165x65 mm was used as collector.

Solutions of 74 mM of Al (1.6%) in distilled water were used and loaded in the syringe. The flow rate, voltage, frequency, and amplitude of vibration control were $2.5x10^{-7}$ m^3/seg, 1 kV, 1000 Hz and 3A, respectively. The syringe internal diameter used was 0.026 m, gauge 30, and the distance between the collector and the nozzle was 0.20 m, unless otherwise stated.

A solution of 100 mM of $CaCl_2$ was used as a crosslinker for 15 minutes. The solution was kept in a cold bath prior to its use. It was slightly stirred during the fabrication process. The Ms were stored in fresh 100 mM $CaCl_2$ solution at 4°C. Fig. 3.3 shows a schematic representation of the electrospraying method and a picture of the encapsulator used.

A parametric study was conducted in which each variable (buffer, Al concentration, syringe internal diameter, amplitude and frequency of the vibration control, electric field magnitude and the distance between the nozzle and collector) was varied one at the time, while other variables were kept constant. The variables and values were selected based on literature protocols, suggestions of the fabricant, and empirical observations [9, 52, 59]. To measure the effect of the buffer solutions of 74 mM of Al were prepared in distilled water, 10 mM MOPS with 20 mM of

D-(-)-Fructose, and 10 mM HEPES with 20 mM of D- (-)-Fructose. The pH of the latter ones was controlled with NaOH until getting a final pH of 7,4. The frequency and amplitude of the vibration control selected was 1800 Hz, and 3, respectively. The flow rate was $1x10^{-7}$ m^3/seg, and the syringe internal diameter was 0.019 m.

Two different syringe internal diameter were tested: 0.019 m (gauge 20), and 0.026 m (gauge 30). The frequency of the vibration control selected was 1800 Hz, and flow rate of $1x10^{-7}$ m^3/seg.

To monitor the effect of the flow rate, it was varied between $2.16x10^{-7}$ m^3/seg and $2.5x10^{-7}$ m^3/seg.

To investigate the optimal frequency, the frequency was changed between 1000 Hz, 1200 Hz, 1500 Hz and 1800 Hz. Similarly, the amplitude of the vibration control was varied with values of 2, 3 and 4. These three parameters influence each other.

To test the effect of the electrical fields, voltages of 0, 0.65 kV, 1 kV, 2 kV were used.

On the other hand, two distances between the nozzle and collector were used, 0.06 m and 0.20 m.

Finally, the effect of the Al concentration was evaluated. Solutions of a mass fraction of 74 mM, 83 mM, and 92 mM (1.6%, 1.8 %, and 2%) were prepared in distilled water.

The table I, summarizes the parameters evaluated in the present study.

3.2 Morphology and size characterization

Alginate microspheres, an inverted microscope (Olympus, CKX41), microscopy calibration slide (Raja), ThorLab digital camera, ThorCam, and ImageJ software were used to monitor the morphology and size of the microbeads.

The obtained microspheres (section 3.1.3) were visualized with the inverted fluorescence microscopy. Micrographs were analyzed using ImageJ. The scale of the images was determined using a calibration slide to establish the pixel size. The particle diameter was obtained using the function <<Analyze particles>>, and it was confirmed with the scale bar tool.

3.3 Modification layer-by-layer

E- Poly-L-Lysine (4130 g/mol, low molecular weight) was purchased from Zhejiang Silver-elephant Bio-engineering Co (China). Chitosan (degree of deacetylation 80%, low viscosity) was purchased from Wako BioProducts (USA). Sodium alginate (MW 216.121 g/mol, 61% mannuronic acid, 39% guluronic acid. low viscosity), and glacial acetic acid (MW 60.05 g/mol) were bought from Sigma-Aldrich (Ontario, Canada). Sodium Chloride (MW 58.44 g/mol), and the pH Benchtop meter were purchased from Fisher Scientific (USA). $CaCl_2$ (MW 147.02 g/mol) was purchased from ACP Chemicals (Montreal, Canada). The Lab Rotator was purchased from LW Scientific. The strainer cup (stainless steel) was acquired from Amazon (Canada). The cell strainers (400 µm) were purchased from pluriSelect (USA).

A solution 0.121 mM (0.05 %) of PLL was prepared in distilled water. Solutions of a mass fraction of 0.5% and 0.05% of Cs were prepared in distilled water. Acetic acid was used to control the pH of the latter one, and to dissolve completely the Cs. The final pH of the solution was 5,4. Solution of 9.2 mM of Al (0.2%) was prepared in distilled water. All solutions were stirred until they were homogeneous.

Fig. 3. 4 illustrates the fabrication process for a) APA Ms and b) Al-Cs. The obtained Ms (section 3.1.3) were immersed and washed in physiological saline solution (1X) to remove unbounded chemical groups using either a strainer cup or a cell strainer. The Ms were immersed in PLL or Cs solution for 10, and 30 minutes, respectively. The Ms were slightly rotated (150 rpm) during the incubation period. In the case of the Ms modified with the external layer of PLL, a second layer of Al was added. The Ms were immersed in a solution of 9.2 mM of Al for 10 minutes.

The Ms were kept wet during fabrication to prevent breakage and adhesion to the surface.

3.4 Cell encapsulation

Immortalized human vocal fold fibroblasts (hVFF, passage 9) were grown from cells donated from the Department of Surgery of the University of Wisconsin (USA). Dubecco's Modified Eagle's Medium, and Phosphate Buffer Saline were purchased from Wisent Inc. (Montreal, Canada). Sodium alginate (MW 216.12 g/mol. 61% mannuronic acid, 39% guluronic acid. low viscosity) was purchased from Sigma-Aldrich (Ontario, Canada). $CaCl_2$ (MW 147.02 g/mol) was purchased from ACP Chemicals (Montreal, Canada). Syringes with an internal diameter of 0.0267 m (gauge 30) were acquired from Cole-Parmer (Canada). The pH Benchtop meter, and corning polystyrene filters (0.22 µm) were purchased from Fisher Scientific (USA). The magnetic stirrer was obtained from Ika Werke basic. The encapsulator IER-20 and nozzles of 300 µm of diameter were purchased from Inotech Corp. A Pyrex dish of 165x65 mm was used as collector of the Ms.

Human vocal fold fibroblasts were cultured with complete media supplemented with 10% FBS and 1% Penicillin-Streptomycin in a commercial incubator at 37°C under humidified atmosphere with 5% CO_2 and 95% air.

Solutions of 74 mM of Al were prepared in distilled water. Afterwards, the solutions were stirred until getting homogeneous mixtures and sterilized with 0.22 µm polystyrene filter.

Fig. 3.5 summarizes the cell encapsulation process. The Fibroblasts were mixed with a solution of 74 mM Al at three different concentrations $2x10^5$, $6x10^5$, and $10x10^5$ cells/ml. The solutions were loaded into the syringe and fabricated as previously described (section 3.1.3). The modifications of Al Ms were done in the biological safety cabinet as previously described (section 3.3.2). All solutions were sterilized prior to their use.

3.5 Effects on cell viability and proliferation

Immortalized human vocal fold fibroblasts (hVFF, passage 9) were grown from cells donated from the Department of Surgery of the University of Wisconsin (USA). Alginate microspheres, APA Ms, and Al-Cs Ms were fabricated as described in section 3.1.2 and 3.3. MTT (MW 413.32 g/mol) was purchased from Tocris (Canada). Dimethyl Sulfoxide (LC- MC grade), and live/dead cell assay (Calcein AM, Ethidium homodimer-1) were purchased from Thermo Fisher Scientific (Canada). Dubecco's Modified Eagle's Medium (without phenol red), and Phosphate Buffer Saline were purchased from Wisent Inc. (Montreal, Canada). 96 well plates, and the vortex were purchased from Fisher Scientific (Canada). Eight-well chambered coverslip were purchased from Ibidi (Germany). The inverted microscope (Axiovert40), the laser scanning confocal microscope (LSM710), and Zen software were purchased from ZEISS (Germany). The spectrophotometer, Victor 3V, and the Wallac Station software were acquired from PerkinElmer (USA).

3.5.1 Live/Dead assay

Approximately 50, 000 human vocal fold fibroblasts were seeded in each well. The cells were cultured overnight with complete media (10% FBS and 1% Penicillin-Streptomycin). Afterwards, the medium was removed, and the cells were washed with PBS to remove dead cells and cellular debris. The cells were cultured with 200 µl of Al Ms, APA Ms, and Al-Cs Ms into DMEM without color, neither FBS nor Penicillin-Streptomycin. The control was the culture of hVFF without Ms. The cells were incubated during 3 h and 24 h in a commercial incubator at 37°C under humidified atmosphere with 5% CO_2 and 95% air.

A solution of 4 µl of ethidium homodimer-1 (part B) and PBS was prepared in sterile conditions. The solution was mixed using the vortex for a few seconds. Afterwards, 1 µl of calcein (part A) was added to the solution. The dye was used immediately to avoid hydrolysis.

The microsphere solution was removed, and the cells were washed with PBS. The ethidium homodimer-calcein solution was added to the microwells for 45 minutes, followed by the visualization of the cells using the CLSM. The wavelengths of the laser were of 488 nm and 543 nm for the live and dead cells, respectively. The bypass filters were between 493 nm and 551 nm for the live cells, and between 548 nm and 606 nm for dead cells. The laser power was two for both live and dead cells. The images were analyzed using the Zen software.

3.5. 2 MTT proliferation assay

A solution of 12 mM (0.5 mg/ml) of MTT was prepared in DMEM without color, neither FBS nor Penicillin-Streptomycin. The solution was filtered (0.2 µm) and stored covered with aluminum foil at 4°C. For the calibration, different cell concentrations (1000, 3000, 10000, 20000, 50000, and 100000) were seeded on 96 well plates. The cells were cultured overnight with complete media (10% FBS and 1% Penicillin-Streptomycin). Afterwards, the medium was removed, and the cells washed with PBS to remove dead cells and cellular debris. MTT solution was added in each well. The cells were incubated during four hours in a commercial incubator at 37°C under humidified atmosphere with 5% CO_2 and 95% air.

The MTT solution was removed. Dimethyl sulfoxide was added and incubated at room temperature for 15 minutes. Cell viability was monitored by measuring light absorbance wavelength at 570 nm for 0.1 seconds. The commercial spectrophotometer Victor3V and a Wallac Station Software were used. The fraction of viable cells was calculated following the equation *(I)*

$$\%\ \boldsymbol{viable\ cells} = \frac{\boldsymbol{abs_s - abs_b}}{\boldsymbol{abs_c - abs_b}} \times \mathbf{100} \qquad (\boldsymbol{I})$$

where the abs_s corresponds to the absorbance of the sample, abs_b designates the absorbance of the media without cells, and abs_c indicates the absorbance of the cells in control conditions, without Ms.

A calibration line was performed associating the absorbance and the number of cells. Fig. 3.6 shows the experimental design for the MTT proliferation assay. The hVFF were seeded in a 96 well plate at a final concentration of 32,280 cells/well. The cells were cultured overnight as previously described. Afterwards, the media was removed, and the cells were washed with PBS prior to the incubation with the Ms. Solutions of 200 µl of Ms in DMEM without color neither FBS nor Penicillin-Streptomycin were prepared. The microsphere solutions covered the surface of the 96 well plate containing hVFF for 6 h, 24 h, and 48 h. The experiments included one row for black, one row for cells without Ms (control), one row for cells with Al Ms, one row for cells with APA Ms, and one row for cells with Al-Cs Ms (0.5% Cs). All the experiments were done in triplicate. After the incubation time, the Ms solution was removed, and the cells incubated with MTT as previously described.

3.6 Determination of membrane thickness

3.6.1 Introduction

The microsphere membrane regulates the influx and outlet of molecules and the degradation rate of the Ms [59]. The membrane thickness is associated with permeability, mechanical properties, including strength and stability, biocompatibility and diffusion properties [83]. The small size of Ms along with the fragile nature of the membrane make difficult the precise thickness determination [84]. Several techniques have been used to determine the membrane thickness, including scanning electron microscopy, transmission electron microscopy and radiolabeled polymers [85]. These techniques require technical expertise for the preparation of the sample. They are destructive which impedes monitor the membrane thickness over the time [86]. In contrast, the confocal laser scanning microscopy (CLSM) is a non-destructive method [87]. Using confocal laser scanning microscopy is possible to obtain high-resolution images without elaborate sample preparation [50]. Usually, the microcapsule membrane is labeled with fluorescent markers, such as

rhodamine B isothiocyanate, fluorescein amine, and fluorescein isothiocyanate prior to encapsulation [88, 89]. These fluorescent markers block the functional groups of the polymers which compose the Ms and are essential for membrane formation leading to a weak binding. The stability, solubility and effect of these fluorescent markers during the process of encapsulation are unknown [34].

Fig. 3.7 shows the chemical composition of genipin, characterized for a cyclopentane bonded with a heterocycle [91]. Genipin is present in unripe genipap fruits. It is a colorless substance. It can react spontaneously with the amine groups and oxygen in the amino acids and proteins. This reaction creates blue pigments, which are frequently used in the food industry as natural coloring [90, 91]. The genipin site of reaction can be identified and visualized with the formation of green color and CLSM [94]. Genipin is used as fluorescent marker for PLL and Cs membranes, because of its stability over time [59, 62, 92].

3.6.2 Methods

Alginate-Poly-L-Lysine microspheres and Al-Cs Ms were fabricated as described in section 3.1.2 and 3.3. Genipin (MW 226 g/mol) was obtained from Wako BioProducts (USA). Sodium Chloride (MW 58.44 g/mol) was purchased from Fisher Scientific (USA). Strainer cup (stainless steel) was purchased from Amazon (Canada). 8-well chambered coverslip was acquired from Ibidi (Germany). Laser scanning confocal microscopy, LSM710, and Zen software was purchased from Zeiss.

Fig. 3.8 shows the complete process to label the membrane of PLL and Cs of the Ms with genipin. It can be noticed, that the process was done after the microsphere formation. The yellow lines correspond to the place were the thickness measurements where taken per sample. A solution of 110 mM of genipin (0.25% wt./v) was prepared in physiological saline solution (1X). The microcapsules were immersed in genipin solution using the strainer cup. The Ms were incubated

for 21 h at room temperature covered in aluminum foil. Afterwards, the Ms were washed and stored in fresh PS (1X) solution.

The confocal laser scanning microscopy was used to visualize the PLL and Cs membrane of the spheres into ibidi wells. All the settings for the confocal microscope and the imaging of Ms were computer-controlled. The wavelength of the used laser was 488 nm, and the power laser was 25 for PLL and 40 for Cs. The digital gain used was 1%. The bypass filter was between 495 nm and 590 nm. Given the size of the Ms, the objective lens used was 10X. The thickness determination was done using the Zen software and the graphics tools. Eight Ms of each type were characterized, at eight different points of the membrane. The thickness and fluorescence intensity were monitored over the time up to 10 days.

3.7 Characterization of mechanical properties

3.7.1 Introduction

The microsphere's mechanical properties determine the *in vivo* performance and general integrity of the Ms [92]. The microsphere's stiffness plays an active role in the regeneration of the tissue without compromising the voice quality [21].

There is a paucity of standard methodologies to evaluate the mechanical properties of Ms *in vitro* since such properties are not frequently evaluated [8, 10, 12, 13, 92, 93]. In the present study, mechanical stability tests and osmotic pressure tests were used to predict the mechanical integrity of the Ms in *vivo*. Mechanical stability tests are used to evaluate the integrity of Ms over the time [94]. Osmotic pressure tests are used for their simplicity, sensitivity, and their validation has been done in *in vivo* experiments [95]. The stiffness of the selected materials was determined using AFM.

3.7.2 Mechanical stability test

Alginate, alginate-Poly-L-Lysine-alginate, and alginate-chitosan Ms were fabricated as described in section 3.1.2 and 3.3. Sodium Chloride (MW 58.44 g/mol), and polystyrene 48 wells plates were purchased from Fisher Scientific (USA). Strainer cup (stainless steel) was purchased from Amazon (Canada). Incubator shaker was purchased from Innova. Inverted microscopy (Axiovert40) was purchased from Zeiss.

Fig. 3.9 shows the mechanical stability test. The microspheres were suspended in fresh PS solution using the strainer cup (1X). 250 µl of microsphere suspension was incubated in 48 well plates. The plates were put in the shaker at 37 °C, using 150 rpm. The microsphere morphology was evaluated using the inverted microscopy at different times up to 10 days. The studies were done in triplicate.

3.7.3 Osmotic pressure test

Alginate, alginate-poly-L-Lysine-alginate, and alginate-chitosan Ms were fabricated as described in section 3.1.2 and 3.3. Sodium Chloride (MW 58.44 g/mol), and Milli-Q water were purchased from Fisher Scientific (USA). The cell strainers (400 µm) were purchased from pluriSelect (USA). Inverted microscopy (CKX41) was purchased from Olympus (USA). Digital camera was purchased form ThorLab (USA). Analyze software was acquired from ImageJ.

Fig. 3.10 illustrates the osmotic pressure test. Aliquots of microspheres were equilibrated in 5 ml of PS (1X) for 30 minutes. After the equilibration, the solution was removed using the cell strainers, and the Ms were exposed to Milli-Q water used as hypotonic solution. The microspheres were observed under the microscope at a 10X magnification after 30, 60, 90, 120 minutes, and 24 h. Representative micrographs were taken and analyzed using ImageJ.

3.7.4 Young's modulus determination

3.7.4.1 Introduction

The functionality, biocompatibility, cell adhesion properties, and regulation of cell phenotype of the biomaterials depend on their Young's modulus (stiffness). For instance, the biomaterials that are stiffer than the native tissue may induce scar formation [16]. In the case of the VFs, the stiffness of the LP determines the mucosal wave motion and voice quality [21].

Different techniques are used to determine the Young's modulus of hydrogels, including rheology and AFM [21].

Rheology describes the deformation of a body under the influence of mechanical stress, and the bulk properties of hydrogels [96]. During rheology, the sample is placed between two parallel plates, and it is deformed during periodic oscillations. The material is exposed to a sinusoidal stress or shear strain, expressed by the equation (II), where Y_0 is the stress amplitude, ω is the oscillation frequency, and *t* is time. The amplitude of the oscillations should be in the linear viscoelasticity limit. Usually, the oscillation frequency is fixed in 1 Hz [97].

$$\gamma = \gamma_0 \sin(wt) \qquad (II)$$

The mechanical response, τ of viscoelastic materials is shown in the equation (III). G´(ω) is the shear storage or elastic modulus, which provides information of the energy stored in the material during deformation. G´´(ω) is the shear loss or viscous modulus, which describes the energy dissipated as heat during the test [97].

$$\tau = G'(w)\gamma_0 \sin(wt) + G''(w)Y_0 \cos(wt) \qquad (III)$$

When the sample is homogeneous, the Young's modulus, or stiffness can be calculated with a simple relationship described by the equation (IV) [97]. In the present study, a torsional rheometer was used to determinate the properties of the Al hydrogels crosslinked with $CaCl_2$.

$$Young's\ modulus = 3\ G'(w) \text{ (IV)}$$

The atomic force microscopy can measure very small forces with nanometer resolution. Fig. 3.11 shows a schematic representation of the basic components of the AFM. This device uses a flexible cantilever. The plate spring of the cantilever is fixed at one end, with a tip supported at the other end. The tip can move across the surface of a sample. The attractive or repulsion force between the tip and the sample causes a deflection of the cantilever towards or away from the sample. The deflection of the cantilever is measured by a laser interferometer. The detection uses a laser beam reflected from the cantilever onto a photodiode [98].

In the present study, contact method, and spherical probes were used to determine Young's modulus of hydrogels coated with PLL, Al, and Cs. The contact mode was selected since it is normally used for measurements of local stiffness [100]. The spherical probes are used for elastic characterization of the material, due to the force can be analyzed more quantitatively, and the measurement is more sensitive [101].

Typical force obtained with the AFM is illustrated in Fig. 3 12, which shows the deflection of the cantilever when the probe is brought vertically toward and then away from the sample surface. The positions A and B show when the tip is approaching the surface. The position B shows when the contact is made. Afterwards, the cantilever bends until reach the limit of the force applied, represented with the letter S. During this step the tip can indent the surface, depending on the relative stiffness of the cantilever with respect to that of the sample. Then, the tip is placed between

positions C and D. In specific applications, in the position D, the tip detaches from the sample. When the tip is between the position D and A, the cantilever returns to its resting position [98].

3.7.4. 2 Methods

E- Poly-L-Lysine (4130 g/mol, low molecular weight) was purchased from Zhejiang Silver-elephant Bio-engineering Co (China). Chitosan (degree of deacetylation 80%, low viscosity) was purchased from Wako BioProducts (USA). Sodium alginate (MW 216.12 g/mol. 61% mannuronic acid, 39% guluronic acid. low viscosity), and glacial acetic acid (MW 60.05 g/mol) were bought from Sigma-Aldrich (Ontario, Canada). Sodium Chloride (MW 58.44 g/mol), the pH Benchtop meter, microscope cover glasses and, the corning polystyrene filters (0.22 µm) were purchased from Fisher Scientific (USA). $CaCl_2$ (MW 147.02 g/mol) was purchased from ACP Chemicals (Montreal, Canada). Glass bottom culture dishes were purchased from MatTek (USA). Torsional rheometer (Discovery HR-2) with parallel plates (top plate size 10 mm) was purchased from TA Instruments (USA). AFM platform was purchased from JPK Nano-wizard 3 (Berlin, Germany). Triangular silicon nitride cantilevers (0.32 N/m) and rectangular silicon cantilevers (0.6 N/m) were purchased from Novascan IA (USA).

3.7.4.2.1 Hydrogels preparation

A solution of 74 mM of Al, 0.121 mM PLL, 9.2 mM Al, and 100mM $CaCl_2$ were prepared in distilled water. Solutions of a mass fraction of 0.5% wt./v of Cs were prepared in distilled water. Acetic acid was used to control the pH of the latter one, and to dissolve completely the Cs. The final pH of the solution was measured to be 5,4. All solutions were stirred until they were homogeneous mixtures and sterilized with 0.22 µm polystyrene filter.

Approximately 200 µl of 74 mM Al was added to at the center of the glass bottom culture dishes. A microscope cover glass was used to distribute uniformly the solution in the dish. The dishes were

immersed in 100 mM $CaCl_2$ for 40 seconds. The $CaCl_2$ was discarded and the hydrogels were modified immersing them into PLL solution for 10 minutes, following by 10 minutes immersion into 9.2 mM Al. Alginate hydrogels were also modified with a solution of a mass fraction 0.5% Cs. The dishes were immersed in the solution for 30 minutes. The hydrogels were characterized on the same day in which they were fabricated.

3.7.4.2.2 Young's modulus of hydrogels using rheometer

The alginate hydrogels were detached from the culture dishes, and their Young's modulus measured with a commercially available torsional rheometer with parallel plates (Discovery HR-2). The top plate size was 10 mm in diameter and its thickness around 500 µm. Mineral oil was used on the outside of the samples to prevent their dehydration. Fig. 3.13 shows the experiment set up. The experiments were done in triplicate for 2 minutes at room temperature (22 °C). Iso-thermo time sweep with 0.1% strain was applied. The ossification frequency was kept at 1 Hz. The shear modulus was recorded and analyzed using TA instruments software. The Young's modulus was calculated by multiplying the shear modulus by 3.

3.7.4.2.3 Young's modulus of hydrogels using atomic force microscopy

A commercially available AFM platform (JPK Nano-wizard 3) was used for nano-indentation tests. Triangular silicon nitride cantilevers (0.32 N/m) and rectangular silicon cantilevers (0.6 N/m) were used (Novascan, IA). 25 µm-in-diameter spherical beads were attached as probes. The cantilever spring constants were determined using the thermal noise method before the experiment. All the indentations were conducted in liquid conditions with samples immersed in the $CaCl_2$ solution. Hertzian contact model was used to fit the indentation data and to calculate Young's modulus. 60 points were measured of each sample.

3.8 Determination of the swelling behavior

3.8.1 Introduction

Alginate is highly hydrophilic due to the presence of OH and COOH in its chain [45, 51, 92]. Therefore, at neutral pH, the water can penetrate its chain to form hydrogen bridges through the -OH and COO- groups and fills up space along the chains and the center of wide pores. Alginate tends to swell. Additional swelling is caused by the presence of ions such as sodium, magnesium, and citrate [92]. The degradation of APA Ms and Al Ms in the body is caused by the water and ions [38]. The swelling behavior of Ms is a useful tool to observe their degradation.

3.8. 2 Methods

Alginate, alginate-Poly-L-Lysine-alginate, and alginate-chitosan microspheres were fabricated as described in section 3.1.2 and 3.3. Phosphate Buffer Saline was purchased from Wisent Inc. (Montreal, Canada). Cell strainers (400 µm) were purchased from pluriSelect (USA). Inverted microscopy (CKX41) was purchased from Olympus (USA). Digital camera was purchased form ThorLab (USA). Analyzes software was acquired from ImageJ.

To assess the swelling behavior, aliquots of Ms were submerged in 5 ml of PBS. The physical integrity and diameter of the microcapsules were monitored for up to 48 h with the microscope at magnifications of 4X and 10X. The percentage of swelling was determined using the equation (V) where D, corresponds to final diameter of Ms, and D_0 corresponds to the initial diameter of Ms.

$$\% \, Swelling = \frac{(D - D_0)}{D_O} \times 100 \qquad \text{(V)}$$

The diameter of the Ms was determined as previously described in section 3.2.

3.9 Evaluation of immune reaction of alginate microspheres

Lymph nodes of fresh dead mice were used to obtain primary monocytes, Dubecco's Modified Eagle's Medium, Phosphate Buffer Saline, Roswell Park Memorial Institute medium were purchased from Wisent Inc. (Montreal, Canada). Alginate Ms were fabricated as indicated in section 3.1.3. Immortalized human vocal fold fibroblasts (hVFF, passage 5) were used [32]. Lipopolysaccharides from Escherichia coli, and sodium Al (MW 216.12 g/mol. 61% mannuronic acid, 39% guluronic acid. low viscosity) were acquired from Sigma Aldrich (Montreal, Canada). One mouse Interleukin 1- beta (IL-1β) ELISA kit was purchased from Abcam Inc. (Toronto, Canada). Twelve well plates, T-flasks, and 5 ml syringes were purchased from Fisher Scientific (Canada). The cell strainers (70 µm) were purchased from pluriSelect (USA). The spectrophotometer, Victor 3V, and the Wallac Station software were acquired from PerkinElmer (USA).

The lymph nodes from fresh dead mice were kept in PBS for 24 h. Afterwards, the monocytes were isolated using physical methods. The lymph nodes were placed on the cell strainers, and the syringe plunger was used to apply pressure on the lymph nodes until the nodes were dissociated. Roswell Park Memorial Institute medium was applied to the filter, and the monocytes were placed in the new fresh solution. Approximately 380, 000 monocytes were seeded in each well of the 12 well culture plates and cultured with RPMI-1640 supplemented with 2% FBS, and 1% penicillin streptomycin for 24 h at 37°C in humidified air containing 5% CO_2. The human vocal fold fibroblasts were cultured in T-flasks with DMEM supplemented with 10% FBS and 1% Penicillin-Streptomycin until reaching confluence.

The human vocal fold fibroblasts were encapsulated as described in section 3.4, with a concentration of $4x10^5$ cells/ml.

Liposaccharides (1 µg/ml) were used to activate the monocytes. Afterwards the monocytes were co-cultured with empty Al Ms, free hVFF, and encapsulated hVFF for 48 h. No activated LPS monocytes were used as a control group. The supernatants were collected and subjected to an enzyme-linked immunosorbent assay of a pro-inflammatory cytokine namely interleukin (IL)-1β. The colorimetric signal was detected with a spectrophotometer (Victor 3V) at 450 nm.

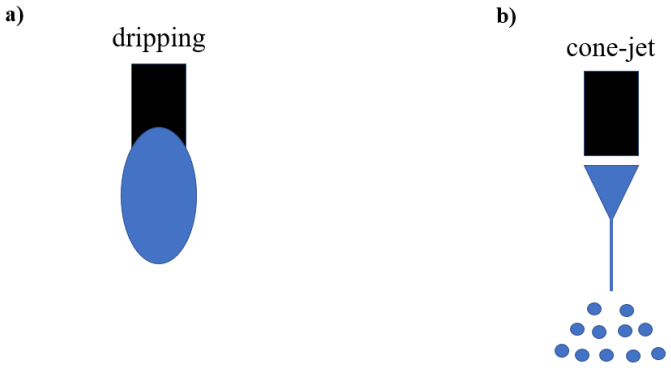

Fig. 3.1 Generation of microspheres by electrospraying. a) Dripping. The liquid rinses the nozzle forming a droplet. b) Taylor cone. The surface tension of the droplet, generated by the electric field, causes the rupture of the droplet into microscale spheres. Imaged modified from [75].

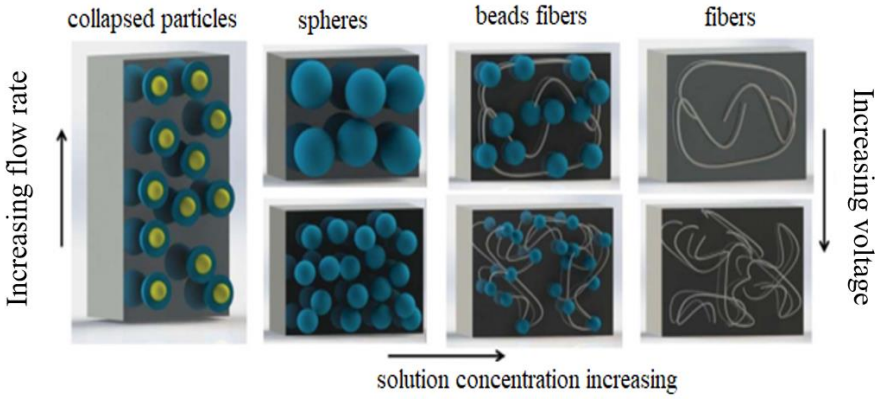

Fig. 3.2 Effect of flow rate, polymer concentration and voltage on electrosprayed microspheres. Imaged reproduced with the permission of Taylor & Francis [78].

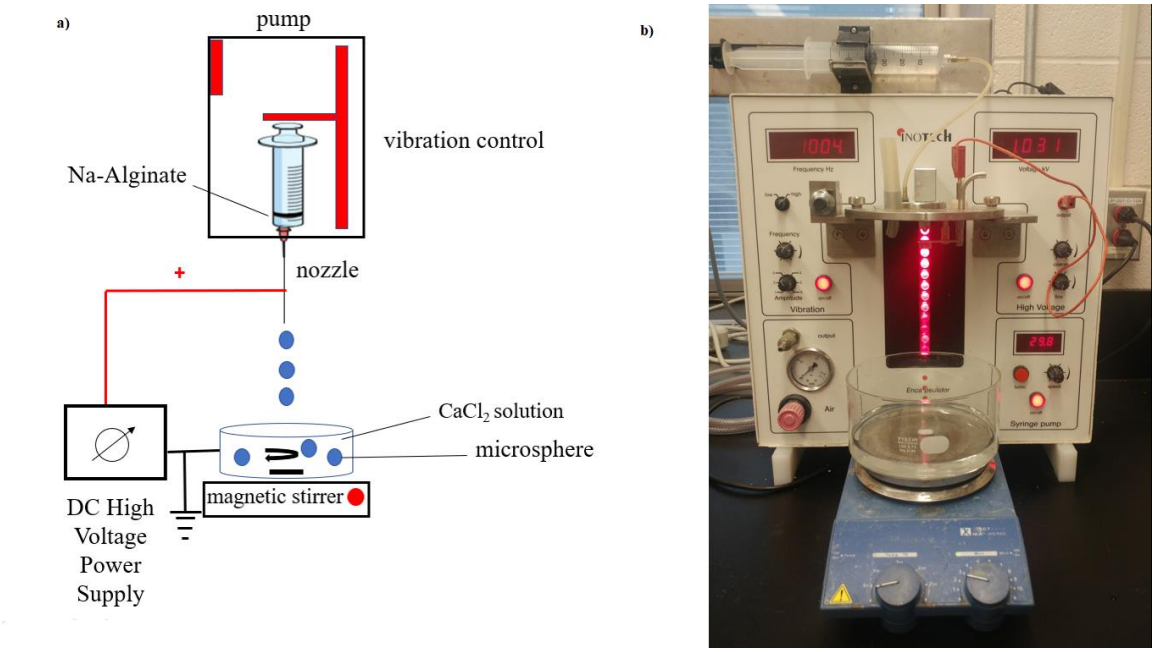

Fig. 3.3 Electrospraying setup. The syringe contains the alginate solution. The electric field charges the nozzle. The droplets are collected and crosslinked in the $CaCl_2$ solution. Fig. 3.3 a). Schematic representation of a typical electrospraying setup. Fig. 3.3 b). Inotech encapsulator, IER-20 used to fabricate the microspheres. Image modified from [81].

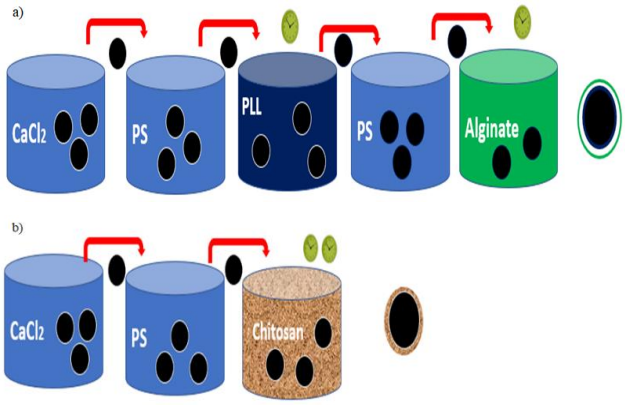

Fig. 3.4 Modification of alginate microspheres using Layer-by-Layer. a) Fabrication of APA Ms. The alginate microspheres were washed with physiological saline solution using the cell strainers or strainer cups and immersed in PLL solution for 10 minutes while keeping in the lab rotator at low speed. After being washed for the second time, the microspheres were immersed in alginate solution for other 10 minutes. b) Fabrication of Al-Cs Ms. The alginate microspheres were washed with physiological saline and immersed in Cs solution for 30 minutes while keeping in the lab rotator at low speed. The final spheres were washed one last time in PS and stored 100 mM $CaCl_2$ solution at 4°C.

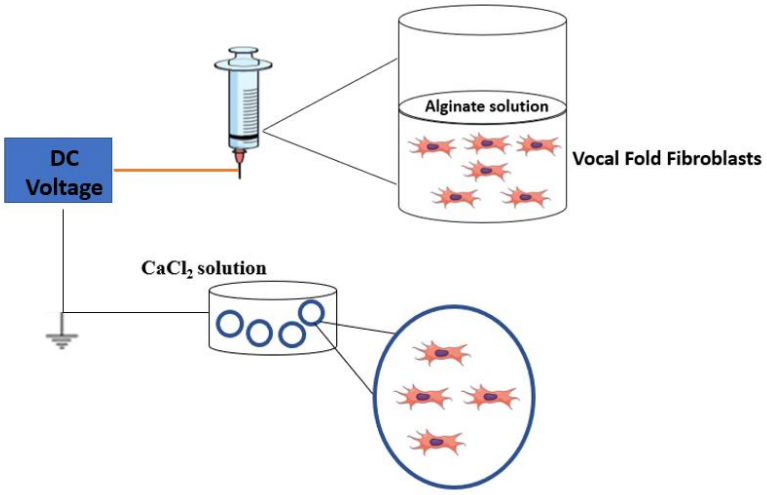

Fig. 3.5 Cell encapsulation process. The human vocal fold fibroblasts were mixed in alginate solution. Afterwards, the mixture was loaded into the syringe. Encapsulated cells were obtained after the electrospraying process.

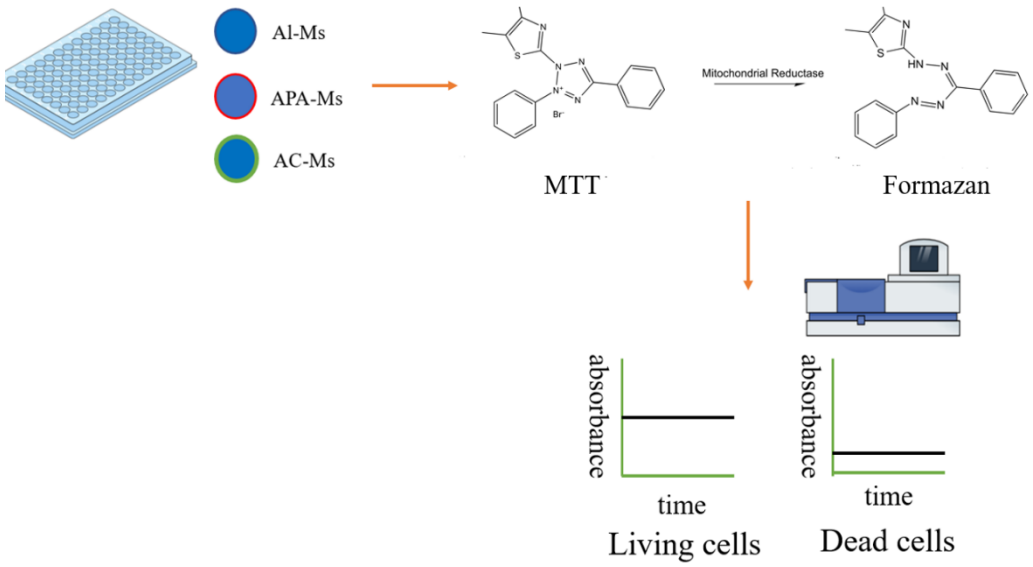

Fig. 3.6 MTT proliferation assay. Experimental Design. The cells were seeded and incubated with the different configurations of microspheres on their surface. The living cells reduce the MTT (yellow) to formazan (deep purple color) The darker the solution, the greater the number of viable, metabolically active cell. Image modified from [82].

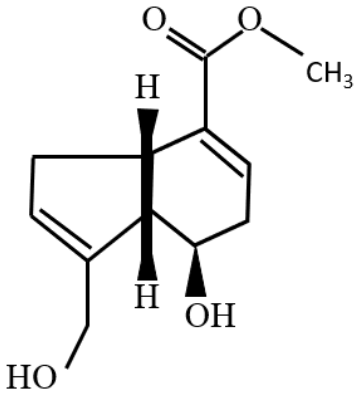

Fig. 3. 7 Chemical composition of genipin. The basic skeleton is composed for a cyclopentane bonded a six-membered heterocycle oxygenate. Imaged modified from [91].

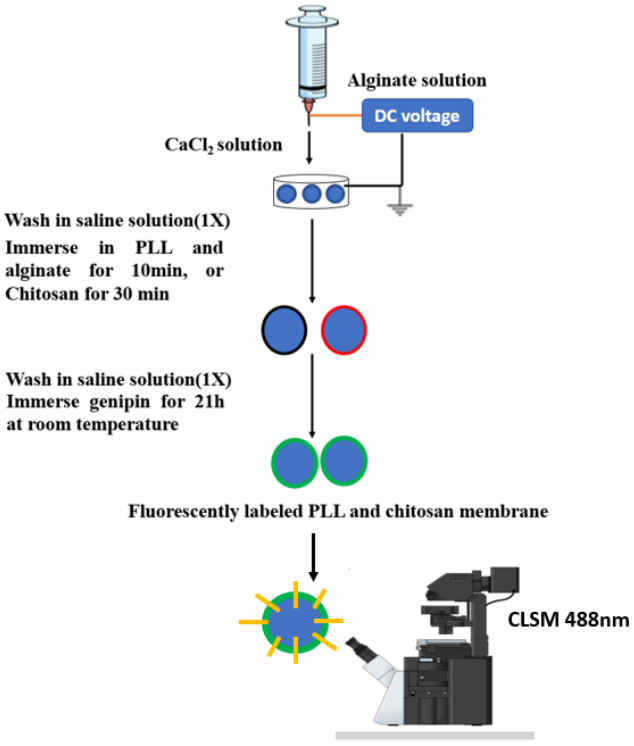

Fig. 3.8 Schematic representation of the process to fluorescently label the PLL and Cs membrane of the microspheres. First, the microspheres were fabricated using electrospraying. The next step was membrane addition LBL. Afterwards, the microspheres were immersed into genipin and incubated for 21 h. Finally, the reaction of the genipin with the polycations was visualized using CSLM. Image modified from [50].

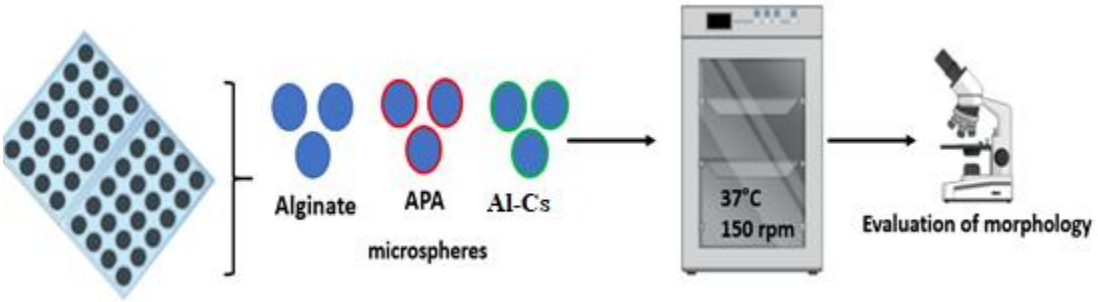

Fig. 3.9 Mechanical stability test. 250 µl of microspheres suspension was incubated at 37°C using 150 rpm. The microsphere's morphology was monitored over time.

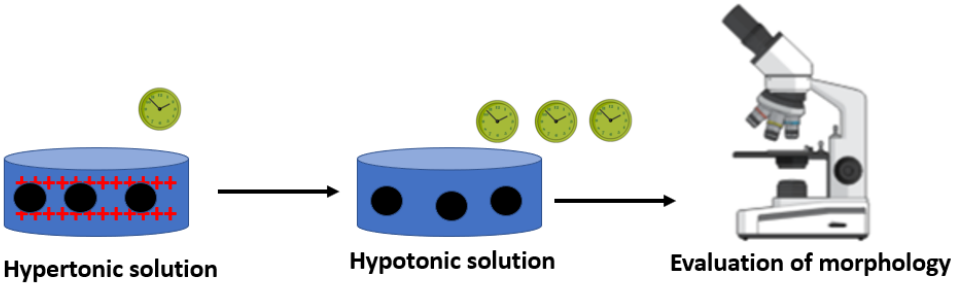

Fig. 3.10 Osmotic pressure test. The microspheres were equilibrated in PS for 30 minutes. Afterwards, the microcapsules were immersed into Milli-Q water. The morphology of the microspheres was evaluated up to 24 h.

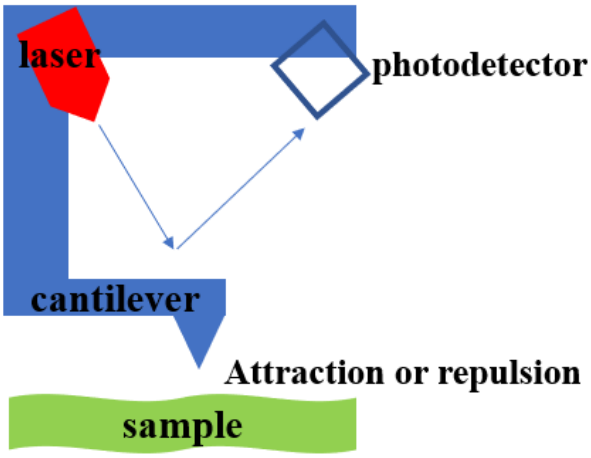

Fig. 3.11 Schematic representation of the basic components of the AFM. The deflection of the cantilever caused by the attraction or repulsion of the sample and the tip is detected with the laser beam and a photodetector, which is further recorded as voltage. Image modified from [99].

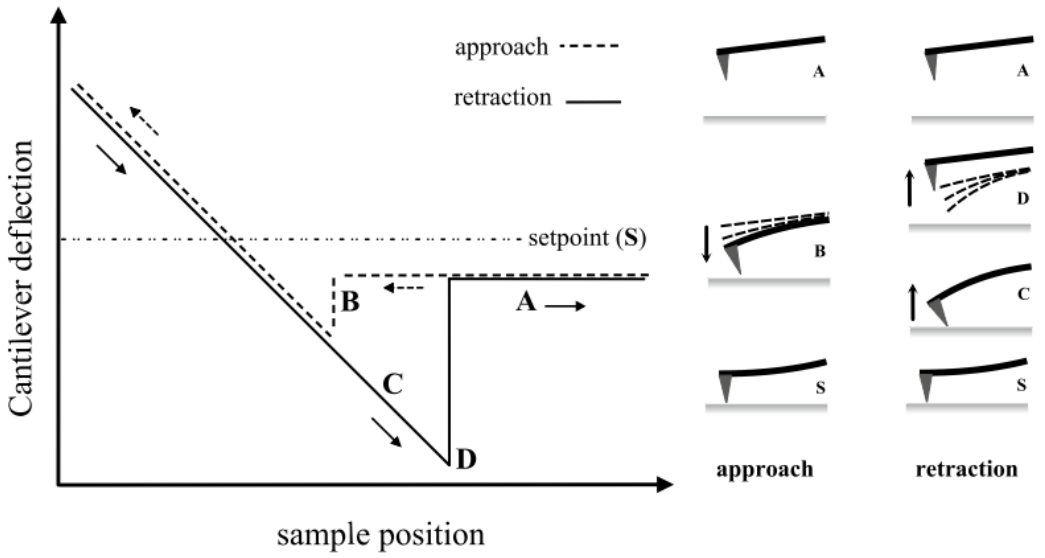

Fig. 3.12 Force obtained with the AFM. A and B show when tip is approaching. Position B shows when the contact between the sample and the tip is done. In this position the tip can indent the sample. Afterwards, the tip is situated between the points C and D. Finally, the positions D and A, show when the tip returns to its resting position. Image reproduced with the permission of Springer Nature from [98].

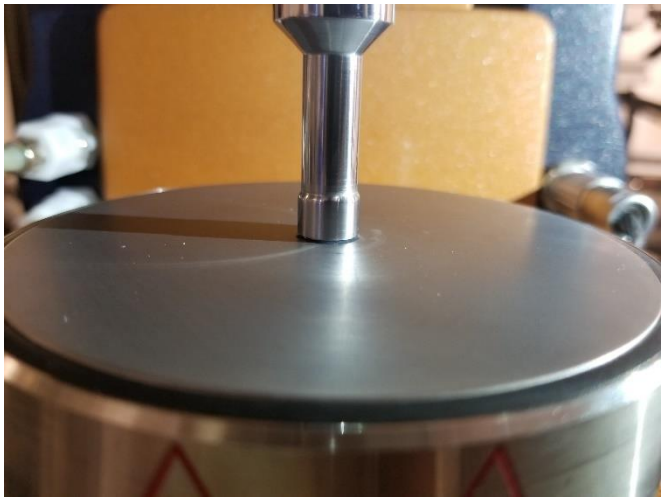

Fig. 3.13 Young's modulus characterization of alginate hydrogels using a torsional rheometer. The sample was placed in the rheometer plate, filling the gap between the parallel plates. Mineral oil was used to protect the sample to be dehydrated.

1) Buffer
10mM MOPS, 20mM D-Fructose, pH 7, 2
10mM HEPES, 20mM D-Fructose, pH 7, 2
H_2O
2) Syringe internal diameter (m)
0.0267
0.019
3) Flow rate (m^3/seg)
$2.16x10^{-7}$
$2.5x10^{-7}$
4) Frequency (Hz) of vibration control
1000
1200
1500
1800
5) Amplitude vibration control
2
3
4
6) Voltage (kV)
0
0.65
1
2
7) Distance between nozzle and collector (m)
0.06
0.2
8) Alginate Concentration (%)
1.6
1.8
2

Table I. Parameters for the optimization of the electrospraying process.

CHAPTER 4

Results

4.1 Fabrication

The microsphere's morphology varied significantly when changing the buffer in which the Al was prepared. Although all the solutions were prepared at neutral pH conditions. The number of broken spheres varied with the selected buffer.

The spheres were considered severely deformed when they were amorphous and fragile as shows Fig. 4.1 a) to c). Slightly deformations, such as elliptical shape were not considered. The table II summarizes all the optimizations done, and the deformed or broken spheres as results of them. The table III shows the impact of the different variables in the size of the Ms.

10 mM of MOPS with 20 mM of D-(-) D-Fructose resulted in 51.73% severely deformed and broken spheres. The use of HEPES buffer, resulted in a drop in the percentage of broken spheres to 23.62%. When using distilled water, the percentage of deformed and broken Ms was only a total of 15.78% without optimizing the syringe internal diameter (SID), flow rate, electrical field, frequency and amplitude of the vibration control, and distance between the nozzle and collector (DNC). The optimization of each parameter was done one at the time. Changing the buffer did not change the size of the Ms. The spheres diameter was between 417 µm and 425 µm.

Variation of the SID improved the microsphere's morphology and affected their size. The use of a syringe of 19.13 mm internal diameter, corresponding to a syringe of 20 ml, yielded 15.78% of broken and deformed spheres. Conversely, the use a syringe of 26.7 mm internal diameter, with a 60 ml total volume, reduced the number of broken and deformed spheres to 7.34%. The corresponding Ms varied from 425 µm to 485 µm, as shown in table II.

When the flow rate, frequency, and amplitude were varied, they affected other parameters. When a frequency of 1000 Hz was used, none spheres were formed with flow rate minor to

$2.16x10^{-7}$ m^3/seg and bigger than $2.5x10^{-7}$ m^3/seg. Therefore, two values of flow rate were tested, using 1000 Hz as a constant frequency: $2.16x10^{-7}$ m^3/seg, and $2.5x10^{-7}$ m^3/seg. No significant difference in the morphology and size of the Ms was found. But it was observed that with a frequency of 1000 Hz and the selected flow rate the Ms were more uniform, than using another combination of frequency and flow rate. A flow rate of $2.5x10^{-7}$ m^3/seg was selected to optimize the values of frequency. Increasing the frequency up to 1800 Hz resulted in more percentage of broken and deformed spheres, and the Ms size increased. For instance, using a frequency of 1000 Hz resulted in 3% of the deformed spheres, while with 1500 Hz this percentage increase up to 5.43%. Using a frequency of 1800 Hz resulted in 10% of broken and deformed spheres. Varying the amplitude did not modify in a significative way the size of the Ms but improved their morphology when the amplitude of 4 was used.

The voltage had a significative impact on the morphology of the Ms. Using low voltages, including 0, and 0.65 kV resulted on 100% and 96%, respectively, of broken spheres. Using 2 kV resulted in 10% of deformed and broken spheres while using 1 kV dropped them up to only 3%. Reducing the distance between the nozzle and the collector, resulted on 32.43% of amorphous spheres. Conversely, using 20 cm of distance, generated uniform Ms.

The Al concentration affected the morphology of the Ms. The most uniform morphology was obtained using 1.6% (wt./v) of Al, resulting in only 3% of deformed Ms. The worst morphology was obtained using 1.8% (wt./v) of Al, resulting in 7.14% deformed Ms.

The optimal conditions were selected for further fabrication. Buffer of H_20 to prepare a solution of mass fraction of 1.6% of Al, 1 kV, $2.5x10^{-7}$ m^3/seg as flow rate, amplitude and frequency of 3, and 1000 Hz, respectively. The distance between nozzle and collector was fixed in 20 cm, and the SID in 26.7 mm.

4.2 Modification layer-by-layer

The modifications done layer-by-layer did not alter the size of the Ms. In all the cases, a constant value of 552. 74 ±7.72 μm was found as a diameter of the microcapsules. In the optical microscopy, none significance difference was observed, except for a slightly bright circumference surrounding the core of the spheres. Some of the APA Ms and Al-Cs Ms had elliptical shape. When the Ms were rinsed completely during the process amorphous capsules were obtained. Al-Cs Ms were the most difficult to manage since Cs solution is very viscous. Therefore, using the strainer cup derived in more control of the Ms and less deformation, compared to cell strainer, which requires more skills. The figure 4.2 shows the Al Ms, APA Ms, Al-Cs Ms obtained and visualized in an inverted microscope.

4.3 Cell encapsulation

The figure 4.3 illustrates the effect of cell concentration loaded into the Ms and its relationship with the percentage of deformed spheres. This type of deformation was not severe in none of the cases, except when $1x10^6$ cells/ml were encapsulated. In this case, the Al core broke by swelling and none further modification could be done as it is shown in Fig. 4.4. Fig. 4.4 shows the cells randomly distributed in the Ms. Some cells were on the edges of the structures.

It can be observed, Fig. 4.3, that without any encapsulated cells in the APA Ms, the Ms deformations (elliptical shape) reached 9.37%. A big number of encapsulated cells, $6x10^5$ cells/ml, decreased the number of Ms deformations to 3.13%. Alginate microspheres and Al-Cs Ms showed the opposite. Increasing the number of encapsulated cells resulted in greater Ms deformations. For Al Ms, the shape irregularities found in the control group, empty Ms, was 3%, and this value increased up to 12.50% when $6x10^5$ cells/ml were encapsulated.

For alginate-chitosan microspheres, a small percentage of deformed Ms was obtained when higher concentration of Cs, %0.5 (wt./v), was used. Conversely, using a smaller

concentration of Cs, 0.05% (wt./v), resulted in greater deformed Ms. For 0.05% (wt./v) Cs, without any encapsulated cells on Al-Cs Ms, the percentage of deformed Ms was 3.1%, and when $6x10^5$ cells/ml were encapsulated on Al-Cs Ms, the percentage of deformed Ms was 12.5%. For 0.05% (wt./v) Cs without any encapsulated cells on Al-Cs Ms none deformed Ms were found, and when $6x10^5$ cells/ml were encapsulated on Al-Cs Ms, the percentage of deformed Ms was 9.37%.

4.4 Effect of microspheres on cell viability and proliferation

4.4.1 Live/Dead assay

The figure 4.5 shows the micrographs of the fibroblasts after being cultured with the different Ms, except for the control group where the cells were cultured in normal conditions. As it can be noticed there was not evidence of cellular death (red color) for neither 3 h nor 24 h, in none of the types of Ms.

4.4.2 MTT proliferation assay

Figure 4.6 and the equation (VI) shows the calibration line, in which the number of fibroblasts was associated with the absorbance detected in the spectrophotometer. The term *nc* expresses the number of cells, and *abs*, the absorbance measured in A.U. As it was expected, a greater number of cells resulted in greater absorbance. From this experiment, it was determined that the optimal concentration of fibroblast was 32, 280 which gave 0.697 A.U. of absorbance.

$$abs = 0.00001(nc) + 0.099 \quad (VI)$$

As it can be noticed in Fig 4.7, that the incubation of fibroblasts with the different configuration of Ms did not compromise neither the metabolic activity nor the proliferation capacity of the cells for 24 h or 48 h. After 3 h of incubation with Al Ms and APA Ms, it was a slightly decrement in the signal corresponding to a viability of 96% and 93% respectively. Nevertheless, after 24 h and 48 h all the materials induced the cell proliferation even more than the control group (no treatment). From all the materials, Al-Cs Ms induced the most abundant

proliferation, following by Al Ms and APA Ms. For instance, after 48 h of cell incubation with Al-Cs Ms, the cell population increased more than the double than the original population.

4.5 Determination of membrane thickness

The membrane of Poly-L-Lysine layer on APA Ms was found to be thicker than the membrane of Cs on Al-Cs Ms. The thickness of the former at day 3 was 21.55±1.88 μm, while the thickness of the Cs at day 3 was 10.625 μm±0.88 μm.

In the case of the APA Ms, the membrane was uniform in all the sphere, and it circumscribed the Al core, as it is shown in Fig. 4.8. Part of the Poly-L-Lysine was deposited inside of the microsphere as it is shown in Fig. 4.9. When the APA Ms reacted with genipin, their color became completely blue.

The Alginate-Poly-L-Lysine Ms with an elliptical morphology showed thinner membrane than that completely spherical ones. Fig. 4.11 shows the deposition of PLL, which was not completely uniform, resulting in regions with a slightly thicker membrane.

The thickness of the APA Ms varied along the time. The original value of 21.55±1.88 μm at day 3 dropped to 14.12μm ± 3.73 μm at day 10. Fig. 4.11 a) shows the thickness at different times, while Fig. 4.11 b) to e) shows the micrographs of PLL membrane of the APA spheres and their changes throughout the days.

The alginate-chitosan Ms did not change their color after the reaction with the genipin. As it is noticed in Fig. 4.12 the membrane circumscribing the Al core was thin and difficult to perceive in the florescent microscope.

The thickness of the Cs membrane varied along time as the PLL deposition in the APA Ms. Fig. 4.14 shows the variability of the thickness of Al-Cs Ms throughout days. The variation was slightly lower than the initial value. The thickness of day 3: 10.625 μm±0.88 μm, decreased to 9.20 μm ± 0.93 μm after 10 days.

Fig. 4.15 shows some broken Al-Cs Ms which were found at day 10, in those broken Al-Cs Ms the Cs membrane remained intact to circumscribe the Al core.

4.6 Characterization of mechanical properties

4.6.1 Mechanical stability test

Alginate Ms were stable until 48 h. Afterwards, the percentage of broken spheres increased up to 6% on day 5, and 7% on day 10. The compromised Ms broke in half. These results are illustrated in Fig 4.16, black line.

The alginate-poly-L-lysine-alginate Ms were the most fragile of the three groups. Fig 4.16 illustrates in red the APA Ms behavior over time. The initial percentage of broken APA Ms was 9.37%, and it increased up to 15.49% by 5 days and up to 28% by day 10. Hollows in the APA Ms were found.

The mechanical stability of the Al-Cs Ms varied according to the Cs concentration used in the process of fabrication. The Ms with 0.05% (wt./v) Cs, Fig. 4.16 blue line, were more fragile. In the first 24 h the percentage of compromised spheres was 6.2%, and on day 10 this value increased up to 12%. In contrast, Al-Cs microbeads with higher Cs concentration, 0.5% (wt./v), Fig. 4. 16, green line, were more resistant to the mechanical disturbance and temperature. During the first 7 days, the percentage of broken spheres was 3% and it remained constant until day 10 in which the percentage increased up to 6%. The alginate-chitosan Ms broke into small pieces.

4.6.2 Osmotic pressure test

The alginate-Poly-L-Lysine-alginate and Al-Cs Ms (0.5% wt./v Cs) showed similar results after the osmotic pressure test. Fig. 4.17 illustrates in the red and blue line, respectively, the percentage of broken spheres over the time. During the first 30 minutes a total of 98% of APA Ms, and 94% of Al-Cs Ms broke. After 24 h, the percentage of broken spheres increased, for APA Ms, the whole 100% of spheres broke, while only 2,3% of Al-Cs Ms remained intact. In both cases,

even after the rupture of the Ms, it was observed the membrane remained to circumscribe the Al core. Fig. 4.18 b), d) and f) illustrates the morphology of the Ms during the first hour of the osmotic pressure test.

According to the osmotic pressure test, the Al Ms were most resistant. In the first 30 minutes, a total of 74% Ms broke. The percentage increase up to 78% during the first hour of the test and remained constant for 120 minutes. After 24 h, this percentage increased up to 82%. The alginate microcapsules swelled and then broke in half. This rupture mechanism is illustrated in Fig. 4.18 b).

4.6.3 Young's modulus determination

4.6.3.1 Young's modulus of alginate hydrogels

Figure 4.19 shows representative shear modulus values for the Al hydrogels. The shear modulus was consistent between the three hydrogels. In all cases the shear or storage modulus after 2 minutes was 1 kPa, and the Young's modulus was around 3 kPa.

4.6.3.2 Young's modulus of hydrogels using atomic force microscope

The Young's modulus of the APA hydrogel was smaller than that of the Al-Cs hydrogel. The APA Young's modulus was 1.92 kPa, with a standard deviation of 432 Pa. The results showed a Gaussian distribution as illustrated in Fig 4.20. A representative force of the APA hydrogel is shown in Fig. 4.21, the red line corresponds to the approach, while the retraction is shown in green. The Young's modulus of the Al-Cs hydrogel was 12.23 kPa with a standard deviation of 4.87 kPa. The results showed a normal distribution illustrated in Fig. 4.22. A representative force of Al-Cs hydrogel is shown in Fig. 4.23. The approach is in red, while the green line shows the retraction.

4.7 Determination of the swelling behavior

The three types of Ms had a different swelling percentage. The worst group was the Al-Cs Ms, at 24 h the swelling percentage was 52.76%, at this point broken spheres were observed. The swelling percentage increased up to 57.47% during 48 h of the test.

Alginate Ms had a swelling percentage of 33.67% at 24 h and 26.03% at 48 h. APA Ms had the best swelling percentage of all the three types of Ms. They had a swelling percentage of 2.32% and 9.01% at 24 h and 48 h, respectively. For Al Ms and APA Ms, none broken spheres were found during the test.

4.8 Evaluation of immune reaction of alginate Ms

Figure 4.24 shows the inflammatory response of activated and non-activated monocytes with different stimuli. In both groups, the empty Ms did not induce any significant inflammatory response. When monocytes were cocultured with free and encapsulated hVFF, significant increases in the IL-1β level were detected compared to the monocyte monocultures. However, the response was much reduced when activated monocultures were cocultured with encapsulated hVFF.

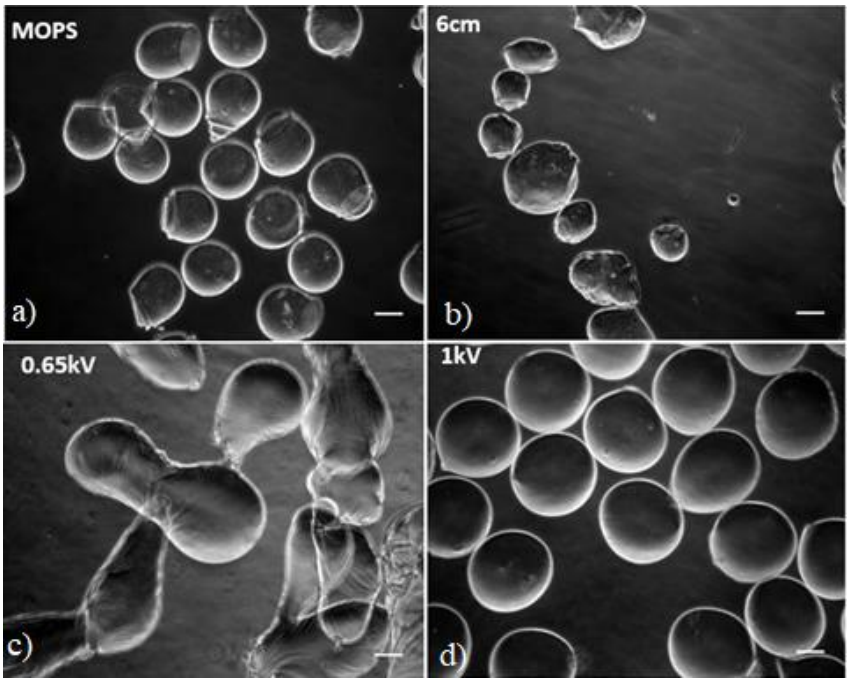

Fig. 4.1. Representative micrographs (4X) of microspheres fabricated under different conditions. a) MOPS buffer, b) distance from collector and nozzle of 6 cm, c) 0.65 kV, and d) 1kV. Scale bar 200 µm.

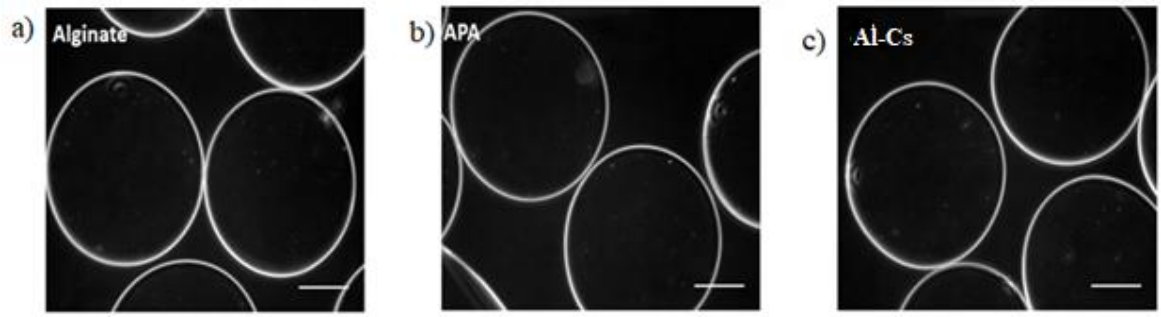

Fig. 4.2 Micrographs of a) Al Ms, b) APA Ms and c) Al-Cs Ms. (10X) Scale Bar 200µm.

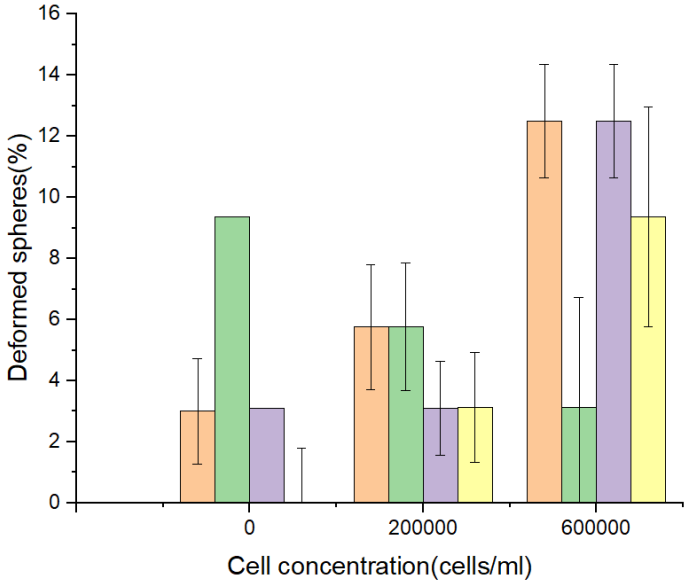

Fig. 4.3 Cell entrapment evaluation. effect of cell concentration on the morphology of the microspheres. : Alginate in orange, : APA in green, : Al-Cs 0.05% (wt./v) Cs in purple, and: Al-Cs 0.5% (wt./v) Cs in yellow.

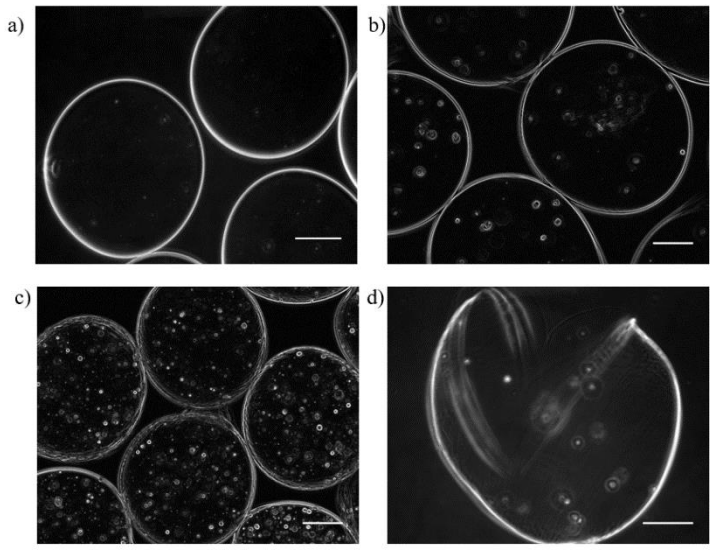

Fig. 4.4 Representative micrographs of alginate (10X) containing different concentrations of fibroblasts (cells/ml) Scale Bar 200 µm. a) alginate microspheres without cells. b) alginate microspheres with $2x10^5$ cells/ml. c) alginate microspheres with $6x10^5$ cells/ml. d) alginate microspheres with $10x10^5$ cells/ml. Increasing the cell concentration up to $10x10^5$ caused severe swelling and rupture of the microspheres.

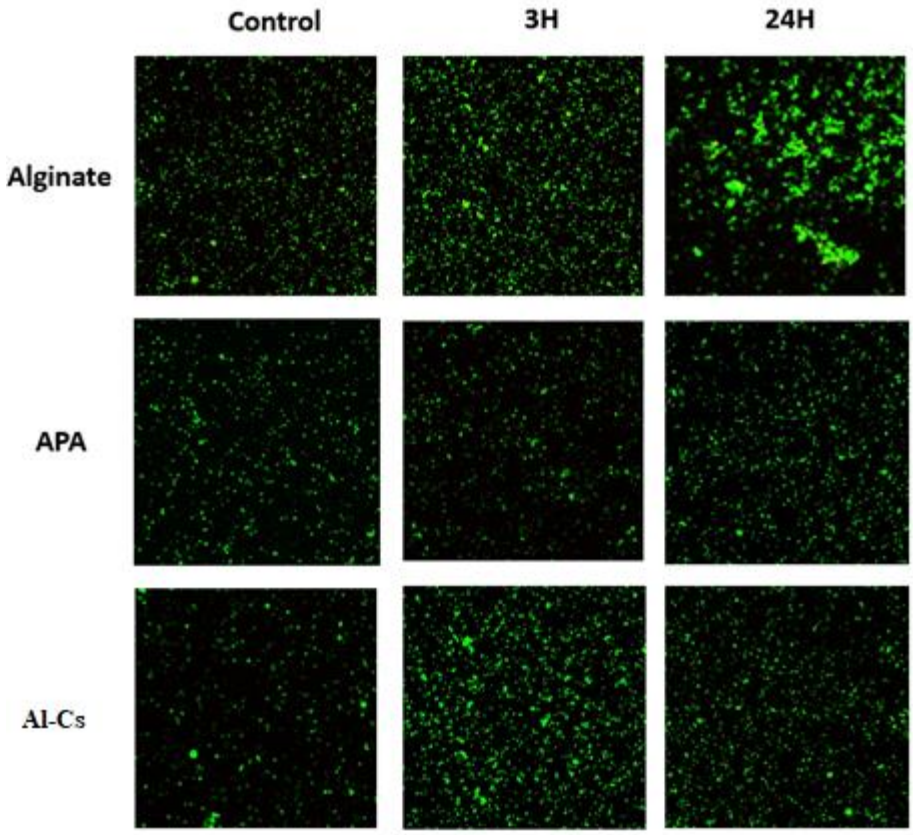

Fig. 4.5 Micrographs of fibroblasts (10X) after 3 h and 24 h incubation with Al Ms, APA Ms, and Al-Cs Ms. Live cells in green, dead cells in red.

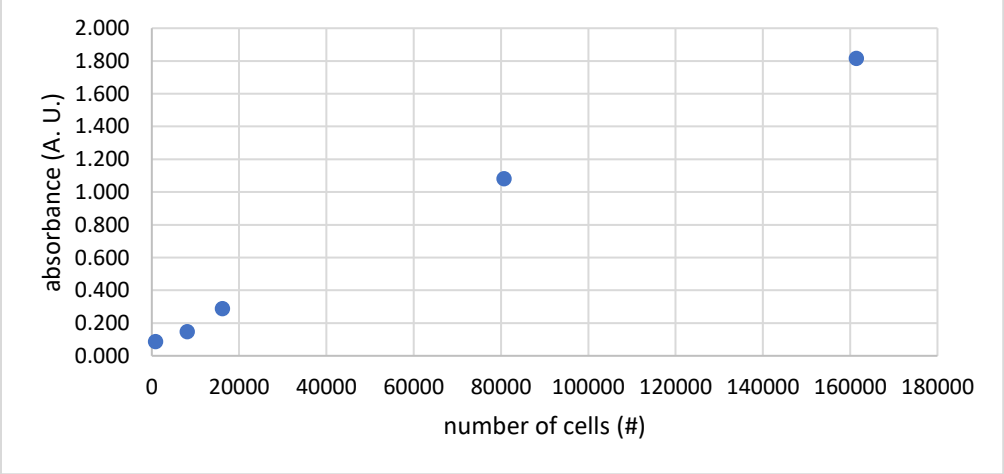

Fig. 4.6 Calibration line of proliferation assay. Fibroblasts and their absorbance. Increasing the concentration of fibroblasts increased the absorbance.

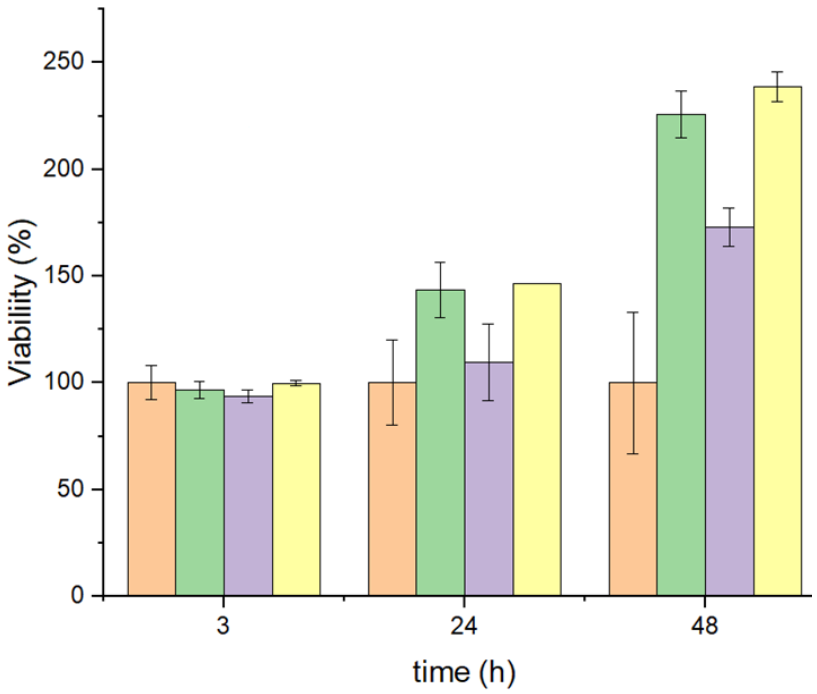

Fig. 4.7 Proliferation assay. Human vocal fold fibroblasts incubated in :standard conditions (orange), with : Al Ms (green) : APA Ms (purple) and : Al-Cs Ms (yellow) for 3 h, 24 h, and 48 h.

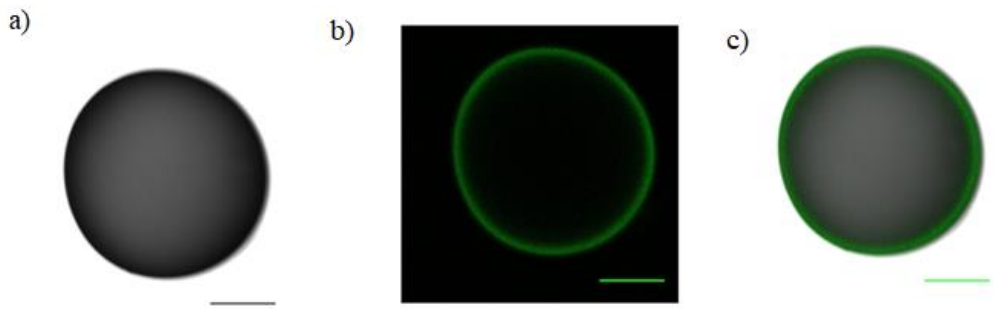

Fig. 4.8 Micrographs of APA Ms (10X). a) Optical channel, blue microcapsules after the reaction with genipin. b) Fluorescence channel, the PLL membrane, in green was visualized using the fluorescence channel. c) Composite channel. Scale Bar 200 µm. The Poly-L-Lysine membrane is circumscribing the Al core of the capsules.

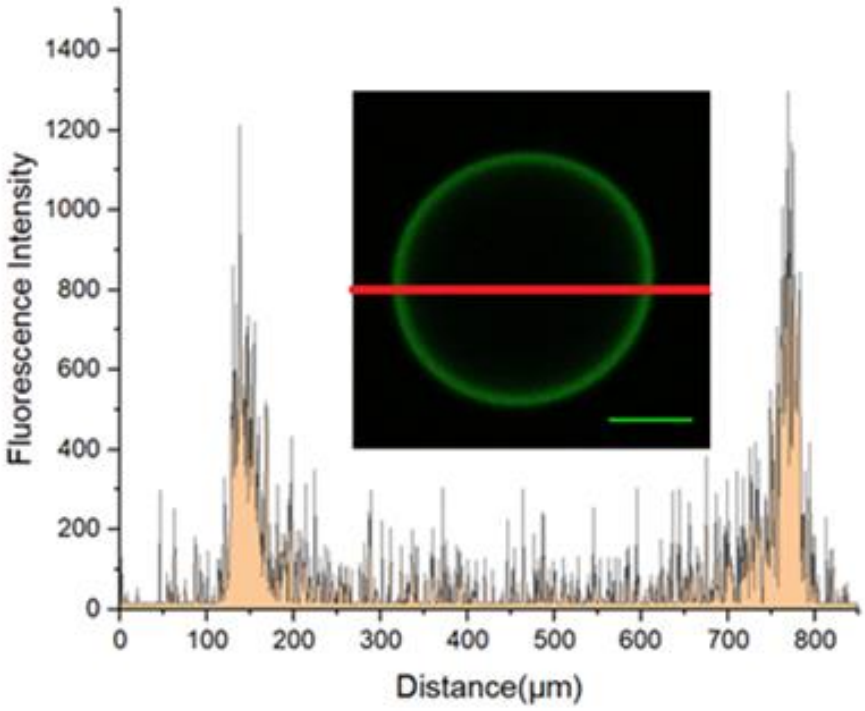

Fig. 4.9 Deposition of Poly-L-Lysine in APA microspheres. The Poly-L-Lysine was mostly deposited in the edge of the microspheres. Little quantities of PLL were found inside of the microspheres, as it is shown in the fluorescence intensity.

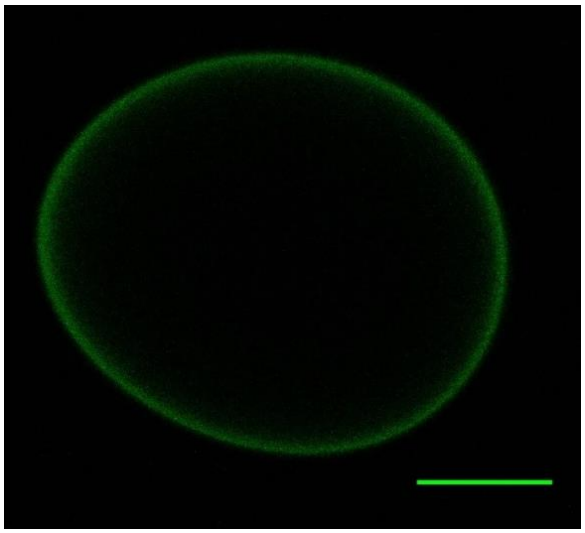

Fig. 4.10 Micrograph elliptical APA microsphere. (10X) The Poly-L-lysine in green is thicker in some parts of the microsphere, while in others is thinner. Scale Bar 200 μm.

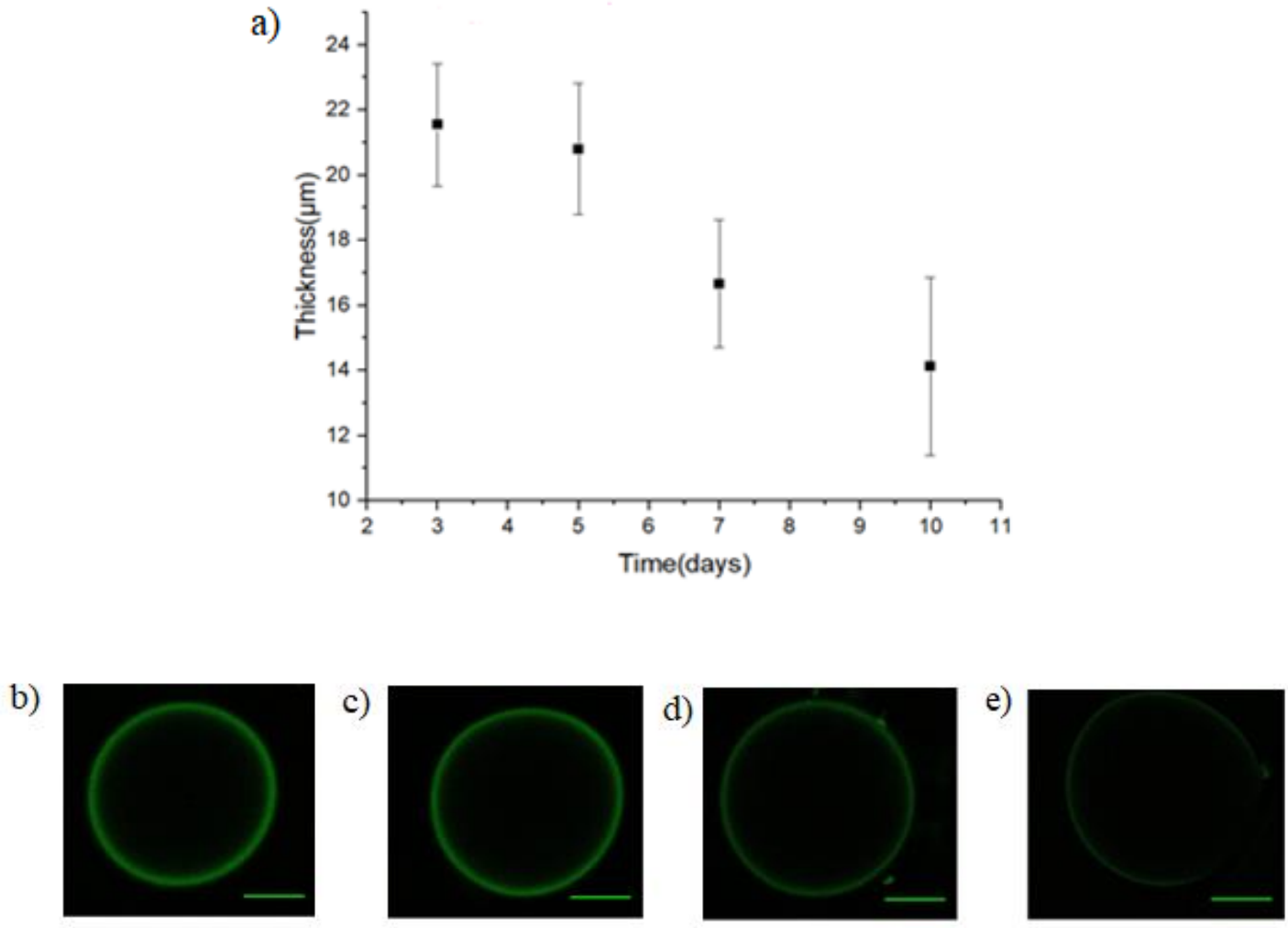

Fig. 4.11 Thickness of Poly-L-Lysine in the APA microspheres over the days. a) The thickness was stable for the first 5 days. Afterwards, it decreased. b) to e) Micrographs (10X) of PLL membrane in APA Ms at different days. b) APA Ms at day 3. c) APA Ms at day 5. d) APA Ms at day 7. e) APA Ms at day 10. Scale Bar 200 µm.

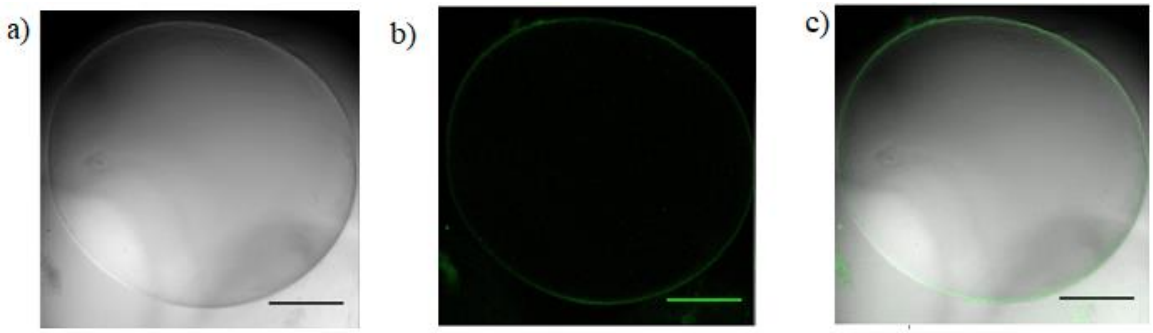

Fig. 4. 12 Micrographs of Alginate-Chitosan Ms (10X). a) Optical channel, Al-Cs Ms after genipin reaction. b) Fluorescence channel, the Cs membrane in green was visualized using fluorescence microscopy. c) composite channel. Scale Bar 200 µm. The membrane is circumscribing the alginate core of the capsules.

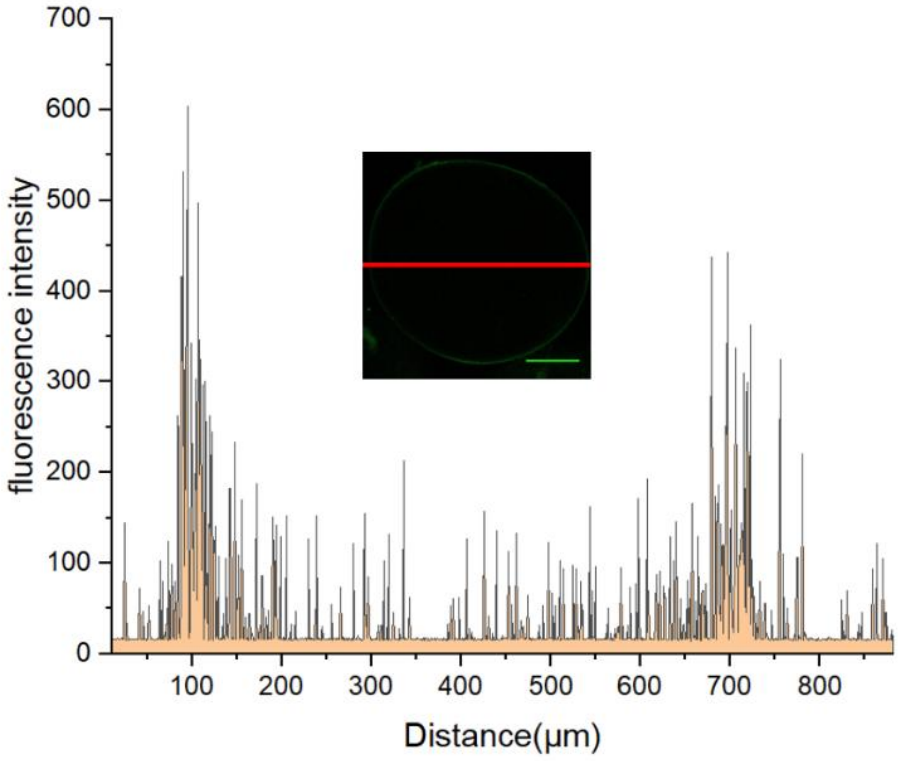

Fig. 4.13 Deposition of Cs in Al-Cs Ms. Chitosan was more abundant in the edge of the Ms, but it did not have a uniform deposition.

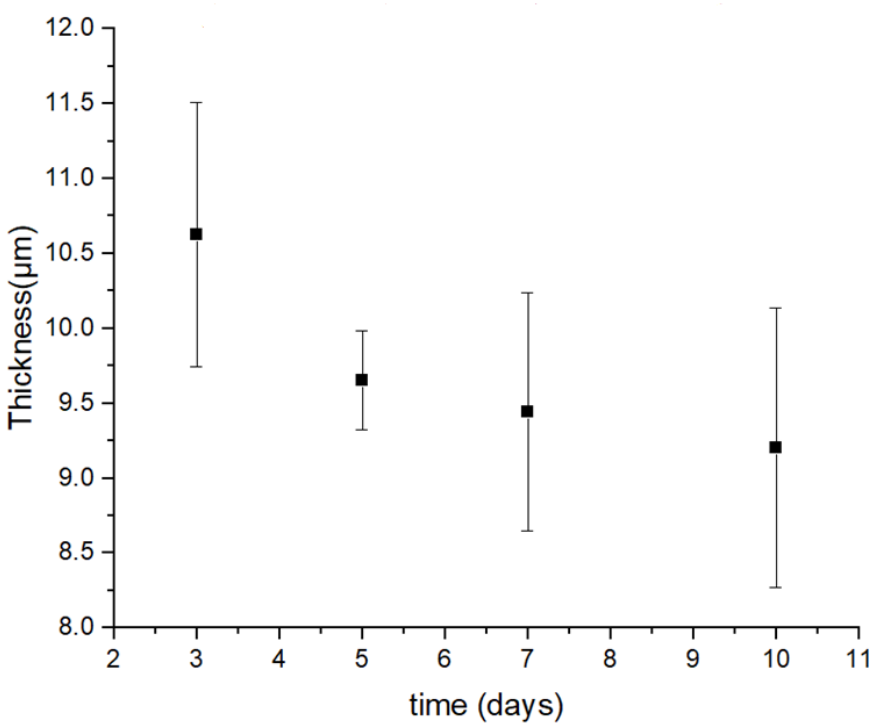

Fig. 4.14 Thickness of Cs in the Al-Cs Ms over the days. The thickness decreased after 5 days, and then it became stable.

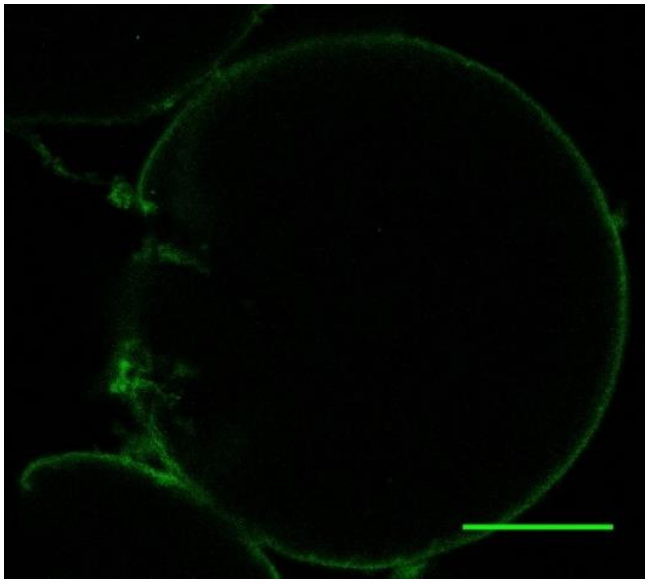

Fig. 4.15 Micrograph of a broken Al-Cs microsphere (10X). Chitosan, in green, remained to circumscribe the alginate core. Scale bar 200 µm.

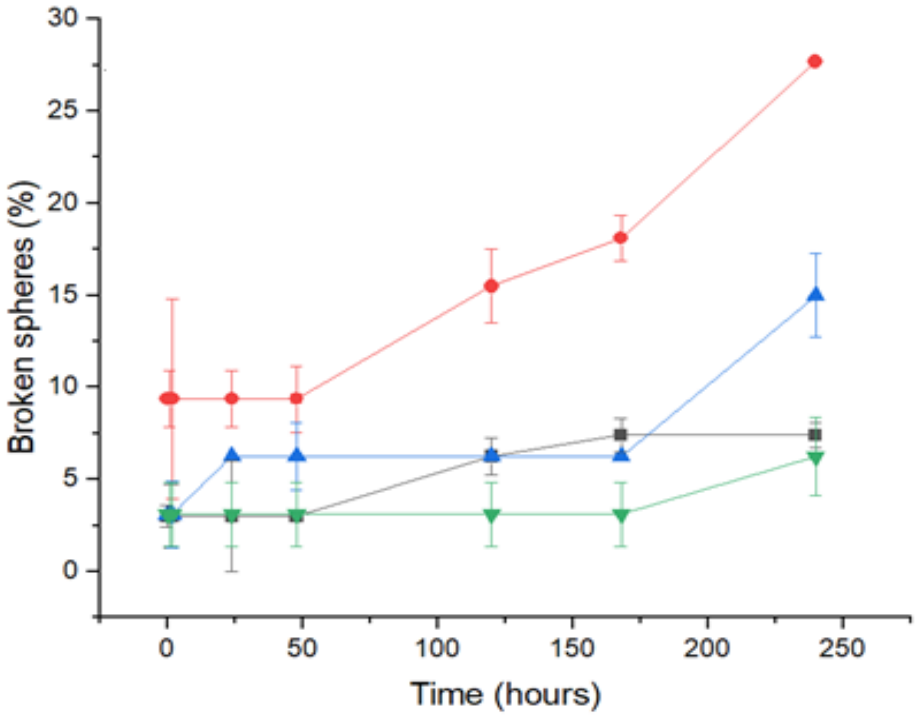

Fig. 4.16. Mechanical stability of the microspheres over the time. ■Alginate microcapsules in black line. ●APA Ms in the red line. ▲Al-Cs Ms with 0.05% (wt./v) of Cs in the blue line. ▼ Al-Cs Ms with 0.5% (wt./v) Cs in the green line.

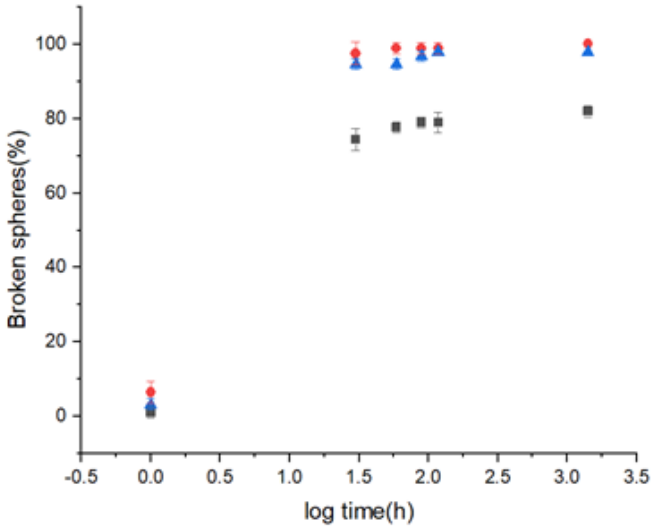

Fig. 4. 17. Osmotic pressure test of microspheres over the time. ■ Alginate Ms, in black squares. ●APA microbeads in red circles, and ▲Al-Cs microcapsules in blue triangles.

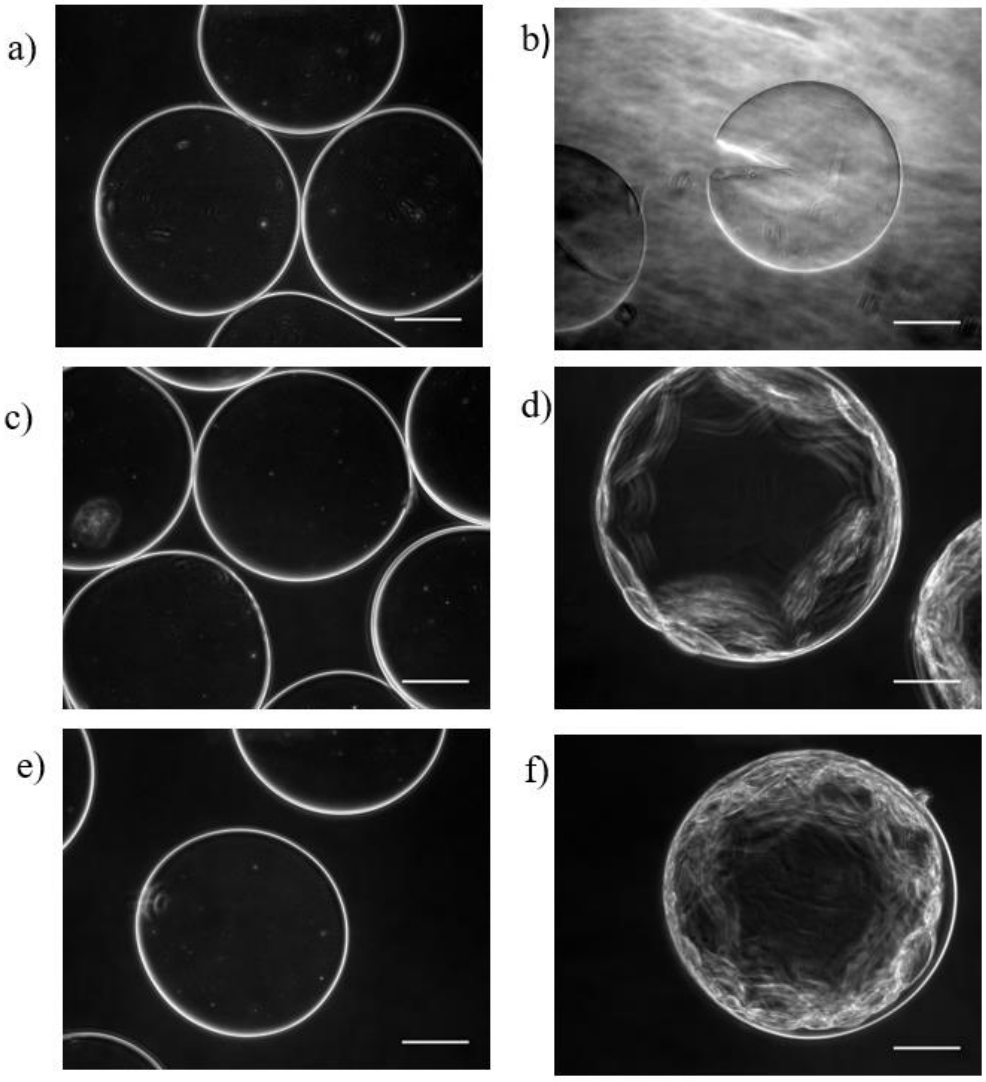

Fig. 4. 18 Micrographs of microspheres during the osmotic pressure test. a) control Al Ms before osmotic pressure test, 10X. b) Al Ms after 1 h of incubation in Milli-Q-water. After swelling, the Ms broke in half, 4X. c) control APA Ms, 10X. d) APA Ms after 1 h of incubation in Milli-Q-water. The PLL membrane circumscribed the microcapsules even after hollows were observed. e) control Al-Cs Ms, 10X. f) Al-Cs Ms after 1 hour of incubation in Milli-Q-water. The Cs membrane was still present in the Ms after their rupture, 10X. Scale bar 200 µm.

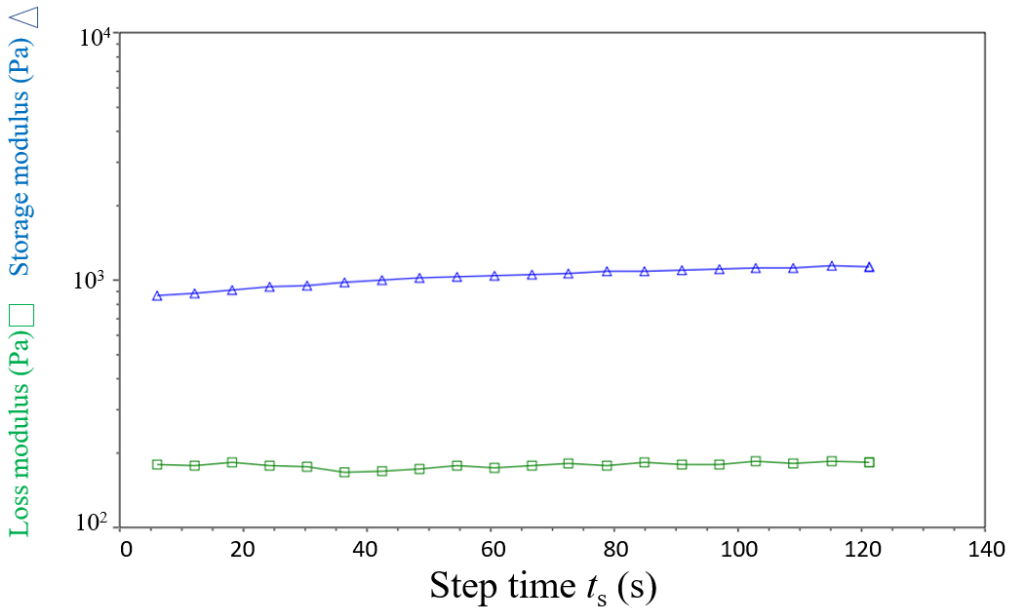

Fig. 4.19 Rheology test in alginate hydrogels. △Storage modulus (blue). □Loss modulus (green) of Al hydrogel. The storage modulus was stable during all the measurement.

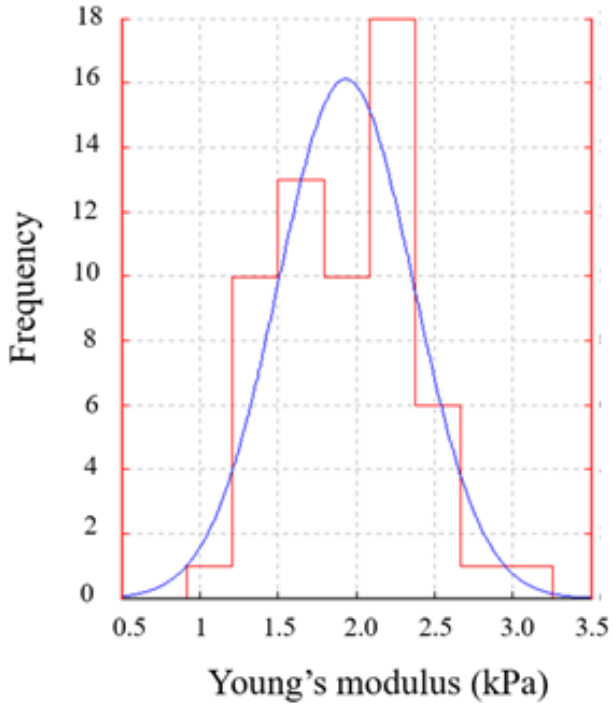

Fig. 4.20 Representative gaussian distribution of the APA hydrogel Young's modulus.

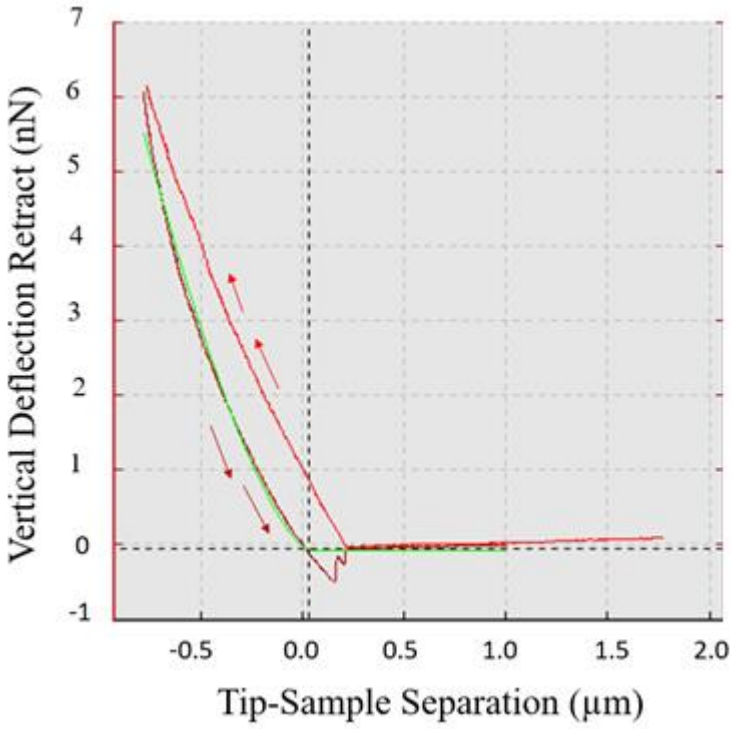

Fig. 4.21 Representative force of the APA hydrogel. The approach is showed in red, while the retraction is showed in green.

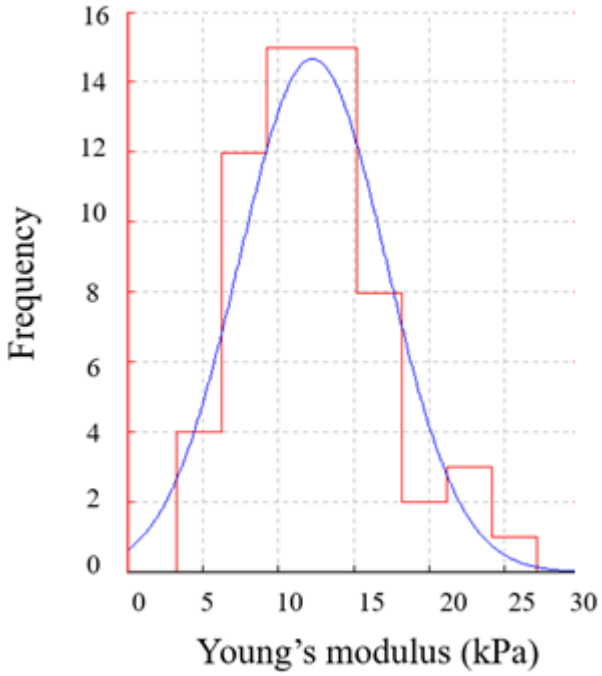

Fig. 4.22 Representative gaussian distribution of the Al-Cs hydrogel Young's modulus.

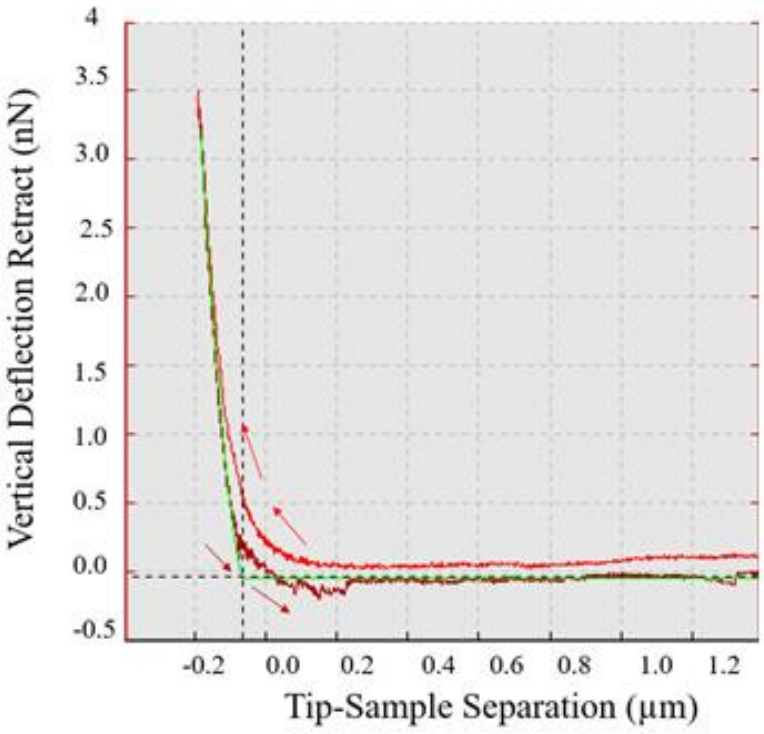

Fig. 4.23 Representative force of the Al-Cs hydrogel. The approach is shown in red, while the retraction is shown in green.

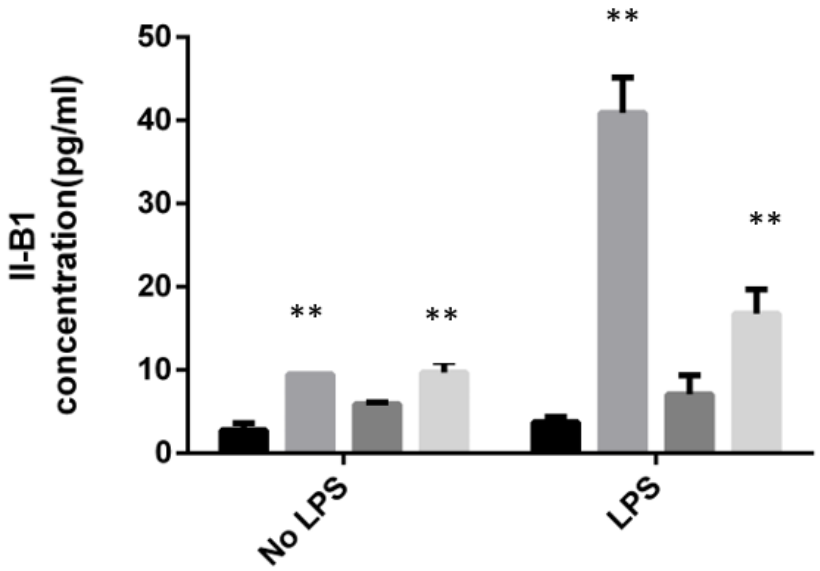

Fig. 4.24 Protein concentration of IL-1β from LPS-activated and non-activated monocytes in co-culture. With : free hVFF, : empty Ms, and :encapsulated hVFF. Bars and error bars are means and standard deviations (n=3). ** $p < 0.05$ from Dunnett's multiple comparisons tests to the monocyte only group to each LPS condition.

Variables	Broken spheres & severe deformities (%)	sd (%)
1) Buffer		
10mM MOPS, 20mM D-Fructose, pH 7,2	51.73	3.9
10mM HEPES, 20mM D-Fructose, pH 7, 2	23.62	3.1
H_2O	15.78	3.1
2) SID (m)		
0.026	7.34	3.1
0.019	15.78	3.1
4)Flow rate (m^3/seg)		
$2.16x10^{-7}$	3.1	0
$2.5x10^{-7}$	3	0
5) Frequency of vibration control (Hz)		
1000	3	0
1200	5.71	0
1500	5.43	0
1800	10	3
6) Amplitude of vibration control		
2	11	2
3	3	0
4	4.76	0
7) Voltage (kV)		
0	100	0
0.65	96	0
1	3	3
2	10	3
8)DNC (m)		
0.06	32.43	5
0.2	3	0.5
9)Alginate Concentration (wt./v)		
1.6	3	1.73
1.8	7.14	3
2	6.9	1.73

Table II. Optimal electrospraying parameters. Effects of buffer, SID, frequency, amplitude, voltage, DNC, and Al concentration on the morphology of the Ms.

Variables	approximate microsphere size (µm)	sd (µm)
1) Buffer		
10mM MOPS, 20mM D-Fructose, pH 7,2	417.065	39
10mM HEPES, 20mM D-Fructose, pH 7, 2	416.243	37.2
H_2O	425.124	38.05
2) SID (m)		
0.026	485.108	17.09
0.019	425.124	38.05
4)Flow rate (m^3/seg)		
$2.16x10^{-7}$	554.023	21.96
$2.5x10^{-7}$	552.74	7.72
5) Frequency of vibration control (Hz)		
1000	552.74	7.72
1200	538.4	39.61
1500	571.23	68.31
1800	589.73	30.74
6) Amplitude of vibration control		
2	568.41	19.81
3	552.74	7.72
4	556.77	19.79
7) Voltage (kV)		
0	na	na
0.65	na	na
1	552.74	7.72
2	571.93	28.61
8) DNC (m)		
0.06	na	na
0.2	552.74	7.72
9)Alginate Concentration (wt./v)		
1.6	552.74	7.72
1.8	566.84	32.41
2	559.31	17.77

Table III. Effects of several electrospraying parameters on the size of the Ms.

CHAPTER 5

Discussion

5.1 Fabrication and optimization

In the present study, optimal conditions for the Ms fabrication were determined. As it is stated in chapter 4, section 4.1, the buffer played a crucial role in the Ms morphology. Other studies successfully used HEPES without compromising the Ms morphology. The fabrication process of this study differed from electrospraying [9]. In addition, the chemical composition of the Al used was not specified [9]. We hypothesize that the chemical groups of the different buffers, HEPES and MOPS, interact with the Al reducing its stability. This hypothesis is supported for previous experiments developed in the Biomedical Technology and Cell Therapy Research Centre, not published [120].

Even though the association between the parameters of electrospraying are not completely well understood, their optimization is necessary [52]. In the present study, the combination of an amplitude of 3 of the vibration controls, a frequency 1000 Hz, and a flow rate of 15 ml/min gave as result the best Ms morphology.

The voltage was a crucial parameter to obtain strong and stable Ms. Before using the INOTECH encapsulator, multiples experiments were developed with a syringe pump without any voltage, as a result, no stable Ms were obtained. The spheres had a diameter of 1 mm, and they broke easily. Other studies tend to use higher voltages, between 3 kV to 5 kV [8, 10], but the INOTECH encapsulator provides a maximum voltage of 2 kV, and the Ms morphology with this voltage was not optimal.

The Al concentration to produce optimal Ms was found to be 74 mM, with agrees with most of the protocols available in the literature [8-10, 59, 62,92].

Because of their diameter of 552.74 ± 7.72 µm. The Ms obtained in the present study, are considered standard [9]. Subsequently, the Ms properties such as diffusion and mechanical stability should be similar to those previously reported [9]. Recently, Ms of 1 mm of diameter have been used [8, 10]. A larger size of Ms reduces the Ms uptake by macrophages [8, 10]. Nevertheless, the standard size achieves the best diffusion properties keeping alive the encapsulated cells. [11, 12, 62]. Future work should explore the effect of the Ms size on their performance. This work was focused on evaluating the properties three different materials of Ms, while the diameter was kept constant.

5.2 Characterization and properties

The microspheres showed favorable and detrimental properties for VF-LP regeneration according to the property investigated.

5.2.1 Cell-biomaterial interaction

5.2.1.1 Cell encapsulation

The results of cell encapsulation, section 4.3, revealed an expected behavior of Al Ms and Al-Cs Ms. Higher cell concentration yielded a higher percentage of deformed Ms. When the cell concentration increased up to $10x10^5$, the Ms broke. In the used methodology, the cells were distributed randomly within the Ms. Some of the hVFF were located near to the membrane caused their rupture or deformation [9]. The two-step process can be used to increase the cell concentration into the Ms while avoiding cell protrusion. However, the involved steps make liquid the core of the Ms which may change their mechanical properties [9, 57]. Interestingly, in the APA Ms, while cell concentration increased, the percentage of deformations decreased, Fig. 4.3. For instance, when none hVFF were encapsulated into APA Ms, they had the biggest percentage of deformed microcapsules, 9.37%. Conversely, when $6x10^5$ cells/ml were encapsulated, the percentage of deformed spheres decreased to 7%. This may be the result of cell interaction with PLL. Other

studies found that PLL and Cs reinforced the Ms [45, 57]. These studies did not consider the interaction between the materials and the cells. The living cells can move and secrete therapeutic agents which may interact with the material in a positive or a negative way [60].

Based on the results, we considered that the optimal cell concentration for the fabricated Ms is around $4x10^5$ cells/ ml, for of Al Ms and Al-Cs Ms, and $6x10^5$ cells/ml for APA Ms. This concentration may change when using another cell line.

5.2.1.2 Biocompatibility

The live/dead assay revealed the biocompatibility of the Ms with the hVFF. Alginate, Cs, and PLL are often used for cell encapsulation [45, 50, 51]. None of them showed any detrimental effect on the cells for 48 hours, as expected. After 3h of incubation of hVFF with the three types of Ms, the proliferation assay exposed a slightly minor signal than the control group. Since the live/dead test did not show any dead cells, we hypothesize that it was due to changes in the metabolic activity of hVFF. This decrease on the signal was not significant. After 24 h and 48 h of incubation, the signal improved. The three groups of Ms (Al, APA, and Al-Cs) induced the proliferation of the hVFF. The alginate-chitosan microspheres and Al Ms doubled the initial cell number after 48 h of incubation. For APA Ms, the original cell concentration increased by 72%. All the Ms can be considered biocompatible. The technique used for evaluating the cytotoxicity of the materials has been used and validated previously. This technique is simple and quantifiable [103].

5.2.2 Membrane properties

The thickness of the PLL membrane was found to be 21.55±1.88 µm at day 3. Fig. 4.11. The thickness of the Cs membrane was found to be 10.625 µm ± 0.88 µm at day 3. Conversely, another research, which used similar conditions to the ones used in the present study, reported a PLL membrane of 4.5 ±0.6 µm, and a Cs membrane of 11. 6±1.7 µm [59]. The study also reported

that the thickness and fluorescence intensity of the PLL was constant over the following 20 days [59]. We found that the thickness of the PLL decreased significantly from 21.55±1.88 μm to 14.12±3.73 μm on day 10. These discrepancies can be explained for the PLL characteristics. The PLL used in the present study did not contain the hydrobromide component, which may do more stable the membrane over the time [59]. Other studies reported similar thickness to the ones obtained in this work [83, 88].

In this work, it was found that the Ms morphology is associated with the uniform deposition of the membrane. When the spheres had elliptical shape, the thickness varied on the same Ms.

The thickness of the Cs membrane obtained in the present study is similar to the one reported previously [56]. The changes in the membrane over time were not significant until day 10, passing from 10.625 μm ± 0.88 μm on day 3, to 9.20 μm ±0.93 μm on day 10. The Al-Cs were stored on pH 7. It is well known that above pH 7, and below pH 2, the Cs starts to disassociate from Al, and the bounding is more stable in acidic conditions [56, 57, 64]. Therefore, it is important for future studies to evaluate the thickness of the Al-Cs Ms at different pH. The alginate-chitosan microcapsules are commonly used to deliver proteins and bacteria on the intestine, in which the pH is mostly acid (pH 2-5) [56]. This is relevant to the study since the VFs are characterized by a neutral pH, which in some cases may be undesirably exposed to gastric reflux [104]. Consequently, the advantages of Cs membrane over PLL or Al Ms may be compromised when injected *in vivo.* In the present study, all the characterizations were developed under neutral pH to reduce the discrepancies between *in vitro* and *in vivo* environments.

The thicknesses of the Ms obtained in this work were previously associated with a permeability up to 40 kDa and 70 kDa [9, 83,88]. This range of permeability is desirable for the system, as it was mentioned in section 2.1 since the therapeutic agents produced by hVFF have a molecular weight of 18 kDa in the case of bFGF, and 34 kDa in the case of HGF [43, 95].

5.2.3 Mechanical properties

5.2.3.1 Mechanical stability and osmotic pressure test

The mechanical stability test has been used previously to compare different crosslinking or crosslinking concentrations on Al Ms, but no for comparing the steadiness of microcapsules made from different materials [94]. We found that Al-Cs Ms and Al Ms have similar stability *in vitro* at 37°C, while APA Ms were the most fragile of the three groups. According to the Osmotic pressure test, Al Ms were the strongest. The alginate-chitosan and APA Ms yielded comparable results, which in the case of APA are consistent with previous reports. Alginate-chitosan microcapsules were not tested previously following the same methodology [92]. Although the Al Ms had the best performance, the percentage of broken capsules, 74%, was still high. Previous studies of Al Ms coated with Cs and genipin reported no broken microcapsules after the osmotic pressure test [92]. Consequently, it is important to determinate if the performance of Al Ms is good enough *in vivo.* During the osmotic pressure test, it was observed that Al Ms swelled and broke in half, while in APA and Al-Cs microcapsules, the Al core shrink creating hollows. The PLL and Cs membrane remained intact. Even though the rupture of the Ms is not desirable, it is better if they break partially instead of bursting, which may lead to scar formation [16].

5.2.3.2 Young's modulus

The Young's modulus or stiffness of injectable biomaterials is an important characteristic, which may determine the efficacy of the treatment. The mismatch of tissue tension of the biomaterials with the one of the VF is associated with an aberrant microenvironment which leads to scar formation [17]. The proper functionality of VF-LP is determined for its stiffness. The voice pitch is associated with the elastic and Young's modulus of the VF [21]. In the present study, Young's modulus of the Ms was determined with a torsional rheometer and with the AFM. The Ms weren't characterized directly, since the high porosity of the Al altered the results. To

characterize directly the Ms in the AFM, they needed to be cut in smaller pieces and attached to a dish with a special glue. Following this procedure, the Al Ms had Young's modulus around 107 kPa, without normal distribution. We hypostasized that the Ms may have adsorbed the glue, altering the results. The stiffness characterization using hydrogels prepared directly in the glass bottom culture dishes, suitable for AFM measurements, provided reproducible and reliable results with similar values reported previously in the literature [100, 105]. The rheometer was used in the present study to characterize the bulk properties of the Al hydrogels [96]. All the measurements were done the same day of the fabrication of the hydrogel to get the initial stiffness. Based in the results, we believe that this method can be suitable to monitor the change of stiffness over time.

The Young's modulus of pure Al hydrogel crosslinked with $CaCl_2$ was 3 kPa. The modification with additional layer of PLL and an additional diluted Al decreased the stiffness by 1.92 kPa. The additional layer of Cs increased the local stiffness up to 12.23 kPa. The stiffness obtained in the present study may explain the results of the mechanical stability test, in which the APA Ms were the most fragile all the three Ms.

There is a wide range of Young's modulus of human VF reported in the literature. For *in-situ* measurements they are in a range of 5.3 kPa up to 13.1 kPa, for *in vitro* measurements, they are in a range of 3.9 kPa up to 5.7 kPa [21]. If the *in-situ* values are considered as the most reliable, it can be concluded that all the hydrogels are suitable for VF-LP regeneration, since the stiffness match the one in VF. However, if the *in vitro* values are more reliable, it can be concluded that alginate-Cs hydrogel is stiffer than the native tissue. Consequently, the regeneration of the VF may be compromised.

5.2.4 Swelling properties

Previous studies suggested that minimizing the swelling of the Ms may help to their stabilization and to slow their degradation [92, 95]. In the present study, APA Ms had the best swelling percentage, 2.32% after 24 h of being incubated with PBS. PBS was selected instead of physiological saline since the chemical composition of the former one helps to evaluate the additional swelling causing by ions such as sodium, magnesium, and phosphate [92]. The swelling of Al Ms was substantially larger than APA Ms, 33.67%. No broken spheres were found because of the swelling. Al-Cs Ms compromised their morphology and got broken by the swelling. This may be caused by the destabilization of the membrane at neutral pH [56]. Similar swelling behavior for the Al-Cs Ms was previously reported [92].

Although Al-Cs Ms had good mechanical stability *in vitro* and promoted the hVFF proliferation, their swelling percentage compromised their overall performance in only 24 h. Subsequently, when injected *in vivo,* it is expected a faster cell release. If allogeneic cells are used, they may be recognized and cleared by immune cells before the regeneration of the tissue. Consequently, these Ms should not be used for VF-LP regeneration until further modifications are made.

5.3 Evaluation of immune response

To mimic the response of the host, monocytes from mice were used and incubated with cells from human origin (hVFF) as xenografts with and without encapsulation. Liposaccharides are critical to the development of inflammation, and their immunomodulatory properties, derived from bacteria, lead to the secretion of proinflammatory cytokines, such as interleukin (IL)-4, IL-1β, and TNF-α [116]. Consequently, the LPS are used to activate macrophages, monocytes, B cells, and dendritic cells [116, 117]. In the control group of monocytes (without LPS) similar levels of IL-1β were found in the coculture and monoculture groups. This indicates the low inflammatory response of hVFF even when transplanted as xenografts, as previously reported [32], and the

biocompatibility of the Ms [51]. When the monocytes were activated with LPS, the hVFF caused the largest production of IL-1β, empty Ms did not produce any significant amount of IL-1β in comparison to the monocyte's monoculture group. The production of IL-1β was reduced when hVFF were encapsulated into Al Ms. This suggests that the Ms fabricated during this study are suitable to protect the host against the immune reaction of xenografts with the cell concentration selected. The immunoprotection by encapsulation allows successful transplantation of cells without immunosuppressants [117]. More research is required to analyze other cytokines, including IL-14 since it has been associated with healing properties [117].

5.4 Summary and novelty of the study

Cell therapy is commonly used for regenerative medicine [9, 12, 51]. As it was mentioned in chapter 1, it has been used for the regeneration of VFs [4, 23, 32, 106]. However, free cells have the drawback of being recognized and cleared by the immune response cells including macrophages and neutrophils [8, 38]. In consequence, the regeneration may not be effective. In addition, adding healthy cells into a damaged microenvironment may compromise the optimal regeneration [14, 16, 17, 31]. The Ms not only protect the cells against the immune response but also provide a temporary microenvironment in which the cells can develop their normal functions [9, 40, 58]. The bulky size of the scaffolds speeds up the process of degradation, compromises the diffusion properties and the viability of the cells [8, 39]. Conversely, the spherical morphology of the Ms enhances diffusion, improving the supply of oxygen and nutrients [8, 9]. The cells encapsulated in these Ms present higher viability and functionality than cells encapsulated in bulky materials [9, 58]. It has been previously demonstrated that Ms reduce foreign body response. Thus, Ms can stay in the system for a longer time without being covered by fibrosis or cellular overgrowth [8]. In the present study, three different types of Ms were fabricated and characterized to evaluate the potential of the biomaterials to protect the cells and withstand to mechanical and ionic

disturbance. The cell-Ms interactions were evaluated in terms of proliferation, and morphology of the Ms. The membrane stability was also evaluated. The stiffness of the materials was determined, since it is desirable that it matches the native rheological characteristics of the VF-LP. Otherwise, the voice quality is compromised [4].

Most of the studies focused on cell therapy to induce the regeneration of the VF-LP, do not use any biomaterial. When biomaterials are used, they are considered as passive cell carriers. Consequently, the characteristics of the biomaterials are neither evaluated nor optimized [4, 23, 106]. Conversely, this study was focused on the optimization of the Ms to provide an adequate substrate to the cells, which improves the hVFF efficiency on regenerating the tissue. Al Ms are easiest to fabricate in comparison with APA Ms and Al-Cs Ms which require further modifications. It was found that Al induces the proliferation of the cells, and it did not compromise their viability. At the same time, it was found that Al Ms had good mechanical stability and had less percentage of broken spheres after the osmotic pressure test. Their swelling percentage, although it is not the best, it did not induce premature degradation as Al-Cs Ms. The Al hydrogel is softer, 3kPa, than the stiffness of the VF-LP reported *in vitro*, 3.9kPa-5.7 kPa [21]. Nevertheless, it is a good approximation. Conversely, when the materials are too stiff, as in the case of Al-Cs hydrogel, 12.23 kPa, the cell viability and voice quality are compromised [4, 14, 21, 60].

5.5 Limitations and future work

The mechanical properties of Al Ms can be improved by increasing the concentration of guluronic acid segment of the Al. Higher content of guluronic acid segment is related with stronger and more ductile materials, as well as low swelling [49, 50]. However, these modifications could modify Young's modulus, porosity and overall protection against the immune response of the host [50]. Nevertheless, the difference in Young's modulus and porosity may be not significant for the application.

An alternative modification of Al Ms can be done fabricating a composite between Al and Cs. The chitosan and Al can be mixed together, to create a core with both materials instead of adding only an external layer of the Cs. With this strategy, the wound healing properties of the Cs can be used, without compromising the swelling or degradation of the Ms [64].

Given some time constraints, there are some characterizations that were not done but are important to determine the feasibility of the Ms in regenerating the VF-LP. Consequently, the next step of this work is to characterize the Ms using the phonomimetic bioreactor which simulates the phonation and the collision between the VFs and the walls pressure [6]. Using the phonomimetic bioreactor with the Ms can be challenging, since the Ms are in solution and may be cleared once starting the test. As an alternative, a different configuration of bioreactor can be used to simulate the vibrations experimented in the VF-LP. A collaborative research group in the University of Delaware fabricated a bioreactor composed of two metal bars, and a water tight vibration chamber, in which the vibration generated by the speaker is translated to the vibration chamber by the oscillating air pressure [107]. This configuration of the bioreactor may facilitate the characterization of the Ms.

Migration is another characterization that was not studied in this work, but it can provide useful information about the biocompatibility of the material, and the overall behavior of the cells inside of the Ms. Cells that do not migrate produce myosin, associated with fibrous deposition around the material, thereby compromising the diffusion of oxygen and other nutrients inside the Ms leading to low viability and metabolic activity [22, 60]. This characterization is an interesting parameter to determine, in special because the core of the Ms is jellified.

The cell type should be optimized. Evaluation of different cell lines, including hVFF (selected in the present study), and stem cells should be done in terms of growth factors production,

antifibrotic agents, and proliferation, to have the best combination between biomaterials and cell type [4]. Most of the studies which use cell therapy to regenerate the VF-LP, use mesenchymal and adipose stem cells for their higher levels of hyaluronic acid production and for their higher rates of proliferation [17, 25, 26, 29].

During this study, it was noticed that, overall, there is more information about the characteristics of scaffolds to induce the regeneration of the VF-LP than the structure itself [4]. This represents a limitation for designing and fabricating biomaterials to mimic the native characteristics of the structure. It is important to characterize the human VF, as well as the rabbit VF since it is the animal model used in the research group.

5.6 Perspective of animal studies and exosomes

The regeneration properties of the Ms along with the cells are normally tested using immunocompromised animals. This kind of study provides a feedback to modify the Ms or the cellular lines [8, 10]. Afterwards, it is important to test the Ms into immunocompetent animals to determine the efficiency of the Ms to protect the cells against the immunological response and degradation. A proper animal study includes free cells group, encapsulated cells, and empty Ms to compare the regeneration in the three groups [9].

The use of exosomes is another interesting approach that can be applied to the VF-LP regeneration. Exosomes (EV) are extracellular vesicles with nanosphere morphology naturally secreted by most of the cells. Exosomes add an alternative to the common cell therapy. They carry diverse molecules including proteins, lipids, and RNA's, which interact with other cells to induce tissue remodeling, regeneration, and antifibrotic activity with immunosuppressive role [108]. In addition, EV have the potential of controlling the inflammatory response, and they are mediators of proliferation and differentiation. It has been previously reported the effects of EV in the

extracellular matrix remodeling, and its long-distance range of action, in which the EV modulate the microenvironment to induce wound healing [109, 110].

Exosomes have the potential of being used alone or in combination with other therapeutic agents as cells, and growth factors or they can coat biomaterials or be mixed with scaffolds [111]. In consequence, in the long-term, the Ms done in the present study can be combined with EV to reduce the immune response of the body after degradation of Ms.

There is preclinical data that support the regenerative effect of EV in cardiovascular diseases, kidney injury, muscle and osteochondral regeneration, and neurological disease [108, 112-114]. The cell origin of the exosomes should be chosen properly. Usually, mesenchymal-derived-EV are used for regenerative and immunosuppressive purposes [109]. There are still challenges with the use of EV. For instance, the proper functionalization and isolation of EV without contaminants is difficult and there is not a standard methodology. In addition, the EV levels change along time upon injury and therefore their use can promote the tissue healing or tissue damage [110]. Nevertheless, the potential of EV to restore the VF-LP can be studied in the future and combined with Ms or scaffolds developed in our research group. An alternative of the Ms can be the direct use of the EV to carry proteins or therapeutic agents to target cells, as previous studies have been done [115].

CHAPTER 6

Conclusions

This study focused on the regeneration of the VF-LP. Voice disorders have a functional and economic impact on around 29% of the adult population. Scarring is a voice disorder that makes stiff the LP, causing voice changes and even aphonic conditions. Scarring currently does not have any effective treatment. The objective of this project was to evaluate the potential of microspheres for the timely delivery of cells and growth factors in the VF-LP for scar treatment as a wounded filler. Several *in vitro* characterization techniques were used to characterize the properties of the Ms.

Electrospraying was used to fabricate Ms with the targeted dimensions, 500 μm, and appropriate morphology. Three different materials were used. Human vocal fold fibroblasts proliferation and viability were found to be excellent when incubated with each type of microspheres over 48 h. For alginate and Al-Cs microspheres, the initial cell concentration doubled after 48 h of incubation. For APA Ms, the original cell concentration increased by 72%.

Alginate microspheres had good mechanical stability over time. Only 7% of the Ms were found to be broken after 10 days of testing. According to osmotic pressure test, it was found that this group is the less prone to break after implantation. Alginate-Poly-L-Lysine microspheres were the most fragile with up to 28% of broken spheres up to day 10. The stability of Al-Cs microspheres varied according to the Cs concentration. Microspheres with higher Cs concentration were more resistant to mechanical disturbance and elevated temperature than Ms with less Cs. With 6% and 12% of broken spheres respectively at day 10. After 24h, an osmotic pressure test did not reveal any significant difference between the percentage of broken APA Ms (100%), and Al-Cs Ms (97%). Alginate microspheres had an adequate stiffness for VF-LP regeneration. Their Young's modulus was slightly softer, 3 kPa than the value reported previously for the vocal cords, 3.9 kPa.

Alginate-Poly-L-Lysine microspheres had a Young's modulus of 1.92 kPa, while Al-Cs Ms had a Young's modulus of 12.23 kPa.

Alginate-poly-L-lysine-alginate microspheres had the lowest swelling percentage of the three groups, 2.32% after 24h of being incubated on PBS, reducing the risk of bursting. Alginate microspheres showed greater but acceptable swelling percentage, 33.67% after 24h of being incubated on PBS, without being prone to bursting during the test. Alginate-chitosan microspheres had a swelling percentage of 52.76% after 24h, and broken spheres were observed.

Alginate microspheres had the most favorable properties for VF-LP regeneration. They were also the easiest to fabricate. Subsequently, empty Al Ms, and hVFF encapsulated in Al Ms were cocultured with monocytes derived from mice which were activated with LPS. The levels of IL-1B after 24h of incubation with empty microspheres were 7.08 pg/ml, and 16.77 pg/ml with encapsulated hVFF. The concentration of IL-1B in the control group was 3.74 pg/ml, and in the free hVFF was 40.88 pg/ml. Microspheres reduced the expression levels of IL-1β, which is an inflammatory cytokine used to monitor the immune response of the host. The results indicated that alginate Ms may provide cell immunoprotection.

These results thus constitute a first step toward the optimal microspheres design and fabrication to promote VF regeneration. Alginate microspheres have significant potential as cell delivery tool. Alginate Ms were resistant to mechanical challenges with a Young's modulus similar to that of the VF-LP. Their swelling rate was low and did not cause bursting. They were found to be showed biocompatible with hVFFs. These properties make alginate Ms adequate biomaterials to be tested in future animal studies. Animals studies are needed to confirm the immunoprotection of microspheres using immunocompetent animals. The viability of encapsulated cells post-implantation needs to be evaluated. Mice will be used, and microspheres will be implanted using intraperitoneal incision. After 14 days post-implantation the microspheres will be retrieved and

analyzed using CLSM and flow cytometry to evaluate the state of the hVFF, and to determine the type of cells attached to the surface of the Ms.

Future work will be aimed to improve the mechanical properties of the microspheres to allow greater cell concentration without compromising the morphology and stability of the microspheres. The line of the cells to load into the microspheres should be determined based on growth factors production, and proliferation capacity.

References

[1] Roy, N., Merrill, R.M., Gray, S.D., Smith, E.M., 2005. Voice Disorders in the General Population: Prevalence, Risk Factors, and Occupational Impact: The Laryngoscope 115, 1988–1995. https://doi.org/10.1097/01.mlg.0000179174.32345.41

[2] K. Verdolini and L. O. Ramig, "Review: Occupational risks for voice problems," Logopedics Phoniatrics Vocology, vol. 26, pp. 37-46, 2001.

[3] Williams, N.R., 2003. Occupational groups at risk of voice disorders: a review of the literature. Occupational Medicine 53, 456–460. https://doi.org/10.1093/occmed/kqg113

[4] Hirano, S., 2015. Regeneration of the Vocal Fold, in: Ito, J. (Ed.), Regenerative Medicine in Otolaryngology. Springer Japan, Tokyo, pp. 171–195. https://doi.org/10.1007/978-4-431-54856-0_12

[5] Chan, R.W., Titze, I.R., 2000. Viscoelastic shear properties of human vocal fold mucosa: Theoretical characterization based on constitutive modeling. The Journal of the Acoustical Society of America 107, 565–580. https://doi.org/10.1121/1.428354

[6] Latifi, N., Heris, H.K., Thomson, S.L., Taher, R., Kazemirad, S., Sheibani, S., Li-Jessen, N.Y.K., Vali, H., Mongeau, L., 2016. A Flow Perfusion Bioreactor System for Vocal Fold Tissue Engineering Applications. Tissue Engineering Part C: Methods 22, 823–838. https://doi.org/10.1089/ten.tec.2016.0053

[7] Liang, Q., Liu, S., Han, P., Li, Xiaofeng, Li, Xiaobing, Zhao, Y., Liang, Y., Deng, Z., Jin, Y., 2012. Micronized acellular dermal matrix as an efficient expansion substrate and delivery vehicle of adipose-derived stem cells for vocal fold regeneration. The Laryngoscope 122, 1815–1825. https://doi.org/10.1002/lary.23330

[8] Veiseh, O., Doloff, J.C., Ma, M., Vegas, A.J., Tam, H.H., Bader, A.R., Li, J., Langan, E., Wyckoff, J., Loo, W.S., Jhunjhunwala, S., Chiu, A., Siebert, S., Tang, K., Hollister-Lock, J., Aresta-Dasilva, S., Bochenek, M., Mendoza-Elias, J., Wang, Y., Qi, M., Lavin, D.M., Chen, M., Dholakia, N., Thakrar, R., Lacík, I., Weir, G.C., Oberholzer, J., Greiner, D.L., Langer, R., Anderson, D.G., 2015. Size- and shape-dependent foreign body immune response to materials implanted in rodents and non-human primates. Nature Materials 14, 643–651. https://doi.org/10.1038/nmat4290

[9] Chang, T.M.S., 2007. Artificial cells: biotechnology, nanomedicine, regenerative medicine, blood substitutes, bioencapsulation, cell/stem cell therapy, Regenerative medicine, artificial cells and nanomedicine. World Scientific, Hackensack, N. J.

[10] Song, W., Lu, Y.-C., Frankel, A.S., An, D., Schwartz, R.E., Ma, M., 2015a. Engraftment of human induced pluripotent stem cell-derived hepatocytes in immunocompetent mice via 3D co-aggregation and encapsulation. Scientific Reports 5. doi:10.1038/srep16884

[11] Kühtreiber, W.M., Lanza, R.P., Chick, W.L. (Eds.), 1999. Cell Encapsulation Technology and Therapeutics. Birkhäuser Boston, Boston, MA. https://doi.org/10.1007/978-1-4612-1586-8

[12] Zhao, S., Xu, Z., Wang, H., Reese, B.E., Gushchina, L.V., Jiang, M., Agarwal, P., Xu, J., Zhang, M., Shen, R., Liu, Z., Weisleder, N., He, X., 2016. Bioengineering of injectable encapsulated aggregates of pluripotent stem cells for therapy of myocardial infarction. Nature Communications 7, 13306. https://doi.org/10.1038/ncomms13306

[13] Liu, X., Jin, X., Ma, P.X., 2011. Nanofibrous hollow Ms self-assembled from star-shaped polymers as injectable cell carriers for knee repair. Nature Materials 10, 398–406. https://doi.org/10.1038/nmat2999

[14] S. Prakash and D. Shum-Tim, Eds., *Stem cell bioengineering and tissue engineering microenvironment*. Singapur; Hackensack, NJ: World Scientific, 2011.

[15] Rodrigues, A. David, ed. Scarless Wound Healing (1). Baton Rouge, US: CRC Press, 2000.

[16] Atala, A., Irvine, D.J., Moses, M., Shaunak, S., 2010. Wound Healing Versus Regeneration: Role of the Tissue Environment in Regenerative Medicine. MRS Bulletin 35, 597–606. https://doi.org/10.1557/mrs2010.528
[17] Forbes, S.J., Rosenthal, N., 2014. Preparing the ground for tissue regeneration: from mechanism to therapy. Nature Medicine 20, 857–869. https://doi.org/10.1038/nm.3653
[18] Wong, V.W., Rustad, K.C., Akaishi, S., Sorkin, M., Glotzbach, J.P., Januszyk, M., Nelson, E.R., Levi, K., Paterno, J., Vial, I.N., Kuang, A.A., Longaker, M.T., Gurtner, G.C., 2012. Focal adhesion kinase links mechanical force to skin fibrosis via inflammatory signaling. Nature Medicine 18, 148–152. https://doi.org/10.1038/nm.2574
[19] X. Z. Shu, Y. Liu, Y. Luo, M. C. Roberts, and G. D. Prestwich, "Disulfide Cross-Linked Hyaluronan Hydrogels," *Biomacromolecules*, vol. 3, no. 6, pp. 1304–1311, Nov. 2002.
[20] J. W. Choi *et al.*, "Small intestine submucosa and mesenchymal stem cells composite gel for scarless vocal fold regeneration," *Biomaterials*, vol. 35, no. 18, pp. 4911–4918, Jun. 2014.
[21] Miri, A.K., 2014. Mechanical Characterization of Vocal Fold Tissue: A Review Study. Journal of Voice 28, 657–667. https://doi.org/10.1016/j.jvoice.2014.03.001
[22] H. K. Heris, N. Latifi, H. Vali, N. Li, and L. Mongeau, "Investigation of Chitosan-glycol/glyoxal as an Injectable Biomaterial for Vocal Fold Tissue Engineering," *Procedia Engineering*, vol. 110, pp. 143–150, 2015.
[23] S. Kanemaru *et al.*, "Destiny of autologous bone marrow—derived stromal cells implanted in the vocal fold," *Annals of Otology, Rhinology & Laryngology*, vol. 114, no. 12, pp. 907–912, 2005.
[24] R. J. Clifton, X. Jia, T. Jiao, C. Bull, and M. S. Hahn, "Viscoelastic response of vocal fold tissues and scaffolds at high frequencies," in *Mechanics of Biological Tissue*, Springer, 2006, pp. 445–455.
[25] X. Jia *et al.*, "Hyaluronic Acid-Based Microgels and Microgel Networks for Vocal Fold Regeneration," *Biomacromolecules*, vol. 7, no. 12, pp. 3336–3344, Dec. 2006.
[26] X. Z. Shu, Y. Liu, Y. Luo, M. C. Roberts, and G. D. Prestwich, "Disulfide Cross-Linked Hyaluronan Hydrogels," *Biomacromolecules*, vol. 3, no. 6, pp. 1304–1311, Nov. 2002.
[27] X. Z. Shu *et al.*, "Attachment and spreading of fibroblasts on an RGD peptide–modified injectable hyaluronan hydrogel," *Journal of biomedical materials research Part A*, vol. 68, no. 2, pp. 365–375, 2004.
[28] S. Ohno *et al.*, "Atelocollagen sponge as a stem cell implantation scaffold for the treatment of scarred vocal folds," *Annals of Otology, Rhinology & Laryngology*, vol. 119, no. 11, pp. 805–810, 2010.
[29] W. Xu, R. Hu, E. Fan, and D. Han, "Adipose-derived mesenchymal stem cells in collagen—hyaluronic acid gel composite scaffolds for vocal fold regeneration," *Annals of Otology, Rhinology & Laryngology*, vol. 120, no. 2, pp. 123–130, 2011.
[30] C. C. Xu, R. W. Chan, D. G. Weinberger, G. Efune, and K. S. Pawlowski, "A bovine acellular scaffold for vocal fold reconstruction in a rat model," *Journal of Biomedical Materials Research Part A*, vol. 92A, no. 1, pp. 18–32, Jan. 2010.
[31] H. Park *et al.*, "Three-dimensional hydrogel model using adipose-derived stem cells for vocal fold augmentation," *Tissue Engineering Part A*, vol. 16, no. 2, pp. 535–543, 2009.
[32] Hanson, S.E., Kim, J., Johnson, B.H.Q., Bradley, B., Breunig, M.J., Hematti, P., Thibeault, S.L., 2010. Characterization of mesenchymal stem cells from human vocal fold fibroblasts. The Laryngoscope 120, 546–551. https://doi.org/10.1002/lary.20797
[33] Orive Gorka, Hernández Rosa María, Gascón Alicia R, Riccardo, M.S. Chang Thomas, De Vos Paul, Hortelano Gonzalo, Hunkeler David, Lacík Igor, Shapiro James, Pedraz José Luis. 2003. Cell encapsulation: progress and promise, Nature Medicine, 109, 104-107.
[34] Prakash, S., Bhathena, J.R., Chen, H., 2007. Introduction to artificial cells: concept, history, design, current status and future, in: Artificial Cells, Cell Engineering and Therapy. Elsevier, pp. 3–41.

[35] LEMARIEa'b, C., 2012. Cell Therapy in Hematology: Hematopoietic Stem Cell Transplantations in 2012. Regenerative Medicine and Cell Therapy 77, 149.
[36] Le Gall, J.Y., Ardaillou, R., 2012. I. Therapeutical Potential of Stem Cells. Regenerative Medicine and Cell Therapy 77, 3.
[37] Chang, T.M.S, 1972. Artificial cells. New York: Charles C Thomas Publisher
[38] Lee, K.Y., Mooney, D.J., 2012. Alginate: Properties and biomedical applications. Progress in Polymer Science 37, 106–126. https://doi.org/10.1016/j.progpolymsci.2011.06.003
[39] O'brien, F.J., 2011. Biomaterials & scaffolds for tissue engineering. Materials today 14, 88–95.
[40] Borlongan, C.V., Skinner, S.J., Geaney, M., Vasconcellos, A.V., Elliott, R.B., Emerich, D.F., 2004. Neuroprotection by encapsulated choroid plexus in a rodent model of Huntington's disease. Neuroreport 15, 2521–2525.
[41] Liu, Z.C., Chang, T.M.S., 2010. Artificial cell microencapsulated stem cells in regenerative medicine, tissue engineering and cell therapy, in: Therapeutic Applications of Cell Microencapsulation. Springer, pp. 68–79.
[42] Singh, A., Gaharwar, A.K. (Eds.), 2016. Microscale Technologies for Cell Engineering. Springer International Publishing, Cham. https://doi.org/10.1007/978-3-319-20726-1
[43] Delrieu, I., 2000. The high molecular weight isoforms of basic fibroblast growth factor (FGF-2): an insight into an intracrine mechanism. FEBS Letters 468, 6–10.
[44] Chan, L.W., Lee, H.Y., Heng, P.W.S., 2006. Mechanisms of external and internal gelation and their impact on the functions of alginate as a coat and delivery system. Carbohydrate Polymers 63, 176–187. https://doi.org/10.1016/j.carbpol.2005.07.033
[45] Rehm, B.H.A., Moradali, M.F. (Eds.), 2018. Alginates and Their Biomedical Applications, Springer Series in Biomaterials Science and Engineering. Springer Singapore, Singapore. https://doi.org/10.1007/978-981-10-6910-9
[46] Szekalska, M., Puciłowska, A., Szymańska, E., Ciosek, P., Winnicka, K., 2016. Alginate: Current Use and Future Perspectives in Pharmaceutical and Biomedical Applications. International Journal of Polymer Science 2016, 1–17. https://doi.org/10.1155/2016/7697031
[47] Bian, L., Zhai, D.Y., Tous, E., Rai, R., Mauck, R.L., Burdick, J.A., 2011. Enhanced MSC chondrogenesis following delivery of TGF-β3 from alginate Ms within hyaluronic acid hydrogels in vitro and in vivo. Biomaterials 32, 6425–6434. https://doi.org/10.1016/j.biomaterials.2011.05.033
[48] Poojari, R., Srivastava, R., 2013. Composite alginate Ms as the next-generation egg-box carriers for biomacromolecules delivery. Expert Opinion on Drug Delivery 10, 1061–1076. https://doi.org/10.1517/17425247.2013.796361
[49] Drury, J.L., Dennis, R.G., Mooney, D.J., 2004. The tensile properties of alginate hydrogels. Biomaterials 25, 3187–3199. https://doi.org/10.1016/j.biomaterials.2003.10.002
[50] Hadjialirezaei, S., 2013. Coating of alginate capsules (master's Thesis). Institutt for bioteknologi.
[51] Sun, J., Tan, H., 2013. Alginate-Based Biomaterials for Regenerative Medicine Applications. Materials 6, 1285–1309. https://doi.org/10.3390/ma6041285
[52] Bock, N., Woodruff, M.A., Hutmacher, D.W., Dargaville, T.R., 2011. Electrospraying, a Reproducible Method for Production of Polymeric Ms for Biomedical Applications. Polymers 3, 131–149. https://doi.org/10.3390/polym3010131
[53] Tibbitt, M.W., Anseth, K.S., 2009. Hydrogels as extracellular matrix mimics for 3D cell culture. Biotechnology and Bioengineering 103, 655–663. https://doi.org/10.1002/bit.22361
[54] Liu-Snyder, P., 2007. Applications of Nanotechnology/Nanomaterials in the Nervous System, in: Nanotechnology for The Regeneration of Hard and Soft Tissues. World Scientific, pp. 135–179.

[55] Webster, T.J. (Ed.), 2007. Nanotechnology for the regeneration of hard and soft tissues. World Scientific, Singapore; Hackensack, N.J.
[56] Cook, M.T., Tzortzis, G., Charalampopoulos, D., Khutoryanskiy, V.V., 2011. Production and Evaluation of Dry Alginate-Chitosan Microcapsules as an Enteric Delivery Vehicle for Probiotic Bacteria. Biomacromolecules 12, 2834–2840. https://doi.org/10.1021/bm200576h
[57] Matricardi, P., Meo, C.D., Coviello, T., Alhaique, F., 2008. Recent advances and perspectives on coated alginate Ms for modified drug delivery. Expert Opinion on Drug Delivery 5, 417–425. https://doi.org/10.1517/17425247.5.4.417
[58] Zhang, Z., Eyster, T.W., Ma, P.X., 2016. Nanostructured injectable cell microcarriers for tissue regeneration. Nanomedicine 11, 1611–1628. https://doi.org/10.2217/nnm-2016-0083
[59] Chen, H., Ouyang, W., Lawuyi, B., Lim, T., Prakash, S., 2006. A new method for microcapsule characterization. Applied biochemistry and biotechnology 134, 207–221.
[60] Currier, C.M., Andrew E. Pelling, n.d. Cells, Forces, and the Microenvironment.
[61] Leick, S., Kemper, A., Rehage, H., 2011. Alginate/poly-l-lysine capsules: mechanical properties and drug release characteristics. Soft Matter 7, 6684. https://doi.org/10.1039/c1sm05676j
[62] Chen, H., Ouyang, W., Jones, M., Metz, T., Martoni, C., Haque, T., Cohen, R., Lawuyi, B., Prakash, S., 2007. Preparation and characterization of novel polymeric microcapsules for live cell encapsulation and therapy. Cell Biochemistry and Biophysics 47, 159–167.
[63] Ribeiro, A.J., Silva, C., Ferreira, D., Veiga, F., 2005. Chitosan-reinforced alginate Ms obtained through the emulsification/internal gelation technique. European Journal of Pharmaceutical Sciences 25, 31–40. https://doi.org/10.1016/j.ejps.2005.01.016
[64] Croisier, F., Jérôme, C., 2013. Chitosan-based biomaterials for tissue engineering. European Polymer Journal 49, 780–792. https://doi.org/10.1016/j.eurpolymj.2012.12.009
[65] Ueno, H., Nakamura, F., Murakami, M., Okumura, M., Kadosawa, T., Fujinaga, T., 2001. Evaluation effects of chitosan for the extracellular matrix production by fibroblasts and the growth factors production by macrophages. Biomaterials 22, 2125–2130.
[66] Wang, Jianmei, Li, Y., Wang, X., Wang, Jianchun, Tian, H., Zhao, P., Tian, Y., Gu, Y., Wang, L., Wang, C., 2017. Droplet Microfluidics for the Production of Microparticles and Nanoparticles. Micromachines 8, 22. https://doi.org/10.3390/mi8010022
[67] Freitas, S., Merkle, H.P., Gander, B., 2005. Microencapsulation by solvent extraction/evaporation: reviewing the state of the art of microsphere preparation process technology. Journal of Controlled Release 102, 313–332. https://doi.org/10.1016/j.jconrel.2004.10.015
[68] Das, S., Rani Nakka David, S., Rajabalaya, R., Kumar Mukhopadhyay, H., Halder, T., Palanisamy, M., Khanam, J., Nanda, A., 2011. Microencapsulation techniques and its practices.
[69] Valo, H., Peltonen, L., Vehviläinen, S., Karjalainen, M., Kostiainen, R., Laaksonen, T., Hirvonen, J., 2009. Electrospray Encapsulation of Hydrophilic and Hydrophobic Drugs in Poly(L-lactic acid) Nanoparticles. Small 5, 1791–1798. https://doi.org/10.1002/smll.200801907
[70] Ding, L., Lee, T., Wang, C.-H., 2005. Fabrication of monodispersed Taxol-loaded particles using electrohydrodynamic atomization. Journal of Controlled Release 102, 395–413. https://doi.org/10.1016/j.jconrel.2004.10.011
[71] Jaworek, A., 2007. Micro- and nanoparticle production by electrospraying. Powder Technology 176, 18–35. https://doi.org/10.1016/j.powtec.2007.01.035
[72] Rayleigh, Lord, 1882. XX. *On the equilibrium of liquid conducting masses charged with electricity*. The London, Edinburgh, and Dublin Philosophical Magazine and Journal of Science 14, 184–186. https://doi.org/10.1080/14786448208628425
[73] Taylor, G., 1964. Disintegration of water drops in an electric field. Proceedings of the Royal Society of London. Series A. Mathematical and Physical Sciences 280, 383–397.

[74] Zeleny, J., 1914. The electrical discharge from liquid points, and a hydrostatic method of measuring the electric intensity at their surfaces. Physical Review 3, 69.
[75] Morad, M.R., Rajabi, A., Razavi, M., Sereshkeh, S.R.P., 2016. A Very Stable High Throughput Taylor Cone-jet in Electrohydrodynamics. Scientific Reports 6. https://doi.org/10.1038/srep38509
[76] Shenoy, S.L.; Bates, W.D.; Frisch, H.L.; Wnek, G.E. Role of chain entanglements on fiber formation during electrospinning of polymer solutions: Good solvent, non-specific polymer-polymer interaction limit. *Polymer* **2005**, *46*, 3372-3384
[77]L R G Treloar (1970), Introduction to polymer science, London, Wykeham Publications; New York, Springer-Verlag, ISBN 978-0-85109-100-6
[78] Alehosseini, A., Ghorani, B., Sarabi-Jamab, M., Tucker, N., 2017. Principles of electrospraying: A new approach in protection of bioactive compounds in foods. Critical Reviews in Food Science and Nutrition 1–18. https://doi.org/10.1080/10408398.2017.1323723
[79] Luo, C. J., Loh, S., Stride, E. and Edirisinghe, M. (2012). Electrospraying and electrospinning of chocolate suspensions. Food Bioprocess Technol. 5 (6):2285–2300. doi: 10.1007/s11947-011-0534-6. Accessed June 27, 2015
[80] Seeram Ramakrishna, Zamani, M., Molamma P Prabhakaran, 2013. Advances in drug delivery via electrospun and electrosprayed nanomaterials. International Journal of Nanomedicine 2997. https://doi.org/10.2147/IJN.S43575
[81] Manojlovic, V., Rajic, N., Djonlagic, J., Obradovic, B., Nedovic, V., Bugarski, B., 2008. Application of electrostatic extrusion–flavour encapsulation and controlled release. Sensors 8, 1488–1496.
[82] Barnabé, M. (*Quartzi).* 2017. Cell viability assays: MTT assay application and protocol. [Online]. [Accessed 25 February, 2018] Available from: https://blog.quartzy.com/2017/05/01/cell-viability-assays-mtt-protocol.
[83] Gugerli, R., Cantana, E., Heinzen, C., Stockar, U. von, Marison, I.W., 2002. Quantitative study of the production and properties of alginate/poly-L-lysine microcapsules. Journal of Microencapsulation 19, 571–590. https://doi.org/10.1080/02652040210140490
[84] Thu, B., Bruheim, P., Espevik, T., Smidsrød, O., Soon-Shiong, P., Skj\a ak-Br\a ek, G., 1996. Alginate polycation microcapsules: I. Interaction between alginate and polycation. Biomaterials 17, 1031–1040.
[85] Krasaekoopt, W., Bhandari, B., Deeth, H., 2004. The influence of coating materials on some properties of alginate beads and survivability of microencapsulated probiotic bacteria. International Dairy Journal 14, 737–743. https://doi.org/10.1016/j.idairyj.2004.01.004
[86] Su, J. F. (2005), *J. Appl. Polym. Sci.* **97,** 1755–1762.
[87] Lamprecht, A., Schäfer, U.F., Lehr, C.-M., 2000. Characterization of microcapsules by confocal laser scanning microscopy: structure, capsule wall composition and encapsulation rate. European Journal of Pharmaceutics and Biopharmaceutics 49, 1–9.
[88] Strand, B. L., Morch, Y. A., Espevik, T., and Skjak-Braek, G. (2003), *Biotechnol. Bioeng.* **82,** 386–394.
[89]Araya-Hermosilla, E., Muñoz, D., Orellana, S., Yáñez, A., Olea, A.F., Oyarzun-Ampuero, F., Moreno-Villoslada, I., 2014. Immobilization of rhodamine 6G in calcium alginate microcapsules based on aromatic–aromatic interactions with poly (sodium 4-styrenesulfonate). Reactive and Functional Polymers 81, 14–21. https://doi.org/10.1016/j.reactfunctpolym.2014.03.017
[90] Djerassi, C., Gray, J. D., and Kincl, F. A. (1960), *J. Org. Chem.* **25,** 2174–2177
[91] NáThia-Neves, G., Nogueira, G.C., Vardanega, R., Meireles, M.A. de A., 2018. Identification and quantification of genipin and geniposide from Genipa americana L. by HPLC-DAD using a fused-core column. Food Science and Technology. https://doi.org/10.1590/1678-457x.17317

[92] Chen, H., Ouyang, W., Martoni, C., Prakash, S., 2009. Genipin Cross-Linked Polymeric Alginate-Chitosan Microcapsules for Oral Delivery: In-Vitro Analysis. International Journal of Polymer Science 2009, 1–16. https://doi.org/10.1155/2009/617184
[93] Lu, Y.-C., Song, W., An, D., Kim, B.J., Schwartz, R., Wu, M., Ma, M., 2015. Designing compartmentalized hydrogel microparticles for cell encapsulation and scalable 3D cell culture. Journal of Materials Chemistry B 3, 353–360. https://doi.org/10.1039/C4TB01735H
[94] Lee, C.-S., Chu, I.-M., 1997. Characterization of Modified Alginate-Poly-L-LysineMicrocapsules. Artificial organs 21, 1002–1006.
[95] Van Raamsdonk, J.M., Chang, P.L., 2001. Osmotic pressure test: a simple, quantitative method to assess the mechanical stability of alginate microcapsules. Journal of Biomedical Materials Research Part A 54, 264–271.
[96] Yan, C., Pochan, D.J., 2010. Rheological properties of peptide-based hydrogels for biomedical and other applications. Chemical Society Reviews 39, 3528. https://doi.org/10.1039/b919449p
[97] Borzacchiello, A., Sala, F.D., Ambrosio, L.A., 2017. Rheometry of polymeric biomaterials, in: Characterization of Polymeric Biomaterials. Elsevier, pp. 233–253. https://doi.org/10.1016/B978-0-08-100737-2.00010-8
[98] Braga, P.C., Ricci, D. (Eds.), 2011. Atomic Force Microscopy in Biomedical Research, Methods in Molecular Biology. Humana Press, Totowa, NJ. https://doi.org/10.1007/978-1-61779-105-5
[99] Vega Manzano O. 2018. Structural Dimensional Limits on Materials Properties: Anisotropic Conduction in Organic Semiconductors and Low Dimensional Ferroelectricity in Organic Ferroelectrics (master's thesis). University of Puerto Rico at Humacao
[100] Monclus, M.A., Young, T.J., Di Maio, D., 2010. AFM indentation method used for elastic modulus characterization of interfaces and thin layers. Journal of Materials Science 45, 3190–3197. https://doi.org/10.1007/s10853-010-4326-6
[101] Butt, H.-J., Cappella, B., Kappl, M., 2005. Force measurements with the atomic force microscope: Technique, interpretation and applications. Surface Science Reports 59, 1–152. https://doi.org/10.1016/j.surfrep.2005.08.003
[102] Chen, X., Thibeault, S.L., 2008. Novel isolation and biochemical characterization of immortalized fibroblasts for tissue engineering vocal fold lamina propria. Tissue Engineering Part C: Methods 15, 201–212.
[103] Yao, L., Phan, F., Li, Y., 2013. Collagen microsphere serving as a cell carrier supports oligodendrocyte progenitor cell growth and differentiation for neurite myelination in vitro. Stem Cell Research & Therapy 4, 109. https://doi.org/10.1186/scrt320
[104] Erickson, E., Sivasankar, M., 2010. Simulated reflux decreases vocal fold epithelial barrier resistance. The Laryngoscope 120, 1569–1575. https://doi.org/10.1002/lary.20983
[105] Matyash, M., Despang, F., Ikonomidou, C., Gelinsky, M., 2014. Swelling and Mechanical Properties of Alginate Hydrogels with Respect to Promotion of Neural Growth. Tissue Engineering Part C: Methods 20, 401–411. https://doi.org/10.1089/ten.tec.2013.0252
[106] Bartlett, R.S., Guille, J.T., Chen, X., Christensen, M.B., Wang, S.F., Thibeault, S.L., 2016. Mesenchymal stromal cell injection promotes vocal fold scar repair without long-term engraftment. Cytotherapy 18, 1284–1296. https://doi.org/10.1016/j.jcyt.2016.07.005
[107] Tong, Z., Duncan, R.L., Jia, X., 2013. Modulating the Behaviors of Mesenchymal Stem Cells Via the Combination of High-Frequency Vibratory Stimulations and Fibrous Scaffolds. Tissue Engineering Part A 19, 1862–1878. https://doi.org/10.1089/ten.tea.2012.0694
[108] Lou, G., Chen, Z., Zheng, M., Liu, Y., 2017. Mesenchymal stem cell-derived exosomes as a new therapeutic strategy for liver diseases. Experimental & Molecular Medicine 49, e346. https://doi.org/10.1038/emm.2017.63

[109] Silva, A.M., Teixeira, J.H., Almeida, M.I., Gonçalves, R.M., Barbosa, M.A., Santos, S.G., 2017. Extracellular Vesicles: Immunomodulatory messengers in the context of tissue repair/regeneration. European Journal of Pharmaceutical Sciences 98, 86–95. https://doi.org/10.1016/j.ejps.2016.09.017

[110] Teixeira, J.H., Silva, A.M., Almeida, M.I., Barbosa, M.A., Santos, S.G., 2016. Circulating extracellular vesicles: Their role in tissue repair and regeneration. Transfusion and Apheresis Science 55, 53–61. https://doi.org/10.1016/j.transci.2016.07.015

[111] Taverna, S., Pucci, M., Alessandro, R., 2017. Extracellular vesicles: small bricks for tissue repair/regeneration. Annals of Translational Medicine 5, 83–83. https://doi.org/10.21037/atm.2017.01.53

[112] Bruno, S., Porta, S., Bussolati, B., 2016. Extracellular vesicles in renal tissue damage and regeneration. European Journal of Pharmacology 790, 83–91. https://doi.org/10.1016/j.ejphar.2016.06.058

[113] Safari, S., Malekvandfard, F., Babashah, S., Alizadehasl, A., Sadeghizadeh, M., Motavaf, M., 2016. Mesenchymal stem cell-derived exosomes: A novel potential therapeutic avenue for cardiac regeneration. Cellular and Molecular Biology 62, 66–73.

[114] Sundaram, B., Herbert, F.J., Kumar, S., 2017. Human Mesenchymal Stem Cell (hMSC) -Derived Exosomes/Exosome Mimetics as a Potential Novel Therapeutic Tool for Regenerative Medicine, in: Mukhopadhyay, A. (Ed.), Regenerative Medicine: Laboratory to Clinic. Springer Singapore, Singapore, pp. 81–97. https://doi.org/10.1007/978-981-10-3701-6_5

[115] Akao, Y., Iio, A., Itoh, T., Noguchi, S., Itoh, Y., Ohtsuki, Y., Naoe, T., 2011. Microvesicle-mediated RNA Molecule Delivery System Using Monocytes/Macrophages. Molecular Therapy 19, 395–399. https://doi.org/10.1038/mt.2010.254

[116] Rodes, L., 2013. Effect of Probiotics Lactobacillus and Bifidobacterium on Gut-Derived Lipopolysaccharides and Inflammatory Cytokines: An In Vitro Study Using a Human Colonic Microbiota Model. Journal of Microbiology and Biotechnology 23, 518–526. https://doi.org/10.4014/jmb.1205.05018

[117] de Vos, P., Smedema, I., van Goor, H., Moes, H., van Zanten, J., Netters, S., de Leij, L.F.M., de Haan, A., de Haan, B.J., 2003. Association between macrophage activation and function of micro-encapsulated rat islets. Diabetologia 46, 666–673. https://doi.org/10.1007/s00125-003-1087-7

[118] Agüero, L., Zaldivar-Silva, D., Peña, L., Dias, M.L., 2017. Alginate microparticles as oral colon drug delivery device: A review. Carbohydrate Polymers 168, 32–43. https://doi.org/10.1016/j.carbpol.2017.03.033

[119] Younes, I., Rinaudo, M., 2015. Chitin and Chitosan Preparation from Marine Sources. Structure, Properties and Applications. Marine Drugs 13, 1133–1174. https://doi.org/10.3390/md13031133

[120] Personal communication with Chen, 2018